European Journal of Medicinal Chemistry 72 (2014) 170–205

Contents lists available at ScienceDirect

European Journal of Medicinal Chemistry

journal homepage: http://www.elsevier.com/locate/ejmech

Invited review

Recent progress in the identification of BRAF inhibitors as anti-cancer agents

Hala Bakr El-Nassan*

Pharmaceutical Organic Chemistry Department, Faculty of Pharmacy, Cairo University, 33 Kasr El-Aini Street, Cairo 11562, Egypt

ARTICLE INFO

Article history:
Received 19 September 2013
Received in revised form
5 November 2013
Accepted 18 November 2013
Available online 27 November 2013

Keywords:
BRAF
Inhibitors
Anti-cancer agents

ABSTRACT

The "RAS/BRAF/MEK/ERK" pathway has been associated with human cancers due to the frequent oncogenic mutations identified in its members. In particular, BRAF is mutated at high frequency in many cancers especially melanoma. This mutation leads to activation of the MAPK signaling pathway, inducing uncontrolled cell proliferation, and facilitating malignant transformation. All these facts make BRAF an ideal target for antitumor therapeutic development. Many BRAF inhibitors have been discovered during the last decade and most of them exhibit potent antitumor activity especially on tumors that harbor $BRAF^{V600E}$ mutations. Some of these compounds have entered clinical trials and displayed encouraged results. The present review highlights the progress in identification and development of BRAF inhibitors especially during the last five years.

1. Introduction

In intracellular signal transduction, signals are transferred from cell surface to the nucleus resulting in modulation of cell proliferation, cell death (apoptosis), motility as well as many other biological processes [1].

Signal transduction is effected through a number of molecules including receptor tyrosine kinases (RTKs), non-receptor tyrosine kinases (NTRKs), serine–threonine kinases (STKs), and G proteins [1].

Receptor tyrosine kinases (RTKs) such as vascular endothelial growth factor receptor (VEGFR), and platelet-derived growth factor receptor (PDGFR) are glycoproteins. RTKs have an extracellular ligand binding domain, a hydrophobic transmembrane domain, and an intracellular catalytic domain [1].

Nonreceptor tyrosine kinases (NRTKs) such as Src, abl, and JAK are cytoplasmic proteins that lack transmembrane domains. Whilst, STKs such as rapidly growing fibrosarcoma (RAF) and AKT/protein kinase B (PKB) are intracellular enzymes and include the key mediators of carcinogenesis [1].

Finally, the G proteins such as Ras, Rho, Rab, Sar1/Arf, and Ran families act as intracellular molecular switches linking RTK and NRTK-mediated activation to control cytoplasmic and nuclear events [1]. Fig. 1 shows a simplified diagram of signal transduction pathways [2].

In "RAS-RAF-MEK-ERK" pathway [sometimes denoted as the mitogen-activated protein kinase (MAPK) cascade], activation of the small G protein Ras results in activation of RAF. RAF phosphorylates mitogen-activated protein kinase (MAPK) which in turn phosphorylates extracellular signal-regulated kinase (ERK). Once phosphorylated, ERK translocates to the nucleus where it activates a number of transcription factors that result in cell proliferation as well as many other biological processes. The formation of side-to-side RAF dimers is required for full kinase activity [3]. Genetic abnormalities in cancer cells may result in increase in the expression and the activity of many signaling molecules [4].

RAF is one of the STKs and RAF kinases were first discovered in 1980s as retroviral oncogenes. The murine sarcoma virus 3611 enhances fibrosarcoma induction in newborn MSF/N mice, and the name RAF corresponds to rapidly accelerated fibrosarcoma [5]. To

Abbreviations: abl, abelson murine leukemia viral oncogene homolog 1; ADME, absorption, distribution, metabolism and excretion; CR, conserved regions; CRD, cysteine-rich domain, DFG, D594, F595, and G596; ELISA, enzyme-linked immunosorbent assay; EMEA, European Medicine Agency; ERK, extracellular signal-regulated kinase; FDA, Food and Drug Administration; GTP, guanosine triphosphate; HCC, hepatocellular carcinoma; IV, intravenous; JAK, Janus kinase; Lck, lymphocyte-specific protein tyrosine kinase; MAPK, mitogen-activated protein kinase; MD, molecular dynamics; NTRKs, non-receptor tyrosine kinases; p38α, mitogen-activated protein kinase 14; PDGFR, platelet-derived growth factor receptor; PET, positron emission tomography; PK, pharmacokinetic; PKB, AKT/protein kinase B; QM/MM, quantum mechanics/molecular mechanics; RAF, rapidly growing fibrosarcoma; RBD, RAS-binding domain; RCC, renal cell carcinoma; RTKs, receptor tyrosine kinases; SCID, severe combined immunodeficiency; STKs, serine–threonine kinases; SRB, sulforhodamine B assay; Src, proto-oncogene tyrosine-protein kinase; VEGFR, vascular endothelial growth factor receptor.

* Tel.: +20 2 23632245; fax: +20 2 23635140.
E-mail address: hala_bakr@hotmail.com.

0223-5234/$ – see front matter © 2013 Elsevier Masson SAS. All rights reserved.
http://dx.doi.org/10.1016/j.ejmech.2013.11.018

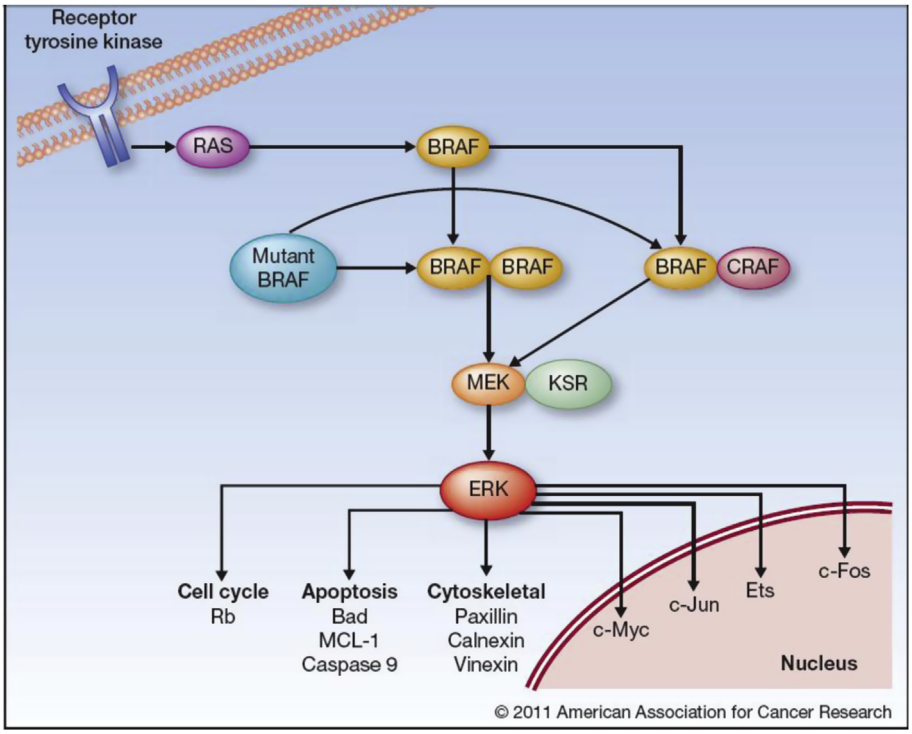

Fig. 1. The MAPK-signaling pathway. The MAPK-signaling pathway is typically initiated through activation of a receptor tyrosine kinase, which activates RAS, which, in turn, facilitates homo- or heterodimerization of wild-type BRAF. Activated BRAF phosphorylates MEK (which is bound to KSR), which phosphorylates ERK, resulting in multiple cellular effects such as proliferation and survival. Mutant BRAF can dimerize and activate MEK without Ras activation. Caronia et al. [2].

date, there are three known RAF isoforms (ARAF, BRAF, and CRAF or RAF-1). CRAF was discovered in 1985, ARAF was discovered in 1986, and BRAF was discovered in 1988. RAF proteins are encoded by the RAF proto-oncogenes, ARAF, BRAF and CRAF, which are located on chromosomes Xp11, 7q32, and 3p25, respectively [5].

RAF may be activated by the G protein Ras, by mutation in cancer cells [5–7] or by other Ras independent elements including the soluble non-RTK Src and Janus kinase 1, which are involved in cytokine signaling [8]. Other Ras-independent activators of RAF include interferon beta, protein kinase C (PKC) alpha, antiapoptotic proteins (e.g., Bcl-2), scaffolding proteins (e.g., ceramide-activated protein kinase), ultraviolet light, ionizing radiation, retinoids, erythropoietin, and dimerization between RAF isoforms [8–15].

Like all protein kinases, the RAF protein kinase domain has the characteristic small *N*-terminal lobe and large *C*-terminal lobe (Fig. 2a). The small *N*-terminal lobe has a predominantly antiparallel β-sheet structure and anchors and orients ATP. It contains a glycine-rich ATP-phosphate-binding loop, sometimes called the P-loop. While, the large *C*-terminal lobe is mainly α-helical. The large lobe binds MEK. The catalytic site lies in the cleft between the small and large lobes [3,7].

All RAF subtypes share highly conserved regions (CR): CR1, CR2, and CR3. CR1 is adjacent to the amino terminus. CR1 is composed of a RAS-binding domain (RBD) and a cysteine-rich domain (CRD), which can bind two zinc ions. CR1 interacts with RAS and with membrane phospholipids. CR2 is a serine/threonine rich domain. CR3 is adjacent to the carboxyl terminus and contains the kinase domain (Fig. 2b) [1,7,16,17]. GTP-bound RAS binds to RAF through its RAS-binding domain (RBD) in the amino terminal regulatory region [1].

BRAF and CRAF form homo- and heterodimers following RAS activation. BRAF–CRAF heterodimers are more active than either homodimer (Fig. 1) [18–20].

ARAF is overexpressed in urogenital tissues (e.g., kidney, ovary, prostate, and epididymis). BRAF is overexpressed in neural, testicular, splenic, and hematopoietic tissues. While, CRAF is expressed in most tissues [1].

"RAS/BRAF/MEK/ERK" pathway has been associated with human cancers due to the frequent oncogenic mutations identified in its members [21–25]. Thus, Ras mutations occur in about 15% of cancers. While, BRAF is mutated at high frequency in certain cancers such as melanoma (~66%), thyroid cancer (35–70%), colorectal cancer (5–20%), liver cancer (~14%) and ovarian cancer (~30%) [17,21–26].

Although more than 95 BRAF mutations have been identified, the most common mutation (90%) is a single base missense substitution (thymidine-to-adenine transversions at nucleotide 1799) which involves replacement of valine with glutamic acid at position 600 (V600E) in the activation loop. This mutation is found adjacent to serine 599, which is phosphorylated during activation of the BRAF. The polarity of glutamic acid in the V600E mutation mimics the polarity of serine phosphorylation in the BRAF activation loop. Therefore, this mutation precludes the need for phosphorylation and thus renders $BRAF^{V600E}$ constitutively active leading to activation of the MAPK signaling pathway, inducing uncontrolled cell proliferation, and facilitating malignant transformation. The V600E BRAF mutations show a 500-fold increase in catalytic activity compared to the wild type [17,21,27–32]. Besides, $BRAF^{V600E}$ contributes to neoangiogenesis *via* stimulating vascular endothelial growth factor secretion [33]. All these facts make BRAF an ideal target for antitumor therapeutic development.

Indeed, many small molecules containing diverse scaffolds were developed as RAF inhibitors. Of the synthesized molecules, the biarylurea derivative Sorafenib (Bay 43-9006, compound **1**), the triarylimidazole derivative SB-590885 (compound **2**), the pyrimidine derivative dabrafenib (GSK2118436, compound **3**), the

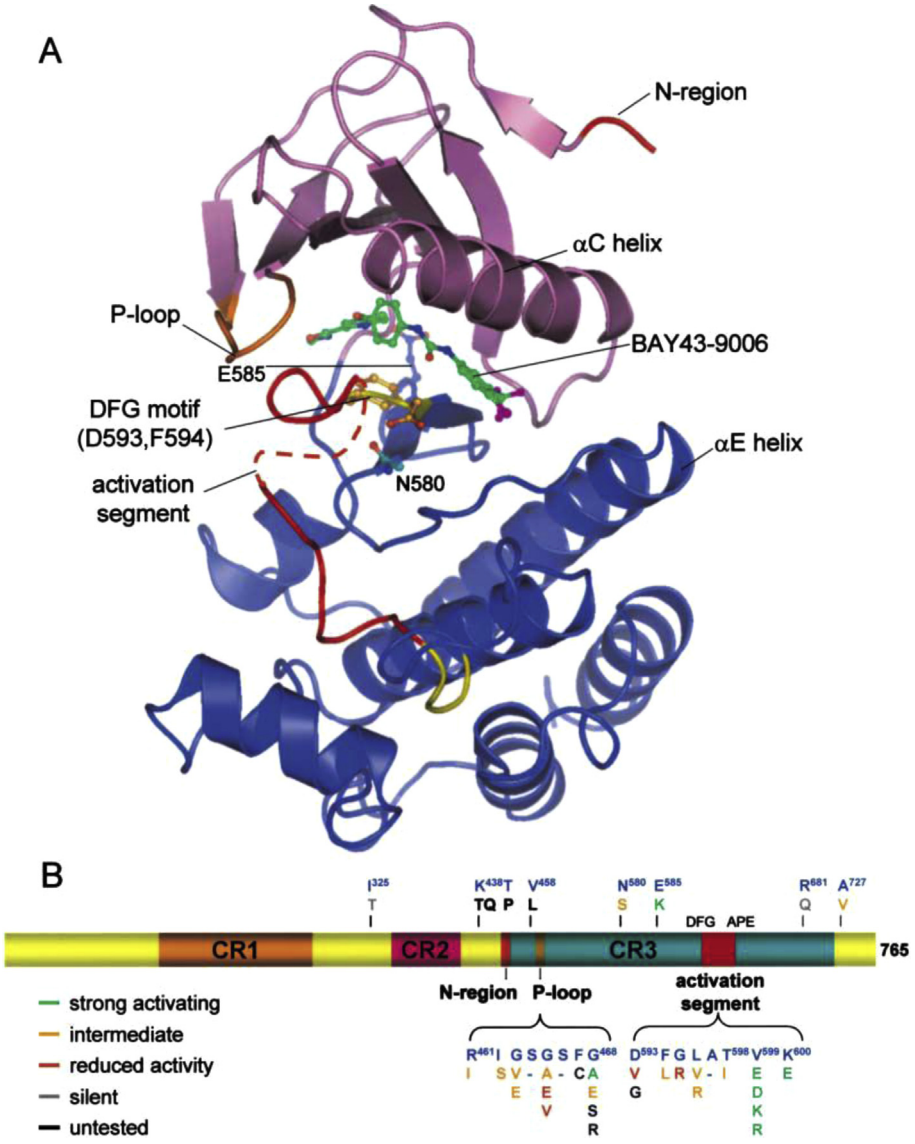

Fig. 2. (a) Ribbons diagram of $BRAF^{WT}$ kinase domain in complex with sorafenib. The positions of Asp593 and Phe594 of the DFG motif, Asn580 of the catalytic loop, and Glu585 are shown, DFG and APE motif in yellow, rest of activation segment and the N region are in red. N lobe is in magenta, C lobe in marine, and P loop in orange. Residues 600–611 of the activation loop are disordered (dashed lines). (b) Schematic of BRAF primary structure, showing functional domains and position of 32 observed cancer-associated mutants of BRAF. The amino acid substitutions are color coded according to their activity class. Wan et al. [17]. (For interpretation of the references to color in this figure legend, the reader is referred to the web version of this article.)

azaindole derivatives Vemurafenib (PLX4032, compound **4**) and PLX4720 (compound **5**) and the benzimidazole derivative (RAF265, compound **6**) have entered clinical or preclinical trials (Fig. 3).

Protein kinases can be classified as type I or type II based on whether they target the protein kinase enzyme in its active or inactive conformations, respectively. Type II inhibitors can be further classified as type IIA and type IIB based on the position of the DFG-motif or αC-helix [34–37]. Targeting the inactive conformation results in more selective kinase inhibitors compared to type I inhibitors [38–40].

X-ray crystal structures of BRAF bound with various inhibitors revealed that BRAF exists mainly as a dimer with a consistent interface. These structures also demonstrate that BRAF can adopt all three commonly observed ATP binding site conformations (active, DFG-out, and αC-helix out). All three classes of BRAF inhibitors can induce RAF dimerization and MAPK activation in $BRAF^{WT}$ cells with different abilities [34].

Type I inhibitors, such as SB-590885 (compound **2**) and PLX4720 (compound **5**), bind to a RAF active conformation featuring DFG-in and αC-helix-in configurations and a preserved ATP binding pocket, including the Lys483-Glu501 salt bridge (Fig. 4a) [41,42]. Type I BRAF inhibitors are potent activators of the MAPK pathway and can promote CRAF homodimerization as well as BRAF/CRAF heterodimerization [19,34]. This can result in serious side effects such as hyperplasia and inflammation accompanied by sustained levels of phosphorylated ERK observed in animal studies treated with type I inhibitors [34,43].

Type IIA inhibitors, such as Sorafenib (compound **1**), bind to the DFG-out, inactive conformation. There are common interactions necessary for high-affinity binding to the DFG-out allosteric pocket of BRAF kinases. The allosteric binding site is an inactive conformation of BRAF enzyme characterized by the movement of an Asp-Phe-Gly (DFG) loop. The allosteric binding site is made accessible by a rearrangement of the activation loop and subsequent movement

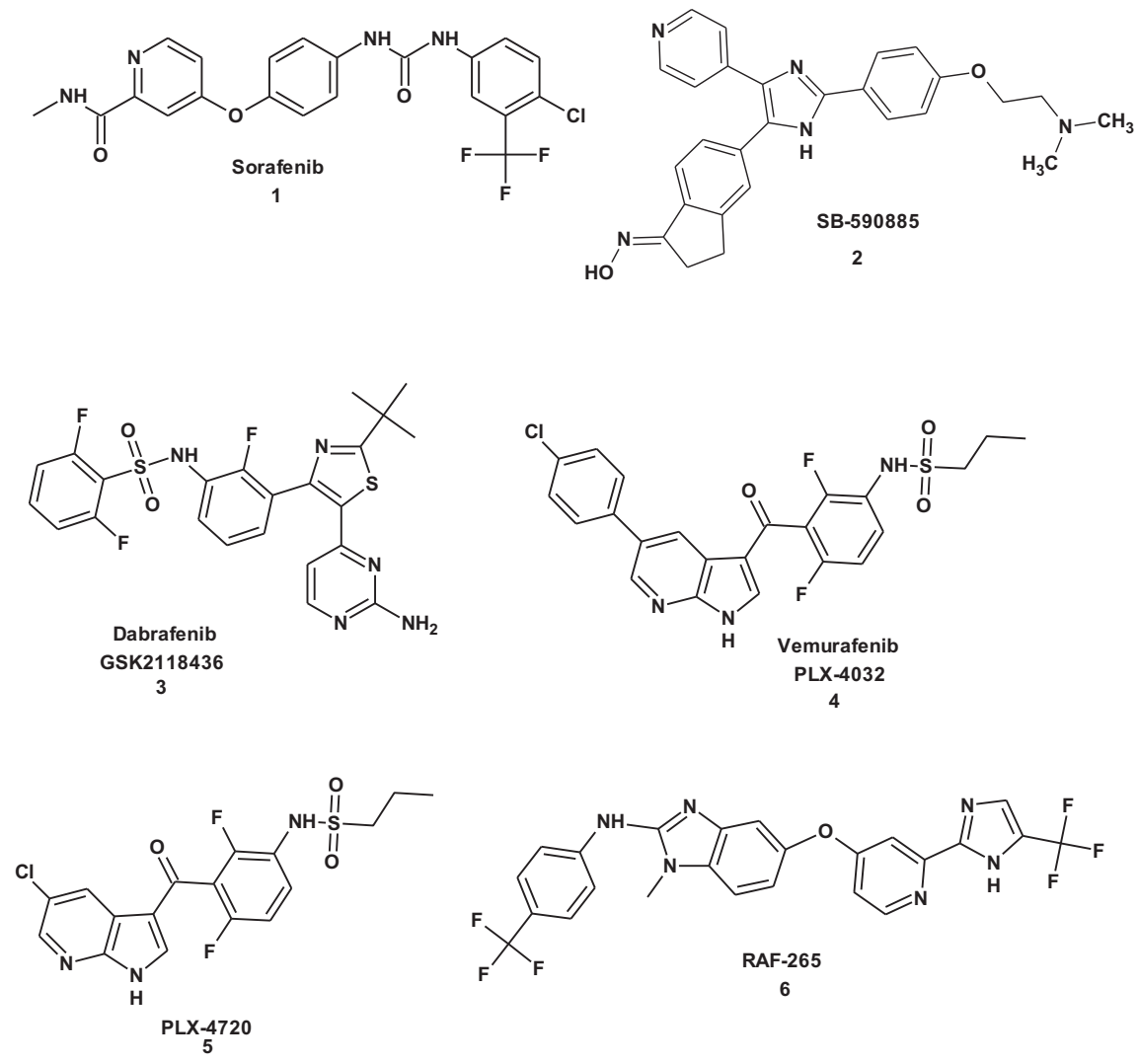

Fig. 3. Structures of known BRAF inhibitors.

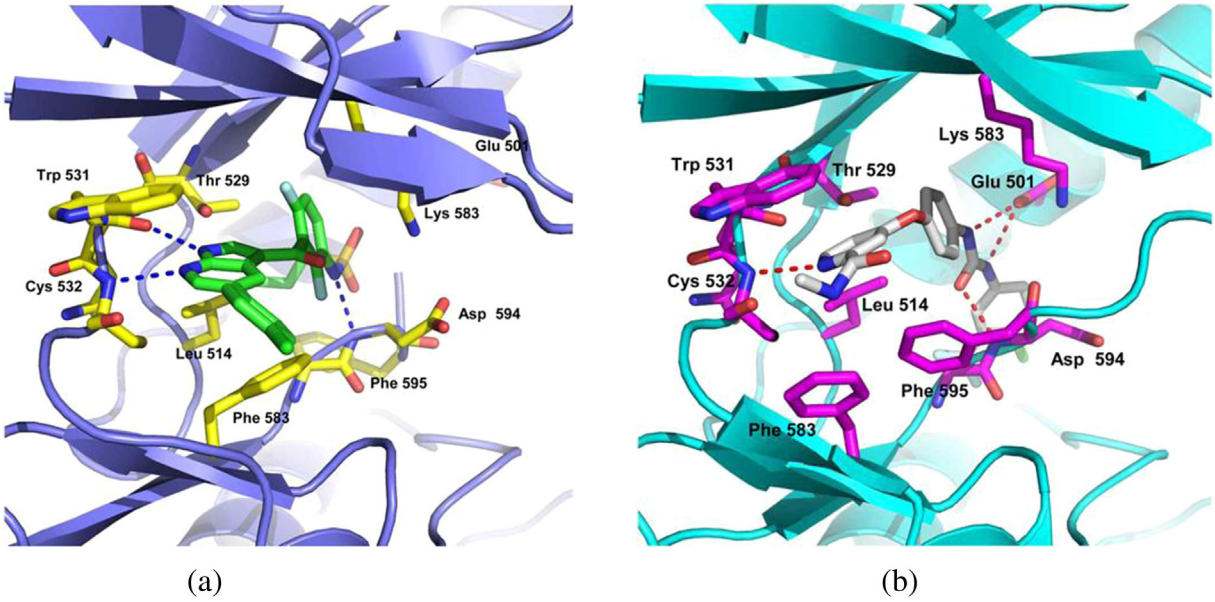

Fig. 4. (a) The co-crystal structure (PDB code: 3C4C) of PLX4720 bound to the kinase domain of $BRAF^{V600E}$. (b) The co-crystal structure (PDB code: 1UWH) of sorafenib bound to the kinase domain of $BRAF^{V600E}$. Kim and Sim [42].

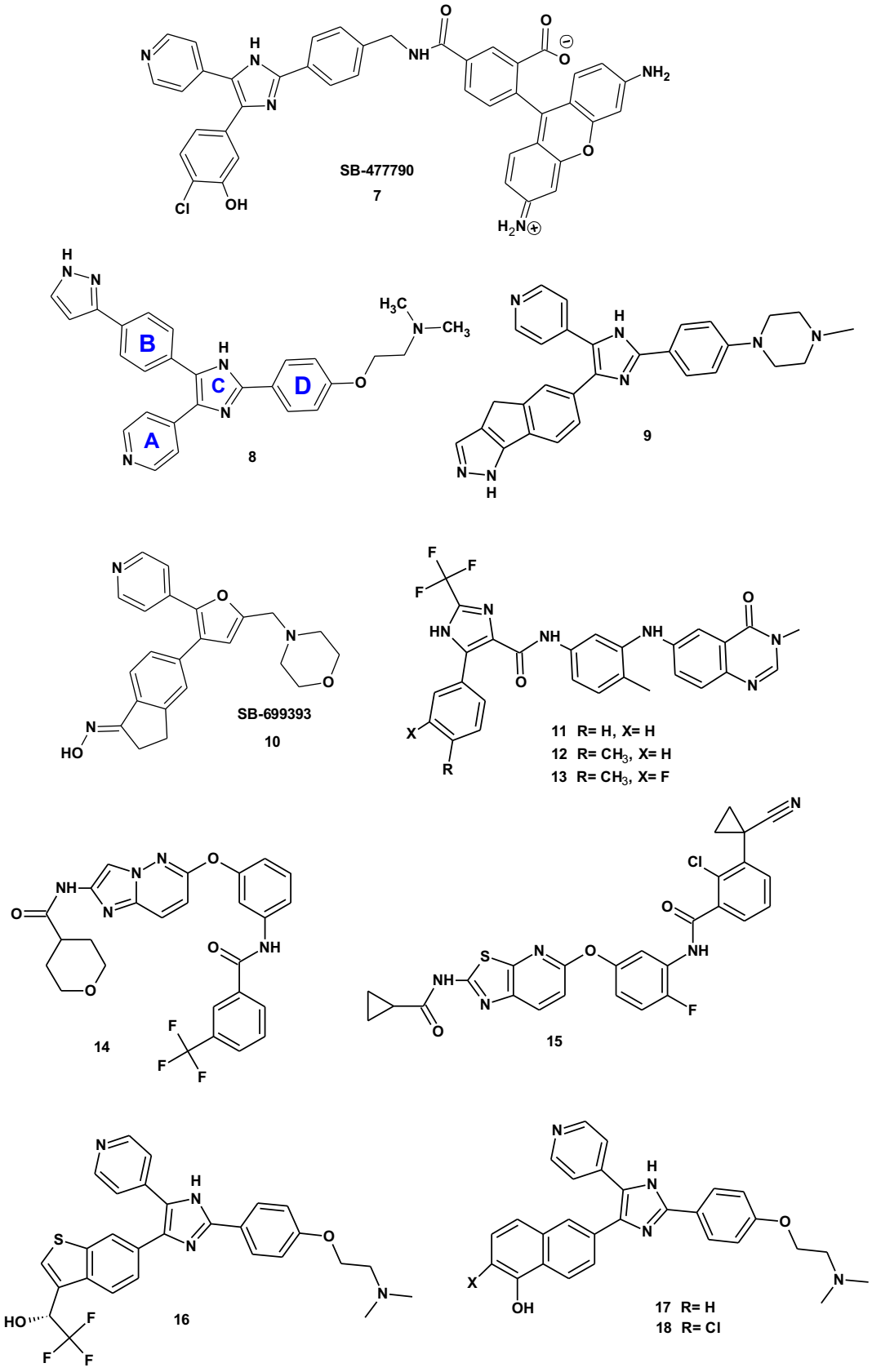

Fig. 5. Imidazoles and their analogs as BRAF inhibitors.

of a phenylalanine side chain out of a large hydrophobic pocket and into the ATP binding site. This movement results in a conformation that is mutually exclusive to ATP binding and also creates a large hydrophobic pocket to which the allosteric kinase inhibitors bind [34].

For inhibitors that bind to DFG-out inactive conformation, four key interactions are made with the enzyme. 1) H-bonding interactions with the hinge region where the adenine ring of ATP normally bound. Here, pyridyl ring of Sorafenib occupied the ATP adenine binding pocket and bound to Cys532 [44]. In fact, the formation of H-bond with the backbone group of Cys532 proved to be necessary for tight binding of the inhibitor in the ATP-binding site and is present in most BRAF inhibitors [45]. 2) H-bond interactions with conserved Glu side chain and the amide N–H from the Asp involved in the DFG loop move. In Sorafenib, urea moiety formed these two H-bonds. 3) Hydrophobic interactions in the allosteric binding region within two selectivity sites. The lower selectivity site which is created when the phenylalanine of the DFG loop flips out of its lipophilic pocket during the DFG loop move and this site is highly conserved among kinases. On contrary, the upper selectivity site is less conserved and afforded unique position to confer selectivity. Sorafenib used its trifluoromethyl phenyl group to bind to lower hydrophobic selectivity site. 4) Hydrophobic interactions in the gatekeeper region which is close to a conserved lysine side chain which is normally involved in triphosphate binding with ATP. As a result of the DFG loop movement, the phenylalanine side chain of this loop typically closes off the gatekeeper region forming a distinct hydrophobic binding site. This region was occupied by the middle phenyl ring in Sorafenib (Fig. 4b) [42,44]. The Lys-Glu salt bridge remains intact, a feature of all type IIA inhibitors. Results for type IIA inhibitors are less consistent among different chemotypes [34].

Type IIB inhibitors such as Vemurafenib (compound **4**) bind to a DFG-in, αC-helix-out, inactive BRAF conformation in which the highly conserved salt bridge between Lys483 and Glu501 is broken. The propyl group of vemurafenib occupied newly formed hydrophobic pocket between the αC-helix and the *N*-lobe β-sheets. Also, the difluorophenyl ring of Vemurafenib occupied a hydrophobic pocket adjacent to the gatekeeper residue, Thr529. Type IIB inhibitors are only weak inducer of RAF dimerization and do not readily promote the translocation of RAF kinases to the membrane, steps considered important in RAF activation. Therefore, type IIB inhibitors showed the lowest proliferative and favorable toxicity profile in $BRAF^{WT}$ cells in preclinical studies which allowed their progression into clinical trials [34,43].

It is noteworthy that type I kinase inhibitors can be converted to type II kinase inhibitors *via* the attachment of a lipophilic group at an appropriate position so that it fills the pocket created by the movement of DFG motif [38].

Sorafenib (Nexavar©) is the first RAF kinase inhibitor that has received clinical approval by the Food and Drug Administration (FDA) and European Medicine Agency (EMEA) for the treatment of advanced renal cell carcinoma (RCC) in 2005 and unresectable hepatocellular carcinoma (HCC) in 2007 and is still under multiple clinical trials for the treatment of other types of cancer. Its clinical activity is attributed to its antiangiogenic effects mediated through inhibition of the receptor tyrosine kinases VEGFR2 and PDGFR [1].

Being non selective, Sorafenib failed to show therapeutic activity in the treatment of malignant melanoma [46] probably due to its poor $BRAF^{V600E}$ cellular activity. Whilst, the selective $BRAF^{V600E}$ inhibitor Vemurafenib showed complete or partial tumor regression in the majority of patients harboring the $BRAF^{V600E}$ mutation with an overall increased median survival time after the treatment. Vemurafenib was approved from FDA in 2011 for the treatment of unresectable or metastatic melanoma with the $BRAF^{V600E}$ mutation [47,48]. Recently, it was reported that combination of RAF and MEK inhibitors can eliminate undesired proliferative effects in animal models [49–51]. Phase I/II clinical trial in patients treated with a combination of BRAF inhibitor and MEK inhibitor displayed no incidences of cutaneous squamous cell carcinoma while producing a high objective response rate [52].

The clinical actions of the most potent BRAF inhibitors were fully discussed in many previously published review articles [1,34,42,53–57].

In spite of the encouraging clinical efficiency of these inhibitors in cancer treatments, recent studies recorded the development of significant drug resistance to these inhibitors [34,48,58–65]. Besides, BRAF inhibitors can activate the RAF-MEK-ERK signaling pathway in cells containing wild type BRAF through RAF dimerization resulting in undesired proliferative effects [47,66]. These facts increase the need for the development of novel more potent and selective $BRAF^{V600E}$ inhibitors that may not suffer from these limitations.

This review highlights the progress in identification and development of potent, selective and specific inhibitors of BRAF especially during the last five years, from 2009 to 2013. Here in, BRAF inhibitors were classified according to their chemical classes and a brief summary of SAR studies done in each class was also introduced.

2. BRAF inhibitors classified by their chemical classes

2.1. Imidazole derivatives

The triarylimidazole derivative, SB-590885 (compound **2**, Fig. 3) was first reported in 2006 by Takle et al. from GlaxoSmithKline as a potent and extremely selective inhibitor of BRAF kinase (BRAF K_d 0.3 nM). SB-590885 was initially identified as neuroprotective agent that can be used in the treatment of stroke [67].

SAR study of the imidazole C-4 position demonstrated that the 3-hydroxyphenyl moiety was optimal for BRAF inhibitory activity. Various groups were tolerated at the imidazole C-2 position that could also affect the physicochemical properties of the resulting compounds. While, the C-5 substituent formed H-bond to the hinge region of the protein and 4-pyridyl group appeared to be optimal for BRAF inhibitory activity although the activity was also retained upon replacement of the C-5 pyridine ring with an alternative H-bond acceptor moieties such as pyrimidinyl- and pyridazinyl-derivatives. The inhibitory activity was completely abolished upon replacement of 4-pyridyl ring with phenyl or 3-pyridyl rings [67].

It was noteworthy that the fluorescent derivative **7** (SB-477790, Fig. 5) was also identified in that study. SB-477790 proved to be suitable for the development of a BRAF fluorescent ligand binding assay (FP) [67].

The general key features of the triarylimidazoles comprised a hinge-binding group, usually pyridine or pyrimidine (ring A), a substituted aromatic group interacting with the hydrophobic pocket adjacent to the gatekeeper residue (ring B), a central imidazole scaffold occupying the ribose position in the ATP-binding pocket (ring C) and a third aryl ring (ring D) extending outside the ATP pocket towards the solvent (Fig. 5) [68].

The incorporation of the H-bond donor pyrazole heterocycle substituent on 'ring B' was investigated and reported in 2010. Pyrazole ring was chosen to act as a potential functional bioisostere of indanone oxime in SB-590885 [68]. Accordingly, (dimethyl-[2-(4-{5-[4-(1*H*-pyrazol-3-yl)-phenyl]-4-pyridin-4-yl-1*H*-imidazol-2-yl}-phenoxy)-ethyl]-amine, (compound **8**) was identified as a lead compound. Indeed, it was found that compound **8** inhibited $BRAF^{V600E}$ at low micromolar concentration (BRAF IC_{50} 1.6 μM,

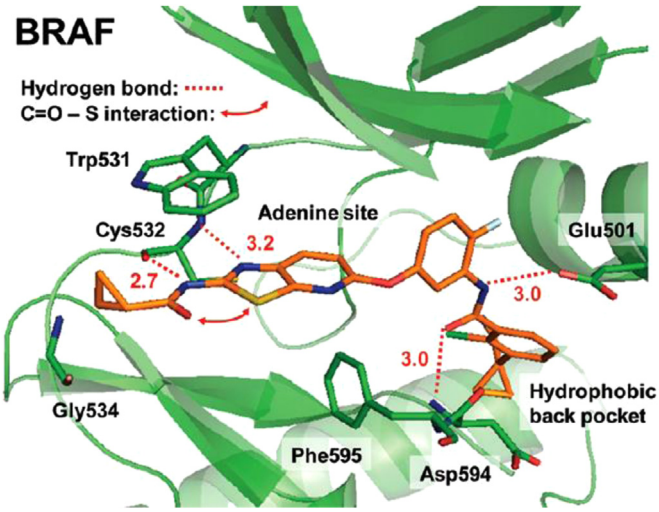

Fig. 6. Co-crystal structure of compound **15** with BRAF (PDB code: 4DBN, 3.1 Å resolution). Okaniwa et al. [72].

pERK IC_{50} 5.8 μM) and showed good antiproliferative activity against melanoma cell line [68]. Structure optimization of the lead compound **8** led to identification of 6-{2-[4-(4-methylpiperazin-1-yl)-phenyl]-5-pyridin-4-yl-3*H*-imidazol-4-yl}-2,4-dihydro-indeno [1,2-*c*]pyrazole (compound **9**) that inhibited BRAF in nanomolar concentration (BRAF IC_{50} 0.24 μM, pERK IC_{50} 0.58 μM). However, its cellular effect on mutant BRAF driven cell line was low [68].

SAR study of the compound **8** indicated that fixation of the pyrazole ring into the tricyclic (1,4-dihydroindeno[1,2-*c*]pyrazole) such as in compound **9** enhanced the inhibitory activity against BRAF five-folds compared to the non-cyclic pyrazole derivative. Besides, this tricyclic system mimiced the indanone oxime moiety in SB-590885. Methylation of the pyrazole NH abolished the enzyme activity consistent with the hypothesis that a H-donor group was beneficial for potent BRAF inhibition. Also, replacement of tricyclic pyrazole by tricyclic triazole or tricyclic pyridazinone analogs led to inactive compounds [68].

Replacement of the imidazole ring with furan-amides reduced BRAF inhibitory activity. However, their cellular activities were enhanced. Replacement of the 2-dimethylaminoethoxy side chain of ring D with *N*-methylpiperazine moiety afforded equipotent BRAF inhibitory activity with significant improvement in the cellular activity due to enhanced physicochemical properties [68].

In analogous study, furan-based derivative SB-699393 (compound **10**) showed potent and highly selective BRAF inhibitory activity (BRAF IC_{50} 7.2 nM) with enhanced CNS penetration. Replacement of imidazole ring with furan ring was done to increase the lipophilicity of the resulting inhibitor by reducing the number of H-bond donors and polar surface area. However, compound **10** did not show significant neuroprotective effects when evaluated in a rodent model of stroke [69].

In 2010, Dietrich and coworkers reported the development of 2,4,5-trisubstituted imidazole derivatives as potent and specific type II inhibitors of BRAF kinase [70]. Here, imidazole derivatives were designed as allosteric DFG-out BRAF inhibitors where a trisubstituted imidazole act as the central core scaffold, the carboxamide group at position 4 of the imidazole ring was expected to make critical H-bonding interactions with Glu501 and Asp594 and the substituents at the 2- and 5-positions of the imidazole ring were varied to optimize the hydrophobic interactions within the selectivity site. 6-(5-Amino-2-methylphenyl)amino-3-methyl-quinazolin-4(3*H*)-one (QUIN) was chosen as hinge region binding motif [70]. Furthermore, a trifluoromethyl group was introduced at position 2 of the imidazole ring to mimic its effect in Sorafenib [70].

Molecular modeling studies suggested that the imidazole core scaffold needed to twist within the selectivity site to relieve sterical clashes with the protein. However, this twisting decreased the lipophilic interactions within the selectivity sites and might result in poor enzyme inhibitory activity. Nevertheless, compounds **11** and **12** inhibited $BRAF^{V600E}$ with IC_{50} of 21 nM and 28 nM,

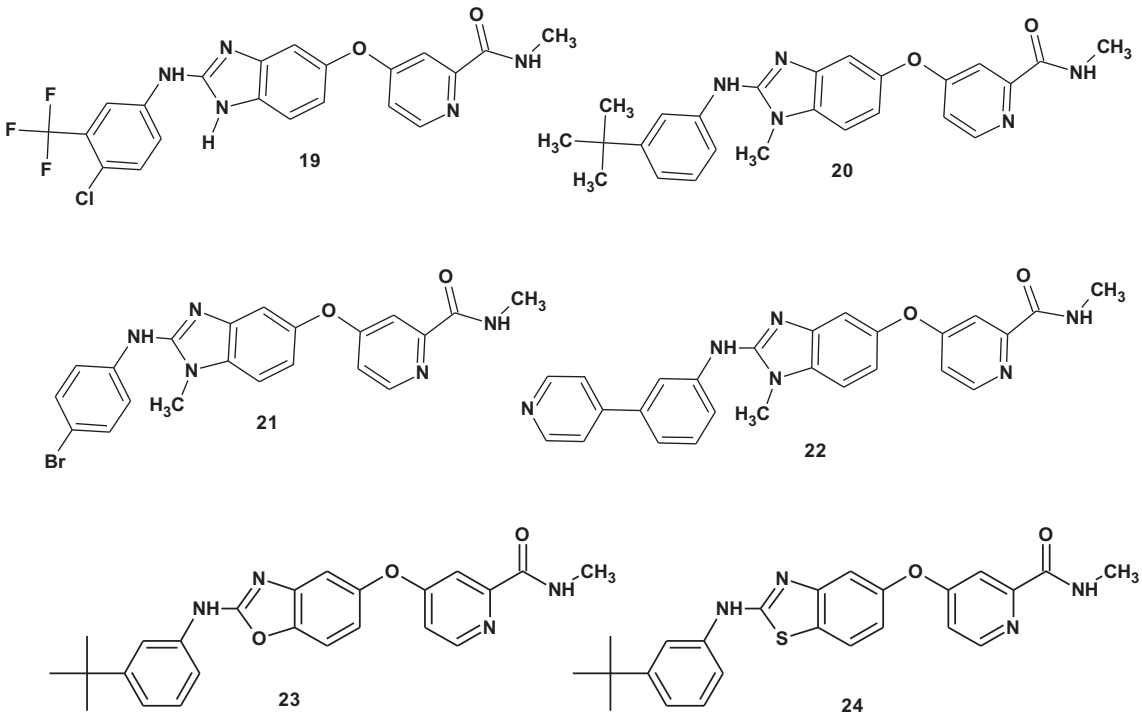

Fig. 7. Benzimidazoles and their analogs as BRAF inhibitors.

respectively which was not consistent with the molecular modeling studies. Compared to Sorafenib, compound **12** was 4-folds more potent against $BRAF^{V600E}$ and 84-fold more selective over p38α [70].

Structure modification of compounds **11** and **12** were made through substitution on the phenyl ring located at position 5 of the imidazole ring or by direct substitution at position 2 of the imidazole ring. Groups at these two positions were thought to bind at the upper and lower selectivity sites of BRAF, respectively [70].

The results indicated that introduction of *para* fluorine atom on the phenyl substituent greatly enhanced the inhibitory activity against both $BRAF^{V600E}$ and p38α. While *meta* substitution with groups larger than fluorine such as methyl, methoxy or trifluoromethyl was not well tolerated. This finding suggested the existence of a large and very hydrophobic upper selectivity pocket. Besides, introduction of *para* methyl group on the phenyl ring increased the selectivity for $BRAF^{V600E}$ over p38α [70]. Compound **13** bearing *meta* fluorine and *para* methyl groups on the phenyl ring retained subnanomolar inhibitory activity against $BRAF^{V600E}$ (IC_{50} 0.3 nM) and meanwhile disfavored p38α inhibition (IC_{50} 100.2 nM) [70]. On the other hand, replacement of trifluoromethyl group at position 2 of the imidazole ring by the larger *t*-butyl or phenyl groups enhanced the potency for p38α and decreased the potency for $BRAF^{V600E}$ [70].

The imidazo[1,2-*b*]pyridazine derivative **14** was identified in 2008 as a hit compound by kinase screening. Compound **14** showed significant inhibitory activities against BRAF and VEGFR2, with IC_{50} values of 43 nM and 3.1 nM, respectively. Compound **14** bound to the inactive DFG-out conformation of BRAF and VEGFR2. However, Western blotting assay for assessing pMEK in HT-29 colon cancer cells indicated that its cellular activity based on $BRAF^{V600E}$ inhibition was insufficient (IC_{50} 3800 nM) [71].

SAR study of compound **14** pointed out that replacement of the pyranyl group with a methyl group increased $BRAF^{V600E}$ inhibitory activity significantly ($BRAF^{V600E}$ IC_{50} 4.1 nM). Larger alkyl groups such as ethyl or isopropyl groups decreased $BRAF^{V600E}$ inhibitory activities ($BRAF^{V600E}$ IC_{50} 6.9 and 31 nM, respectively). Bulky lipophilic groups might stabilize the DFG-out binding conformation and increase cellular activity [72].

Structure modification of compound **14** was done by replacing imidazopyridazine ring by various [5,6]-fused bicyclic rings such as benzimidazole, 1,3-benzothiazole, imidazo[1,2-*a*]pyridazine, imidazo[4,5-*b*]pyridine, [1,3]thiazolo[5,4-*b*]pyridine and imidazo[1,2-*a*]pyridine [72]. The results suggested that the presence of nitrogen atom adjacent to the phenoxy group enhanced $BRAF^{V600E}$ inhibitory activities. Thus, imidazo[1,2-*a*]pyridazine, imidazo[4,5-*b*]pyridine and [1,3]thiazolo[5,4-*b*]pyridine analogs were more active than imidazo[1,2-*a*]pyridine, benzimidazole and 1,3-benzothiazole, respectively [72].

This structure modification led to discovery of [1,3]thiazolo[5,4-*b*]pyridine derivative **15** as potent inhibitor of both BRAF and VEGFR2 with significantly improved metabolic stability against human liver microsomes and good PK profiles in mice. Compound **15** was formulated as solid dispersion formulation (spray-dried SD formulation) in order to maximize its oral absorption in rats and the formulation showed significant suppression of ERK1/2 phosphorylation in an A375 melanoma xenograft model in rats. Compound **15** also showed *in vivo* antitumor activity in rats. These results suggested that dual inhibition of $BRAF^{V600E}$ and VEGFR2 might provide strong antitumor efficacy [72]. BRAF cocrystal structure of compound **15** (PDB code 4DBN) revealed that the compound occupied the ATP-binding site and stabilized the inactive DFG-out conformation of BRAF (Fig. 6) [72].

2,4,5-Trisubstituted imidazoles substituted at position 4 (ring B) with naphthyl or benzothiophene groups were reported in 2013 as potent BRAF inhibitors. For example, *R* 1-(6-{2-[4-(2-dimethylamino-ethoxy)phenyl]-5-(pyridin-4-yl)-1*H*-imidazol-4-yl}benzo[*b*]thiophen-3-yl)-2,2,2-trifluoroethanol (**16**) exhibited BRAF inhibitory activity with IC_{50} 190 nM and with cellular GI_{50} 2100 nM. While, 6-{2-[4-(2-dimethylamino-ethoxy)-phenyl]-5-(pyridin-4-yl)-3*H*-imidazol-4-yl}-naphthalen-1-ol (**17**) displayed BRAF inhibitory activity with IC_{50} 9 nM and GI_{50} 220 nM [73]. Furthermore, chloro analogs of compound **17** (compounds **18**) which was more acidic than naphthol **17** displayed lower kinase inhibition (4-fold decrease) with parallel decrease in cellular activity [73].

These derivatives were developed in an attempt to enhance the activity of imidazole derivative **9**. The structure modification also focused on exploring the effect of the nature of ring B on the enzyme inhibitory activity. Three rings were examined, namely, benzofuran, benzothiophene and naphthyl substituted with H-bond donors [73]. In these compounds, the imidazole ring was kept constant, the 2-substituent was (2-(disubstituted amino)ethoxy) phenyl, which was used as a solubilizing group, and the 5-substituent was 4-pyridyl group, which was used as hinge-binder [73].

The benzofurans and benzothiophenes were selected due to their structural similarity to the indane scaffold of the indanone oximes, the key group responsible for the activity of SB-590885 (compound **2**). While, naphthyls substituted with H-bond donors such as oximes, phenols or pyrazoles were previously reported to enhance the activity against BRAF. Therefore, they were selected for investigation [67,69].

The results indicated that benzothiophenes with more acidic H-bond donors such as trifluoroethanol (compound **16**) was highly active (BRAF IC_{50} 0.33 μM for racemic mixture and 0.19 μM for R-enantiomer). This result indicated the beneficial effect of presence of relatively acidic hydroxyl group on ring B for potent BRAF inhibition [73].

In addition, the more lipophilic naphthyl group substituted with H-bond donors (like hydroxyl group) in a rigid framework (naphthols **17** and **18**) were also highly active BRAF inhibitors [73]. Besides, the position of the hydroxyl group on the naphthyl ring affected the inhibitory activity of the resulting inhibitor (1-naphthols were more potent than 2-naphthols) [73].

2.2. Benzimidazole derivatives

Arylaminobenzimidazoles were first identified as RAF kinase inhibitors in 2008. They were developed during structural optimization of the urea derivative Sorafenib (compound **1**). Although, Sorafenib **1** was potent CRAF and BRAF inhibitor (IC_{50} 0.001 μM for both) and entered clinical trial, it suffered from its poor physicochemical properties and the lack of downstream modulation on the MAP kinase axis on cells [74].

Structure improvement of Sorafenib **1** was achieved by eliminating the urea moiety and closing the urea onto ring to give arylaminobenzimidazoles **19** (Fig. 7) which was less potent than Sorafenib **1** but still potently inhibited C and mutant B isoforms of RAF (CRAF IC_{50} 0.076 μM and $BRAF^{V600E}$ IC_{50} 0.28 μM) [74].

Substituted aniline moiety was essential for potent RAF inhibition. Substitution at the *meta* and *para* positions of the aniline phenyl ring especially with lipophilic substituents led to higher enzyme activity than substitution at the *ortho* position. *para* Bromine substituent showed 200-fold enhancement in the enzyme activity while trifluoromethyl group exhibited 770-fold improvement in the activity relative to the unsubstituted analog [74]. Among the tested compounds, the 3-*tert*-butylanilino derivative **20** exhibited the most impressive antiproliferative activity (SKMEL-28 EC_{50} 0.89 μM) and inhibitory activity on Erk phosphorylation (pERK

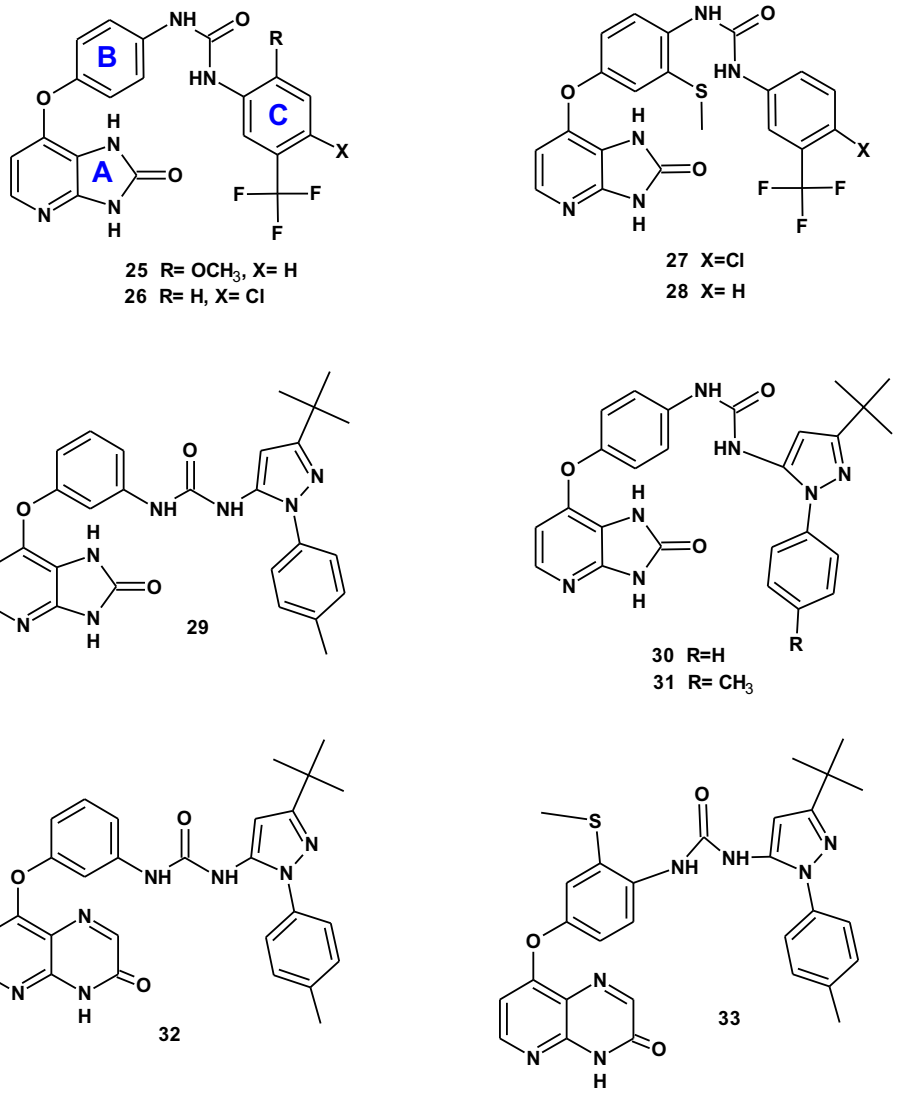

Fig. 8. Imidazopyridines and pyridopyrazines as BRAF inhibitors.

EC_{50} 0.28 μM). Compound **20** inhibited both $BRAF^{V600E}$ and CRAF with IC_{50} 0.045 μM and 0.004 μM, respectively [74].

N-Methylation of benzimidazole ring as in compounds **21** and **22** improved the activity against both isoforms of RAF compared to the Sorafenib **1**, ($BRAF^{V600E}$ IC_{50} 0.002 μM and 0.014 μM, respectively) and (CRAF IC_{50} 0.001 μM and 0.010 μM, respectively) [74].

The introduction of lipophilic groups on the aniline ring enhanced the enzymatic potency, but resulted in limited solubility. Therefore, the pyridyl end of the molecule was substituted with water soluble groups in order to modify the physicochemical properties [74]. While the solubility of Sorafenib **1** was <0.005 μg/mL at pH 7, that of compound **21** was 4.9 μg/mL at pH 7. Incorporation of a solubilizing group on the amide moiety like the 2-morpholinoethyl group resulted in further improvement in the solubility (7.3 μg/mL at pH 7 and 29 μg/mL at pH 5.5) [74].

Regarding the PK parameters of **21** and **22**, compound **21** exhibited low clearance, low volume of distribution, long half-life, and almost complete oral bioavailability. Compound **22**, on the other hand, exhibited a higher clearance, slightly higher volume of distribution, and shorter half-life than **21** but also had almost complete oral bioavailability [74]. Compound **22** demonstrated significant *in vivo* antitumor activity against HT29 human colorectal tumor xenograft model [74]. It is noteworthy that further work on this scaffold led to identification of RAF-265 (compound **6**) with improved enzymatic and cellular activities.

Structure optimization of 3-*t*-butylanilinobenzimidazole amide **20** led to identification of benzoxazole amide and benzothiazole amide derivatives **23** and **24**, respectively, as potent BRAF kinase inhibitors ($BRAF^{V600E}$ IC_{50} 0.006 μM and 0.004 μM, respectively) [75].

SAR study of these analogs pointed out that the *meta tert*-butylanilino moiety in benzoxazoles and benzothiazoles was essential for *in vitro* potency and inhibition of ERK phosphorylation. The *ortho* substituents on the aniline group showed inferior activity to the *meta* or *para* substituents. Compounds substituted at the *meta* position potently inhibited both CRAF and mutant-BRAF [75].

While both benzoxazole and benzothiazole series yielded extremely potent RAF inhibitors, neither series inhibited phosphorylation of ERK and thus their cellular potencies were inferior to that of benzimidazole derivatives [75].

2.3. Imidazopyridine derivatives

Type II BRAF inhibitors based on 1*H*-imidazo[4,5-*b*]pyridin-2(3*H*)-one as a hinge-binding scaffold were first reported by Niculescu-Duvaz and coworkers in 2009 [76]. SAR study of the

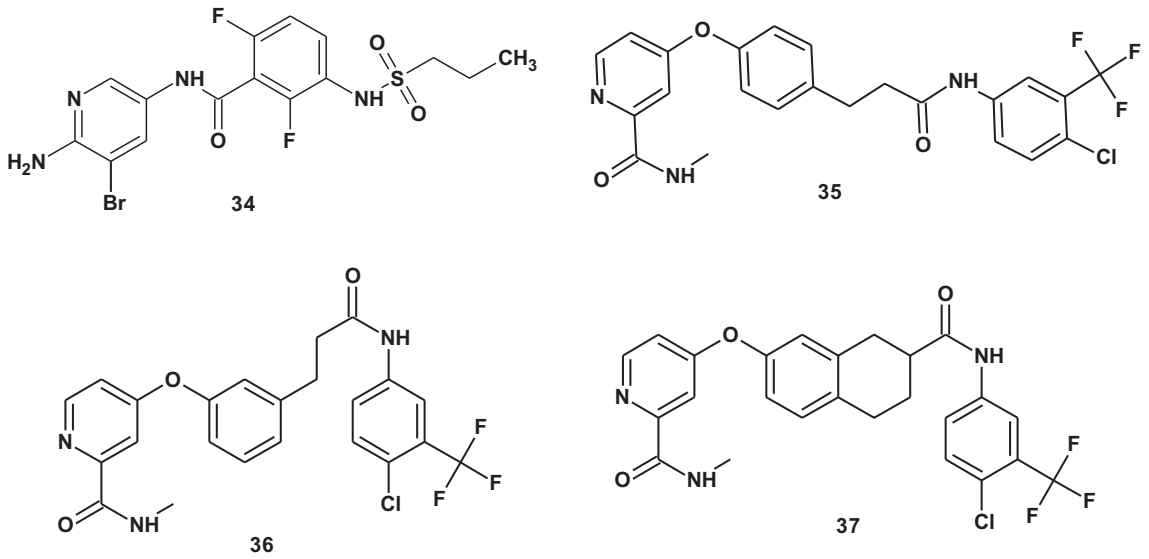

Fig. 9. Pyridines as BRAF inhibitors.

synthesized imidazopyridin-2-ones indicated that mono or dimethylation at the *N*1 or *N*3 position of the imidazolone ring was tolerated and resulted in lower metabolism and better PK profile. While, substitution with the two bulkier ethyl groups at both *N*1 and *N*3 positions of the imidazolone ring decreased the activity by 10-folds [76].

SAR study also revealed that replacement of the oxygen linker with sulfur linker had no effect on the BRAF inhibition, but enhanced cell growth inhibition. This might be attributed to the increase in lipophilicity and hence cell membrane permeability in case of sulfur linker. Regarding the phenyl group on urea linker, *meta* substitution of this phenyl group with lipophilic groups like *tert*-butyl and trifluoromethyl groups enhanced the BRAF inhibitory activity while their removal or transfer to the *para* position abolished the enzyme activity. Further enhancement in the cellular activity could be achieved by a second substituent like halogen or methoxy on the phenyl ring [76]. On the other hand, replacement of the urea moiety with thiourea, an amide or sulfonamide moiety decreased the enzyme activity [76].

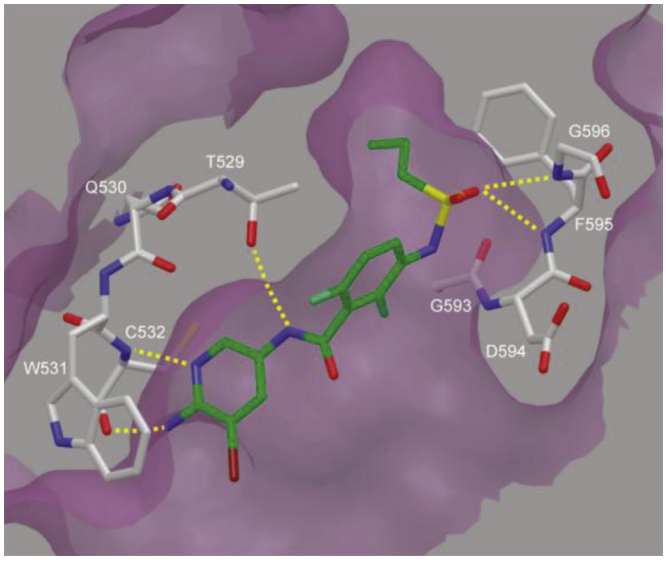

Fig. 10. X-ray crystal structure of compound **34** in complex with $BRAF^{WT}$. The cleft surface is rendered in violet, select residues are depicted in white, and the inhibitor is green. Hydrogen-bonding interactions are illustrated with yellow dashed lines. The DFG sequence (D594-G596) resides in its active (DFG-in) conformation. Wenglowsky et al. [83]. (For interpretation of the references to color in this figure legend, the reader is referred to the web version of this article.)

Among the compounds synthesized, compounds **25** and **26** (Fig. 8) showed BRAF IC_{50} 12 nM and 23 nM, respectively, with low micromolar cellular potency against WM266.4 cell line (SRB IC_{50} 4.2 μM for both compounds) [76].

These inhibitors were designed as type II inhibitors that targeted the inactive conformation of $BRAF^{V600E}$. In these compound, the 1*H*-imidazo[4,5-*b*]pyridine-2(3*H*)-one (ring A, Fig. 8) acted as the hinge binding moiety and a number of substituted phenyl (ring C) interacted with the allosteric binding site created by the displacement of the DFG loop. Besides, various groups were introduced on the central phenyl (ring B) to control the potency of the compounds as $BRAF^{V600E}$ inhibitors. Ring B occupied the lipophilic DFG-out pocket [77].

Meta substitution of ring B afforded more potent inhibitors than *ortho* substitution. Hydrophobic groups enhanced the cellular activity and provided submicromolar compounds in pERK and SRB assays. It was found that substitution of the central phenyl ring (ring B) with 3-fluoro, 3-thiomethyl group or complete replacement by naphthyl group enhanced the enzyme activity (IC_{50} of these compounds were below 1 nM) and the antiproliferative activity [77].

An examination of cocrystal structure of BRAF bound to Sorafenib revealed a space in the lipophilic pocket adjacent to the adenine binding site formed in the DFG-out conformation. This space could accommodate the substitutions on ring B resulting in higher selectivity for BRAF [77].

Compounds **27** and **28**, each substituted with a thiomethyl group, notably achieved a $BRAF^{V600E}$ IC_{50} of 1 nM. Moreover, this 3-thiomethyl substitution, as for the naphthyl group, increased the potency on melanoma cells greatly with GI_{50} in the nanomolar range [77].

A new series of selective type II BRAF inhibitors in which ring B connected to rings A and C in a *meta*-substitution pattern was described in 2010. This series which was discovered using docking studies afforded more selective BRAF inhibitors in comparison with the *para* series [78].

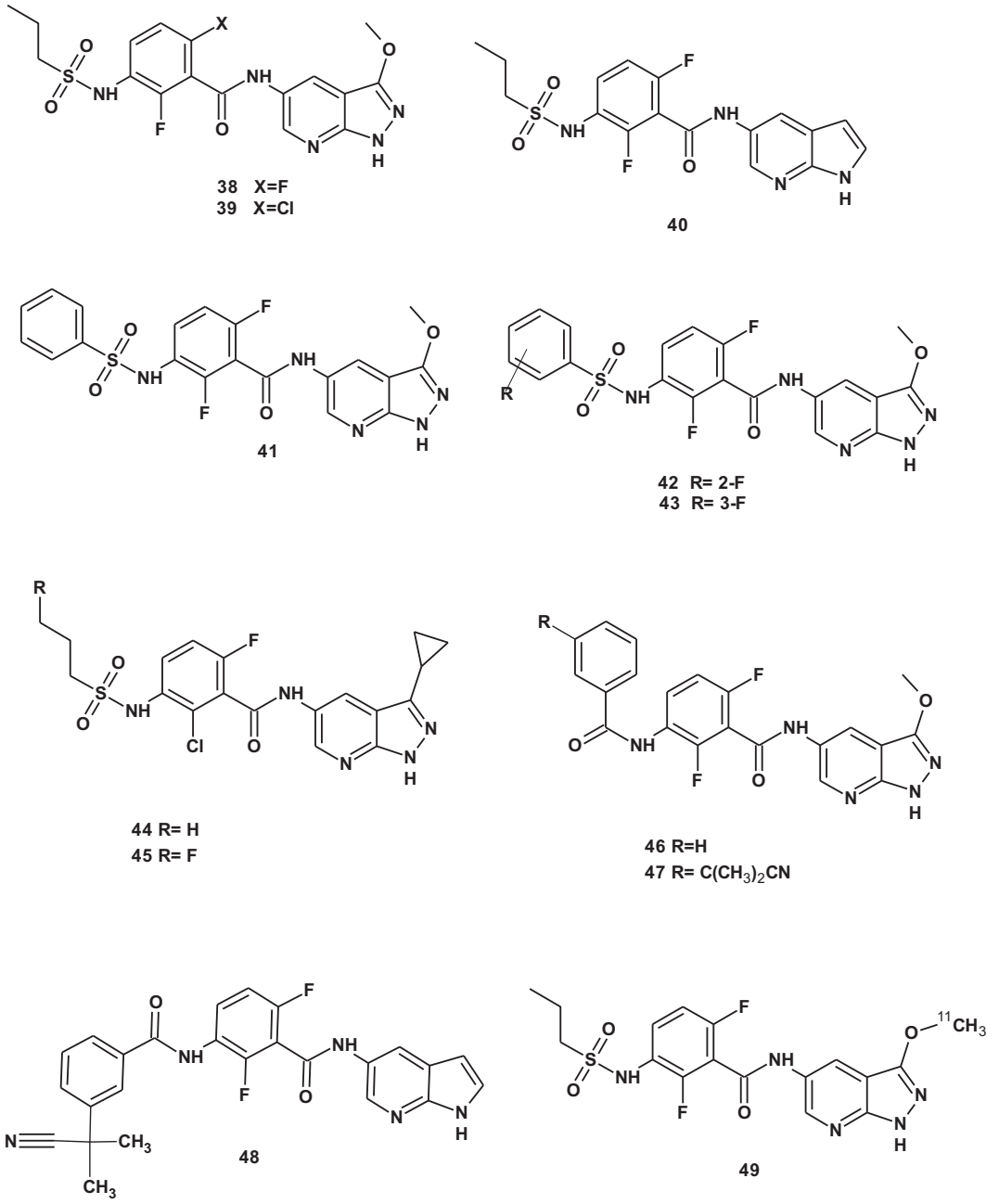

Fig. 11. Pyrrolopyridines and pyrazolopyridines as BRAF inhibitors.

The *meta* substituted ring B series allowed a wider range of linkers compared to its *para* counterpart. Thus, amides, sulfonamides, and urea linkers were proved to be active in the *meta* substituted series, while in the *para*-substituted series only the urea group was tolerated. However, the selectivity of the *meta* compounds was further enhanced when the urea linker was replaced by an amide [78].

Replacement of phenyl ring (ring C) with different aromatic heterocycles improved the cellular potencies of the resulting inhibitors. Thus, substituted pyrazoles, particularly 3-*tert*-butyl-1-aryl-1*H*-pyrazoles, increased the cellular potencies significantly [78]. Compound **29** represented one of the most effective compounds discovered in that study with BRAF IC_{50} of 128 nM, however, its cellular potency was relatively weak (pERK IC_{50} of 830 nM and SRB GI_{50} of 705 nM) [78].

Introduction of heteroaromatic ring C was done in order to improve the cellular activity of *para* substituted ring B series. Here, ring C was mainly 1,3-disubstituted-1*H*-pyrazole core linked at 5-position to ring B *via* a urea linker [79]. SAR study of these derivatives indicated that methylation at the *N*-1 position of the pyridoimidazolone ring enhanced the activity whilst methylation at *N*-3 position had a detrimental effect on the BRAF inhibitory activity probably due to removal of NH H-bonding interaction with the hinge region. As reported before, the introduction of thiomethylphenyl, fluorophenyl or naphthyl as ring B enhanced the enzyme and cellular activities [79]. Besides, substitution of the oxygen linker with a sulfur linker slightly decreased the enzyme activity but improved the cellular activity by a factor of ~10 on pERK and ~30 in the SRB assay, due to the higher lipophilicity of the resultant compounds. As a result, compounds **30** and **31** were

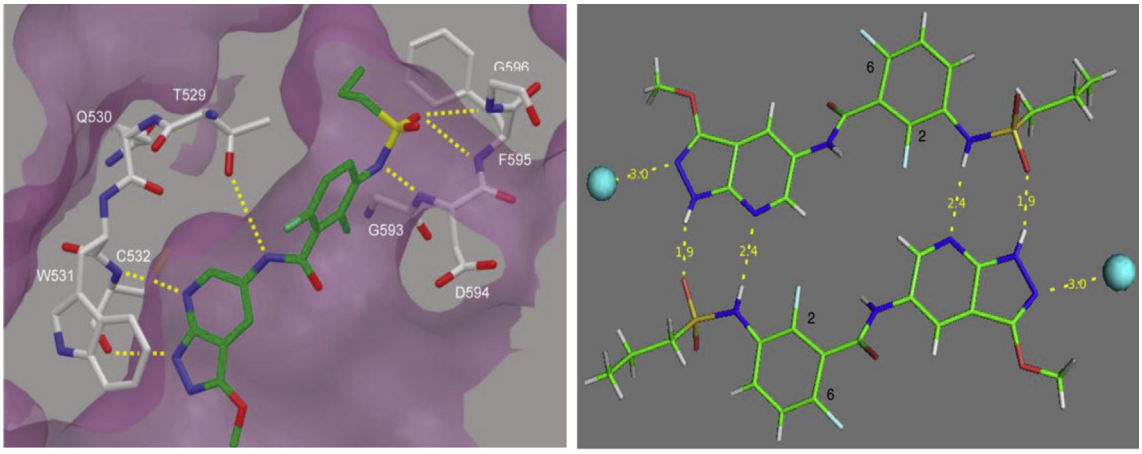

Fig. 12. (a) X-ray crystal structure of compound **38** in complex with $BRAF^{WT}$. The cleft surface is rendered in violet, selected residues are depicted in white, and the inhibitor is green. Hydrogen-bonding interactions are illustrated with yellow dashed lines. The propyl group resides in a pocket that is enlarged by an outward shift of the αC-helix. The DFG sequence (D594-G596) resides in its active (DFG-in) conformation. The sulfonamide NH of compound **38** is in close contact to the main chain NH of Asp594, indicating that the sulfonamide is deprotonated. Wenglowsky et al. [83]. (b) X-ray crystal structure of compound **38**. Water molecules are represented as blue spheres. Carbon atoms are rendered in green, hydrogen in white, nitrogen in blue, oxygen in red, fluorine in light blue and sulfur in yellow. H-bond interactions are illustrated with yellow dashed lines and H-bond distances are given in Angstroms. Wenglowsky et al. [85]. (For interpretation of the references to color in this figure legend, the reader is referred to the web version of this article.)

discovered with BRAF IC_{50} of 94 nM and 142 nM, pERK IC_{50} of 620 nM and 420 nM and SRB GI_{50} of 390 nM and 300 nM, respectively [79].

Molecular modeling study combining QM-polarized ligand docking, molecular dynamics, free energy calculation, and 3D-QSAR study of the compounds described in the after mentioned research articles was published in 2011 [80]. The aim of the study was to understand the binding mode between the inhibitors and $BRAF^{V600E}$ enzyme and demonstrate the structural requirements for the inhibitory activity. The study revealed that van der Waals interaction represented the main driving force for the interaction between the inhibitors and $BRAF^{V600E}$. Besides, the H-bond interactions between the inhibitors and Glu501 and Asp594 stabilized the DFG-out conformation [80].

2.4. Pyridopyrazine derivatives

Further structure optimization of the type II BRAF inhibitors 2,3-dihydroimidazo[4,5-*b*]pyridin-2-ones led to the identification of pyridopyrazine analogs that carried novel hinge binding group [81].

Examining the docking poses of imidazo[4,5-*b*]pyridin-2-ones pointed out that changing the hinge binder groups could allow the H-bond donor of the bicyclic ring to form a more favorable interaction with the enzyme and thus enhancing the inhibitory potency towards BRAF. In addition, the terminal carbonyl group of the imidazolone group pointed out toward the solvent, and thus it could be used to improve the solubility and pharmacokinetics properties of the series [77,80].

Fusion of pyridine ring with a range of five- and six-membered rings bearing H-bond donor and acceptor groups was investigated and reported in 2010. Docking studies revealed that the best fitting was obtained with pyrido[2,3-*b*]pyrazin-3(4*H*)-one ring since the extension of the second ring of the bicyclic system to a six-membered cycle moved the lactam moiety closer to the carbonyl group of Cys532, while maintaining the H-bond between the pyridine ring and the amide moiety of Cys532. On the other hand, the pyrido[2,3-*b*]pyrazin-3(4*H*)-one ring contained only one H-bond donor and thus was expected to improve the pharmacokinetic properties and cell permeability of the resulting inhibitor relative to the pyridoimidazolone ring which included two H-bond donors [81].

Replacement of pyridoimidazole with pyridopyrazin-3(4*H*)-one afforded more potent compounds in terms of both enzymatic and cellular activities. Notably, the presence of an amino group at the 2 position of the pyrazinone ring led to a slight decrease in enzymatic activity. In addition, introduction of water-soluble groups on the pyridopyrazine at the 2 position decreased the enzyme activity probably due to removal of a H-bond donor from the hinge binder. On contrary, the presence of a lipophilic methyl group in the same position led to a 2-fold improvement in cellular activity [81]. Besides, pyridopyrazin-2(1*H*)-one derivatives were generally less active than their pyridopyrazin-3(4*H*)-one counterparts in both the enzymatic and cellular assays [81].

As observed for the pyridoimidazolones [79], the introduction of 3-*tert*-butyl-1-phenyl-1*H*-pyrazole or a 3-*tert*-butyl-1-*p*-tolyl-1*H*-pyrazole group significantly enhanced the potency in the cell-based pERK and the SRB cell proliferation assays [81].

Regarding the effect of ring B on the enzyme and cellular potency, it was found that the potency increased in the order of phenyl < naphthyl < 3-F-phenyl < 3-MeS-phenyl [81]. This effect was similar to that observed for pyridoimidazolone derivatives [77,79]. Also, connecting ring B to the allosteric pocket binder in a *meta* substitution pattern afforded BRAF inhibitors with nanomolar level of inhibition in enzymatic and cellular assays [81].

Compound **32** (Fig. 8), with a tolylpyrazole ring C, (BRAF IC_{50} 0.087 μM, pERK IC_{50} 0.274 μM and SRB GI_{50} 0.019 μM) showed an improved oral bioavailability compared with its phenylpyrazole analog [81].

Notably, compound **33** [1-(3-*tert*-butyl-1-*p*-tolyl-1*H*-pyrazol-5-yl)-3-(2-(methylthio)-4-(3-oxo-3,4-dihydropyrido[2,3-*b*]pyrazin-8-yloxy)phenyl)urea] showed high oral bioavailability along with a long half-life, representing an improvement in PK properties compared to the imidazopyridine inhibitors previously reported [79]. This, combined with the potency of the compound (BRAF IC_{50} 0.019 μM, pERK IC_{50} 0.005 μM and SRB GI_{50} 0.001 μM) suggested potential effect suitable for therapeutic efficacy *in vivo* in human tumor xenograft models [81].

Indeed, clinical studies of compound **33** (CCT239065) was reported in 2010. The results indicated that compound **33** inhibited

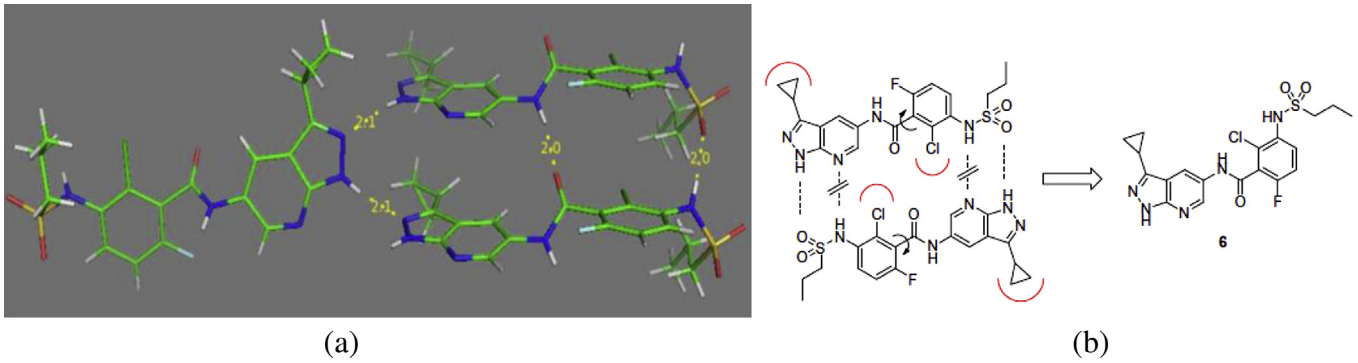

Fig. 13. (a) X-ray crystal structure of compound **44**. Carbon atoms are rendered in green, hydrogen in white, nitrogen in blue, oxygen in red, fluorine in light blue and sulfur in yellow. H-bond interactions are illustrated with yellow dashed lines and H-bond distances are given in Angstroms. (b) Conformation change of compound **44** due to the incorporation of sterically demanding substituents. Wenglowsky et al. [85]. (For interpretation of the references to color in this figure legend, the reader is referred to the web version of this article.)

signaling downstream of $BRAF^{V600E}$ in cancer cells, blocked DNA synthesis, and inhibited proliferation. Compound **33** was also more selective for mutated BRAF cancer cell lines compared with wild-type BRAF cell lines. The inhibitor was well tolerated in mice and exhibited excellent oral bioavailability (F = 71%). Molecular modeling study suggested that compound **33** bound to BRAF inactive conformation and thus act as type II inhibitor [82].

2.5. Pyridine derivatives

Structure optimization of Vemurafenib (PLX4032, compound **4**) resulted in the discovery of aminopyridine derivative **34** (Fig. 9) as potent BRAF inhibitor but its cellular activity remained insufficient for *in vivo* efficacy (BRAF IC_{50} 110 nM and pERK IC_{50} 310 nM) [83]. Here, the 6-aminopyridine ring act as H-bond donor and acceptor, which was postulated to bind to the −NH and carbonyl of hinge residue Cys532. The presence of 5-bromine atom enhanced the enzymatic and cellular activity by 8-folds probably due to its lipophilic interactions with the enzyme which was apparant from X-ray crystal structure of compound **34** with BRAF (Fig. 10) [83].

This X-ray picture revealed two characteristic conformational features of the amide series; a near co-planar arrangement of the amide group with the hinge-binding scaffold and a near 90° torsion angle of the amide relative to the 2,6-dihalo substituted central phenyl ring. This resulted in a near orthogonal spatial arrangement between the propyl sulfonamide bearing phenyl ring and the hinge-binding pyridine ring, and allowed them to interact optimally with residues in the ATP pocket. The amide linker lacked the required chemical and metabolic stability. Indeed, potentially toxic aniline metabolites generated from *in vivo* cleavage of the amide bond were observed [83].

On the other hand, structure optimization of Sorafenib (compound **1**) by replacement of the urea moiety with propionamide moiety afforded the pyridine derivative **35**. This modification was done to explore the importance of the two H-bonds formed by urea moiety in Sorafenib on the enzyme affinity. Interestingly, the enzyme tolerated the increase in chain length and the loss of one of the H-bond donor groups of the urea ($BRAF^{V600E}$ IC_{50} 61 nM). The *meta* substituted analog **36** was slightly more potent ($BRAF^{V600E}$ IC_{50} 47 nM) than its *para* analog **35**, however, cellular activities of both compounds were very high (pERK IC_{50} > 25,000 nM). Constraint of the flexible central core of compound **36** by cyclization into tetralin ring (compound **37**) improved the cellular activity while maintained the enzyme potency ($BRAF^{V600E}$ IC_{50} 32 nM, pERK IC_{50} 2900 nM) [84].

2.6. Pyrrolopyridine and pyrazolopyridine derivatives

In an attempt to improve the *in vivo* efficacy of the aminopyridine derivative **34**, pyridine core was replaced by bicyclic cores like imidazopyridine, pyrrolopyridine, and pyrazolopyridine. These bicyclic cores were designed to form a bidentate H-bonding interaction at the hinge region [83].

The imidazopyridine derivatives showed good enzymatic activity superior to that of aminopyridines but with poor cellular activity. The pyrrolopyridine derivatives displayed similar enzymatic activity to imidazopyridines with better cellular activity. Whilst, the pyrazolopyridine derivatives provided the most potent and orally bioavailable $BRAF^{V600E}$ inhibitors in that study [83].

Varying the substituent at position 3 of the pyrazolopyridine ring system resulted in improvements in both the enzymatic and cellular activities and meanwhile modulating their pharmacokinetic and physicochemical properties. 3-Methoxy group was found to be optimal for both enzymatic and cellular activities and afforded more potent inhibitors than 3-alkyl, 3-halo or 3-amino group. The substitution of chloro atom by fluoro atom at position 6 of the benzamide ring provided significant effects on pharmacokinetic and physicochemical properties. Thus, compounds **38** and **39** (Fig. 11) were discovered as the most potent and selective inhibitors in the amide series ($BRAF^{V600E}$ IC_{50} 4.8 and 1.7 nM, respectively) (pERK IC_{50} 19 and 20 nM, respectively). Both compounds had similar potency to PLX4032 on the A375 cell line but were 3-fold more potent on Malme-3M cell line. Compounds **38** and **39** also exhibited favorable ADME and pharmacokinetic profiles and demonstrated potent antitumor activity in the Colo205 mouse xenograft model. However, their aqueous solubility was low (<10 μg/mL at pH 6.5 and 7.4) [83].

X-ray crystal structure of compound **38** in complex with BRAF revealed that the kinase adopted the DFG-in conformation and that the pyrazole portion of the bicycle made π-stacking interaction with the side chain indole of Trp531 which might account for the improvement in potency over the pyridine amides. Besides, the propyl sulfonamide tail occupied the small lipophilic pocket formed by an outward shift of the αC-helix and this might account for the selectivity of these inhibitors towards $BRAF^{V600E}$ (Fig. 12a) [83]. The X-ray crystal structure of compound **38** also revealed a head-to-tail dimer formation in the crystal lattice (Fig. 12b) [85]. Thus, four intermolecular H-bonds between the pyrazolopyridine hinge binding template and the propyl sulfonamide tail contributed to the dimer formation resulting in high melting point (mp = 229 °C) and high crystal lattice energy [83]. Consequently, compound **38** required formulation as amorphous dispersion and

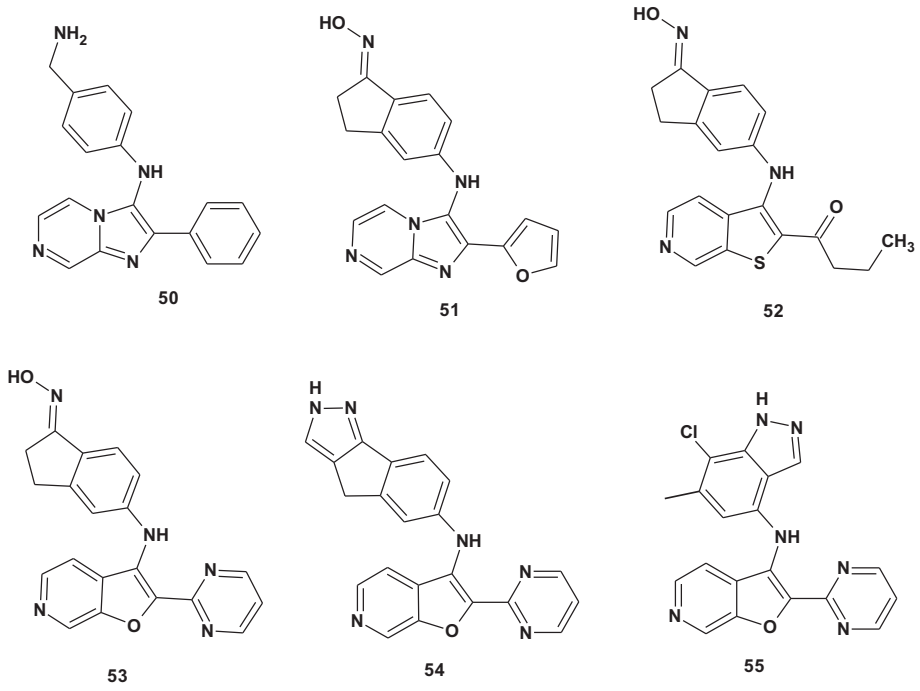

Fig. 14. Furopyridines and their analogs as BRAF inhibitors.

achieved less than 25% bioavailability at efficacious doses in mice [86].

Pyrrolopyridine derivative **40** was also identified in that study as $BRAF^{V600E}$ inhibitor ($BRAF^{V600E}$ IC_{50} 38 and pERK IC_{50} 94 nM), although it was less potent than pyrazolopyridine derivatives **38** and **39** [83].

Molecular modeling studies done on compounds **38** and **40** indicated that the dihaloaryl ring occupied the hydrophobic pocket adjacent to the gatekeeper residue Thr529 and thus further substitution could be done at positions 2, 5 and 6 of the ring. Indeed, different groups were introduced at these positions including halogen, alkyl and alkoxy groups. The results showed that chloro and fluoro substituents were well-tolerated in positions 2- and 6- of the phenyl ring with the 2,6-difluoro substituent as the optimal combination for cellular activity across both pyrazolopyridine and pyrrolopyridine series [87]. On the other hand, introduction of fluorine atom at position 5 of the phenyl ring resulted in a 2–5-fold loss in cellular activity, while other substituents like Me, MeO and CF_3 were not well tolerated. In all the tested compounds, 3-methoxypyrazolopyridine derivatives showed higher activity in both enzymatic and cellular assays than pyrrolopyridine ones [87].

Introduction of different substituents at position 3 of the pyrrolopyridine core was done in an attempt to mimic the interactions of 3-methoxypyrazolopyridines [88]. The results showed that small, lipophilic substituents at this position improved the potency of the pyrrolopyridine series. Whilst, groups larger than methyl abolished the cellular activity. Nevertheless, attempts to prepare 3-methoxypyrrolopyridine failed probably due to insufficient chemical stability [87].

Although X-ray crystal structure of compound **38** suggested that the lipophilic pocket occupied by the propyl group would not likely accommodate an aromatic ring, phenyl sulfonamide derivative **41** was equipotent to compound **38** (BRAF IC_{50} 1.6 and pERK IC_{50} 17 nM). Besides, *ortho* and *meta* fluorine groups on phenyl sulfonamide moiety were well tolerated (compounds **42** and **43**), while *para* fluoro resulted in a significant loss of potency [87]. Compounds **42** and **43** inhibited BRAF with IC_{50} of 1.8 and 0.7 nM, respectively, and showed potent cellular activity (pERK IC_{50} 9.1 and 12 nM, respectively) [87].

Attempts to disrupt the crystal packing of compound **38** were reported by Wenglowsky et al. in 2012. The attempts were based on replacement of 3-methoxy group with the small and more branched cyclopropyl ring (out of plane substituent) and incorporation of chlorine atom in place of the fluorine atom at position 2 of the central phenyl ring. This resulted in compounds **44** and **45** (BRAF IC_{50} of 3.8 and 0.6 nM, respectively). The study showed that both changes were required to decrease the crystal lattice energy resulting in a substantial reduction in melting point (mp = 164 and 154 °C, respectively). The X-ray structure of compound **44** revealed no head-to-tail dimer formation which led to fewer π-stacking interactions than seen in compound **38** (Fig. 13). Besides, significant improvement in the aqueous solubility of these two compounds was noticed [85].

Structure modification of compound **38** was reported in 2012 aiming to synthesize type II kinase inhibitors. This structure modification focused mainly on the propyl sulfonamide moiety. Thus, replacement of the sulfonamide with an amide moiety, and the propyl with phenyl group, led to benzamide derivative **46** (BRAF IC_{50} 39 nM, pERK IC_{50} > 12,000 nM) [89]. The benzamide derivative **46** was predicted to form the required H-bonds with Glu501 and Asp594, while the phenyl ring would occupy the hydrophobic back pocket [89]. SAR of the central ring suggested that removal of the fluoro substituent adjacent to the amide carbonyl group improved the enzymatic activity, while removal of both fluoro substituents resulted in a 7-fold loss in the cellular activity [89].

The 3-(2-cyanopropan-2-yl) group was previously reported as an optimized substituent in related type II BRAF inhibitors [90]. Incorporation of this group led to compound **47** with a significant improvement in cellular activity over compound **46** (BRAF IC_{50} 2.3 nM, pERK IC_{50} 180 nM). Compound **47** was considered as a new lead compound with only 10-fold less potency than sulfonamides **38** and **39** [89].

Similar to the previously reported results, the pyrrolopyridine **48** was less potent than its analogous 3-methoxypyrazolopyridine **47** in both the enzymatic and cellular assays (BRAF IC_{50} 6.8 nM, pERK IC_{50} 440 nM). Here also, elimination of the substituents at position 3 of the pyrazolopyridine core decreased the enzyme and

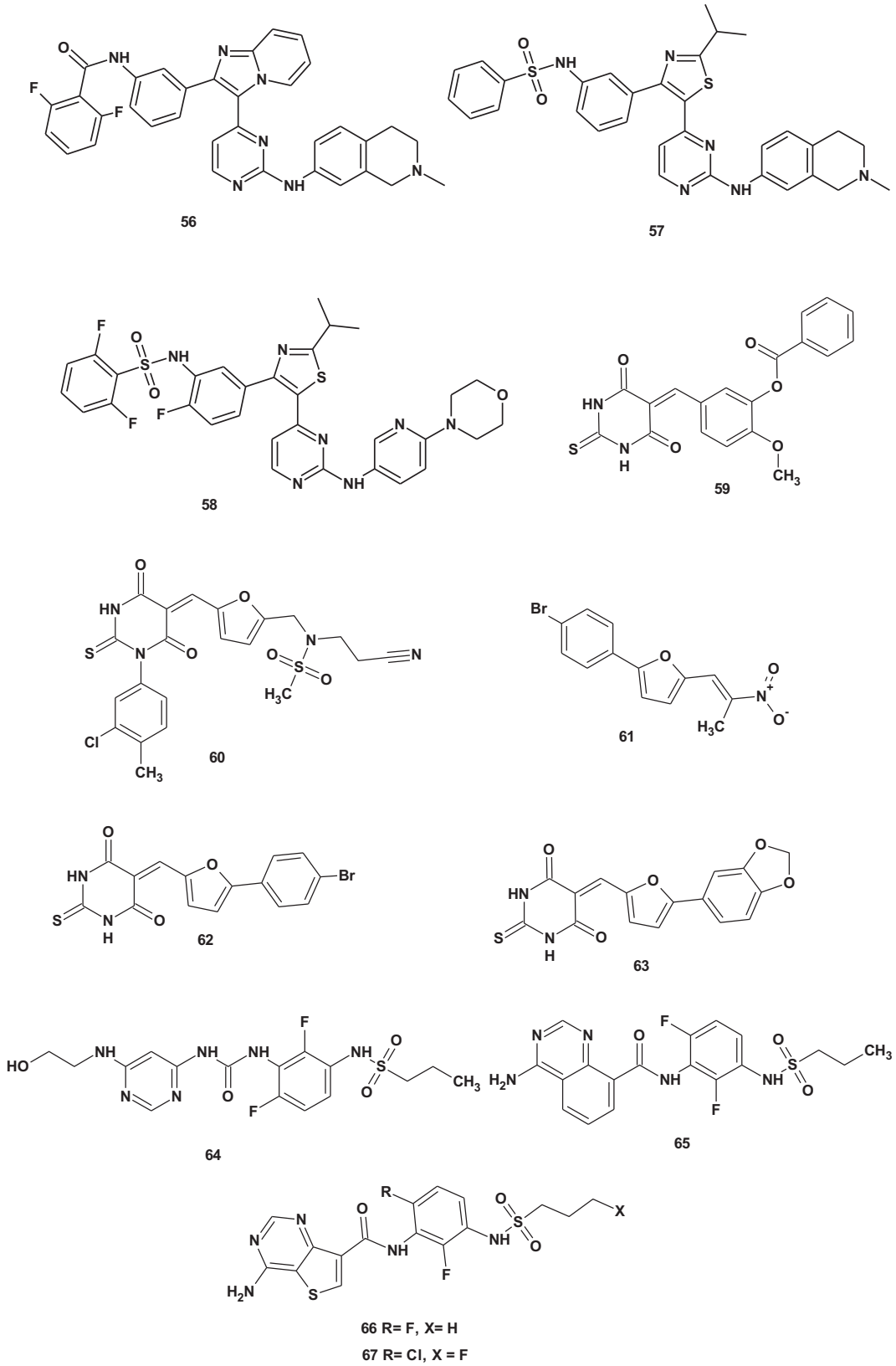

Fig. 15. Pyrimidines as BRAF inhibitors.

cellular activity [89]. Thus, 3-alkoxypyrazolopyridine proved to be the superior hinge-binding group for potency against $BRAF^{V600E}$ across two series of compounds that inhibited this kinase by two distinct binding modes.

Since $BRAF^{V600E}$ is an attractive target for molecular imaging of cancer, the search for specific and selective cancer $BRAF^{V600E}$ imaging agent to detect cancers and guide chemotherapy becomes essential. Therefore, [2,6-difluoro-*N*-(3-[^{11}C]methoxy-1*H*-pyrazolo

[3,4-*b*]pyridine-5-yl)-3-(propylsulfonamidio)benzamide], compound **49**, was prepared as a new specific and selective potential imaging agent for positron emission tomography (PET) to image $BRAF^{V600E}$ in cancers [91].

2.7. Furopyridine and thienopyridine derivatives

Buckmelter et al. described the identification of imidazo[1,2-*a*] pyrazine **50** (Fig. 14) as inhibitor of mutant BRAF (BRAF IC_{50} 1400 nM) *via* initial virtual and high-throughput screening. The authors pointed out that introduction of the indane–oxime moiety provided a boost in the enzyme inhibitory activity and pERK inhibition, for example compound **51** showed BRAF IC_{50} 4 nM and pERK IC_{50} 1400 nM [92].

Further structure optimization led to identification of the analogous thieno[2,3-*c*]pyridine derivatives. These derivatives showed only slight improvements in both enzyme and cellular potencies. Compound **52** displayed BRAF $IC_{50} < 2$ nM and pERK IC_{50} 140 nM [92]. This improvement was attributed by the authors to that thienopyridines made an additional hydrophobic interaction with Ile463 of the P-loop of BRAF enzyme [92]. However, thienopyridine ring system suffered from its propensity to inhibit multiple CYP P450s at sub-micromolar concentrations [93]. Therefore changing the thienopyridine into its analogous furopyridine was done. Indeed, this caused a dramatic change in the both enzyme and cellular potencies with better P450 profile [92].

SAR study of the effect of substituents at position 2 in furopyridine on the enzyme potency indicated that substitution with secondary amides was superior to tertiary amides. Besides, heteroaryl substituents showed better results than aryl ones. Accordingly, the 2-pyrimidinyl-furopyridine derivative **53** was identified as the most potent and selective BRAF inhibitor in that study (BRAF IC_{50} 0.2 nM and pERK IC_{50} 5 nM) [92].

In spite of the remarkable *in vitro* potency of furopyridine derivatives, they displayed very high clearance rate and hence insufficient plasma exposure in rats for *in vivo* efficacy. This might be attributed to oxime metabolism [92].

In order to improve the inhibitor pharmacokinetic profile, the indanone–oxime head-group was replaced by different groups including naphthol, phenol and hydroxyamidine [94]. Unfortunately, all the after mentioned groups demonstrated poor pharmacokinetic exposure in mice in spite of their enzyme and cellular potencies [94].

Nevertheless, introduction of the more metabolically stable groups such as the tricyclic pyrazole (compound **54**) and the indazole (compound **55**) provided potent BRAF inhibitors with good pharmacokinetic profiles in mice [94]. Besides it was found that substitution of the furopyridine ring at position 2 with 2-pyrimidinyl ring enhanced the enzyme and cellular activity in all the tested series [94].

2.8. Pyrimidine derivatives

In 2011, researchers from GlaxoSmithKline reported the development of pyrimidine derivatives as novel potent and selective BRAF kinase inhibitors. The identified compounds showed excellent activity in cellular assays as well as good oral bioavailability in rats. The key structural features of the developed compounds were an arylsulfonamide headgroup, a thiazole core, and fluorine atom *ortho* to the sulfonamide nitrogen [95].

These pyrimidine derivatives were developed *via* structure optimization of compound **56** (Fig. 15) which was identified from GlaxoSmithKline oncology directed kinase programs as BRAF inhibitor. Compound **56** possessed an imidazopyridine core and a large hydrophobic benzamide headgroup [95].

Although compound **56** displayed good activity in the $BRAF^{V600E}$ enzyme assay ($BRAF^{V600E}$ IC_{50} 9 nM), it had little activity in both cellular (pERK $EC_{50} > 10{,}000$ nM) and anti-proliferative cell based assays using the $BRAF^{V600E}$ mutant SKMEL28 cell line (EC_{50} 5316 nM) [95]. Structural optimization of compound **56** was achieved by replacing the imidazopyridine core with thiazole core and replacing the benzamide headgroup with arylsulfonamide headgroup. These modifications led to compound **57** with comparable $BRAF^{V600E}$ enzyme inhibition ($BRAF^{V600E}$ IC_{50} 12 nM) and striking improvement in both cellular (pERK EC_{50} 52 nM) and anti-proliferative activity against SKMEL28 cell line (EC_{50} 287 nM) [95].

Further structure modifications of compound **57** led to identification of compound **58** which exhibited excellent enzymatic activity ($BRAF^{V600E}$ IC_{50} 3.8 nM), cellular activity (pERK EC_{50} 23 nM) and *in vitro* cytotoxic activity against mutant BRAF cell line SKMEL28 (EC_{50} 47 nM). In compound **58**, the introduction of 2,6-difluorinated atoms at the headgroup enhanced the BRAF inhibitory activity and marginally improved the metabolic stability of the compound. The good oral bioavailability in rats observed for compound **58** as well as its metabolic stability might be attributed also to the presence of 6-fluorine atom next to the sulfonamide nitrogen [95].

However, pyrimidine derivative **58** suffered from very high clearance and poor bioavailability in nonrodent species. Besides, metabolite identification studies conducted in dog and monkey liver microsomes identified several major metabolites clustered in the tail and core regions of the molecule. Therefore, it was postulated that drug exposure after an oral dose in the higher species was limited by rapid compound metabolism [96].

Structure optimization of compound **58** was done by fluorination of the phenyl thiazole ring, replacing the isopropyl group with a *tert*-butyl group, and utilizing the unsubstituted aminopyrimidine tail group. These modification afforded dabrafenib (GSK2118436, compound **3**) as a highly selective inhibitor of RAF kinases with potent *in vitro* activity in oncogenic BRAF driven melanoma and colorectal carcinoma cells (BRAF IC_{50} 0.7 nM, pERK IC_{50} 4 nM, SKMEL28 IC_{50} 3 nM, A375P F11 IC_{50} 8 nM, Colo205 IC_{50} 7 nM). On the other hand, dabrafenib showed minimal effect *in vitro* on cells with wild-type BRAF (HFF $IC_{50} = 3.0$ μM) and on tumor cells not harboring the activating $BRAF^{V600E}$ mutation. Additionally, acceptable rat and dramatically improved dog pharmacokinetic profiles were observed [96].

Dabrafenib displayed potent *in vivo* antitumor and pharmacodynamic activity in mouse models of $BRAF^{V600E}$ human melanoma. Accordingly, dabrafenib was identified as a development candidate, and early clinical results demonstrated significant activity in patients with BRAF mutant melanoma. Dabrafenib is currently in phase III clinical development for the treatment of activating BRAF mutant tumors [96].

Dabrafenib displayed remarkable efficacy in melanoma patients with activating BRAF mutations, including patients with brain metastases, and had further shown enhanced clinical activity in combination with the MEK inhibitor, trametinib [27,97–99]. Further clinical studies conducted on dabrafenib were published in recent reviews dealing with BRAF clinical drugs [42,57].

In 2012, a group of Chinese researchers reported the discovery of 5-benzylidene-2-thioxodihydropyrimidine-4,6(1*H*,5*H*)-dione **59** as novel $BRAF^{V600E}$ inhibitor ($BRAF^{V600E}$ IC_{50} 4 μM) using pharmacophore-based virtual screening [100].

Scaffold hopping of compound **59** inspired by molecular docking led to the discovery of 5-(furan-2-ylmethylene)-2-thioxodihydropyrimidine-4,6(1*H*,5*H*)-dione as a new and better scaffold. Further structure modification afforded compound **60** which was found to be 10-fold more potent than the hit **59** ($BRAF^{V600E}$ IC_{50} 0.31 μM), and acquired comparable BRAF inhibitory

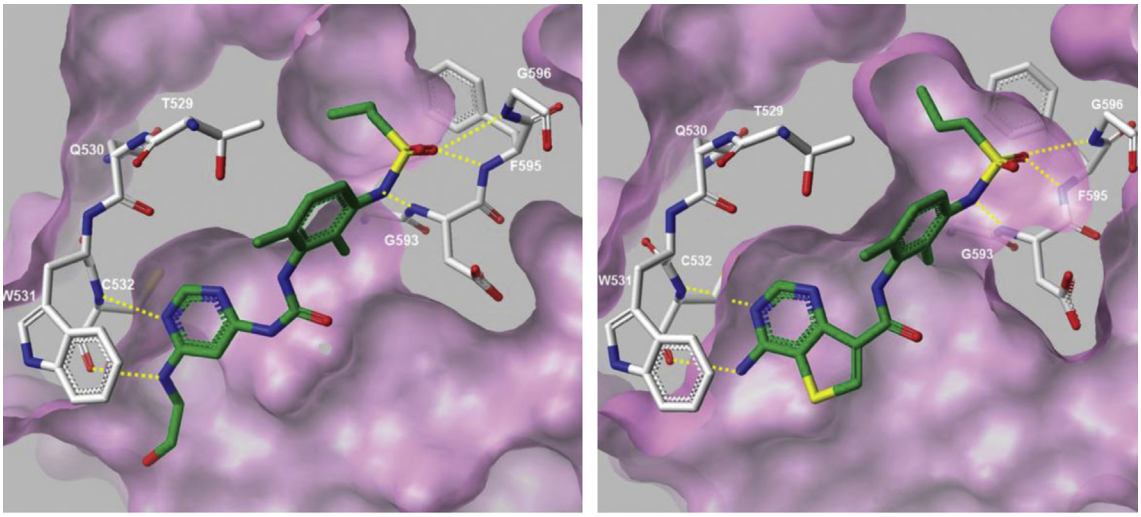

Fig. 16. (a) X-ray crystal structure of compound **64** (in green) in complex with $BRAF^{V600E}$. (b) X-ray crystal structure of compound **66** (in green) in complex with $BRAF^{WT}$. The cleft surface is rendered in violet, and select residues are depicted in white. H-bond interactions are illustrated with yellow dashed lines. Mathieu et al. [86]. (For interpretation of the references to color in this figure legend, the reader is referred to the web version of this article.)

activity to that of the marketed drug Vemurafenib (compound **4**, BRAF IC_{50} 0.29 μM) [100].

In another study, 5-(furan-2-ylmethylene)-thiobarbituric acid derivatives were identified as selective $BRAF^{V600E}$ inhibitors *via* combined ligand- and structure based virtual screening in conjunction with hierarchical hit optimization. First, virtual screening resulted in the discovery of nine hit compounds with low micromolar IC_{50} values as $BRAF^{V600E}$ inhibitors [101]. Among them, furan derivative **61** displayed high ligand efficiency and promising anti-proliferation activity. The molecular modeling study of compound **61** into the ATP-binding site of BRAF indicated that potency and selectivity could be enhanced by varying the hinge region binder and the substituent on the benzene ring [101].

Further structure optimization and SAR analysis led to the identification of 2-thiobarbituric acid derivatives with improved inhibitory potency and $BRAF^{V600E}$ selectivity. The most potent inhibitors in that study were compounds **62** [5-[5-(4-bromophenyl)-furan-2-ylmethylene]-2-thioxo-dihydropyrimidine-4,6-dione] and **63** [5-[5-(3,4-methylenedioxy)-furan-2-ylmethylene]-2-thioxo-dihydropyrimidine-4,6-dione] (BRAF IC_{50} 0.47 and 0.3 μM, respectively). Both compounds showed selectivity for $BRAF^{V600E}$ *in vitro* and exhibited potent cytotoxicity against $BRAF^{V600E}$ cancer cell lines [101].

The improved selectivity of compound **63** for $BRAF^{V600E}$ (IC_{50} 0.3 μM) over $BRAF^{WT}$ (IC_{50} 1.15 μM) could be attributed to the H-bond interaction between the *meta*-substituted H-bond acceptor (in this case the conformationally constrained 3,4-methylenedioxy substituent) and the main chain NH of Asp594 in the BRAF binding site, which potentially stabilized the DFG-in conformation and the active conformation of BRAF [101].

Structure optimization of the pyrazolopyridine derivative **38** [83] was conducted *via* replacement of the amide linked pyrazolopyridine hinge binding motif by a urea-linked aminopyrimidine scaffolds. The latter scaffolds were designed so that they were geometrically held in place *via* an intramolecular H-bond between the urea NH and the pyrimidine nitrogen atom and thus provided equivalent planarity of the hinge binding system of pyrazolopyridine [86].

Urea-linked aminopyrimidines showed better solubility and pharmacokinetic profiles than pyrazolopyridine **38**. The improved solubility at gastric pH was attributed to the presence of basic center in the hinge binding moiety [86].

Indeed, urea-linked pyrimidine derivatives were found to have good $BRAF^{V600E}$ inhibitory activity, for example, compound **64** showed potency against $BRAF^{V600E}$ with IC_{50} equal to 64 nM and cellular potency pERK with IC_{50} equal to 3400 nM [86].

X-ray crystallography of compound **64** (Fig. 16a) indicated that 4-aminopyrimidine moiety formed similar H-bond interactions with the hinge residue Cys532 as the previous lead compound **38** [86]. The −NH and $-SO_2$ portions of the sulfonamide interacted with Asp594 and Phe595-Gly596, respectively, and the propyl tail moiety filled a narrow lipophilic pocket in the enzyme [86].

However, urea-linked pyrimidines suffered from chemical stability problems especially under acidic conditions which were attributed to the intramolecular H-bond; therefore, the related "reverse amide" linked 4-aminoquinazoline and 4-aminothienopyrimidine series were investigated. Both were structural alternatives to urea-linked pyrimidine that maintained the geometrical arrangement including the intramolecular H-bond at the hinge binding region. The urea linker was replaced with a more stable amide-linked 4-aminoquinazoline core [86]. Both systems were characterized by high p*K*a values affording very good solubility at gastric pH and resulting in high exposures after dosing as crystalline suspension [86].

Amide-linked 4-aminoquinazoline derivative **65** displayed excellent enzyme and cellular potencies ($BRAF^{V600E}$ IC_{50} 2 nM and pERK IC_{50} 10 nM) without any chemical stability issues at low pH. The aminoquinazoline moiety of **65** provided a basic center with a considerably higher p*K*a. Accordingly, the solubility of compound **65** at pH 1.2 was substantially increased, with a value of >1000 μg/mL (the solubility at pH 6.5 and 7.4 remained low at 1 μg/mL) [86].

Alternatively, the amide-linked thieno[3,2-*d*]pyrimidine analogs **66** and **67** (G945) emerged as highly potent and selective BRAF inhibitors ($BRAF^{V600E}$ IC_{50} 3.2 and 0.18 nM, respectively) with potent cellular activity (pERK IC_{50} 15 and 4.6 nM, respectively) [86].

Cocrystal structure of compound **66** with BRAF (Fig. 16b) showed H-bond interactions similar to those observed for the aminopyrimidine analog **64** [86].

The thieno[3,2-*d*]pyrimidines exhibited higher oral exposure than their quinazoline counterparts which could be attributed to

both the lower clearance and the better thermodynamic solubility at neutral pH observed for the thienopyrimidine series [86].

Both compound **66** and **67** exhibited favorable physicochemical properties so that they can be used in crystalline suspension, and were highly effective in a $BRAF^{V600E}$ mutant Colo205 mouse xenograft model compared to compound **38**. Although no adverse safety signals were recorded for compounds **66** and **67** in mouse efficacy studies, observations reported in higher species precluded the advancement of these compounds [86].

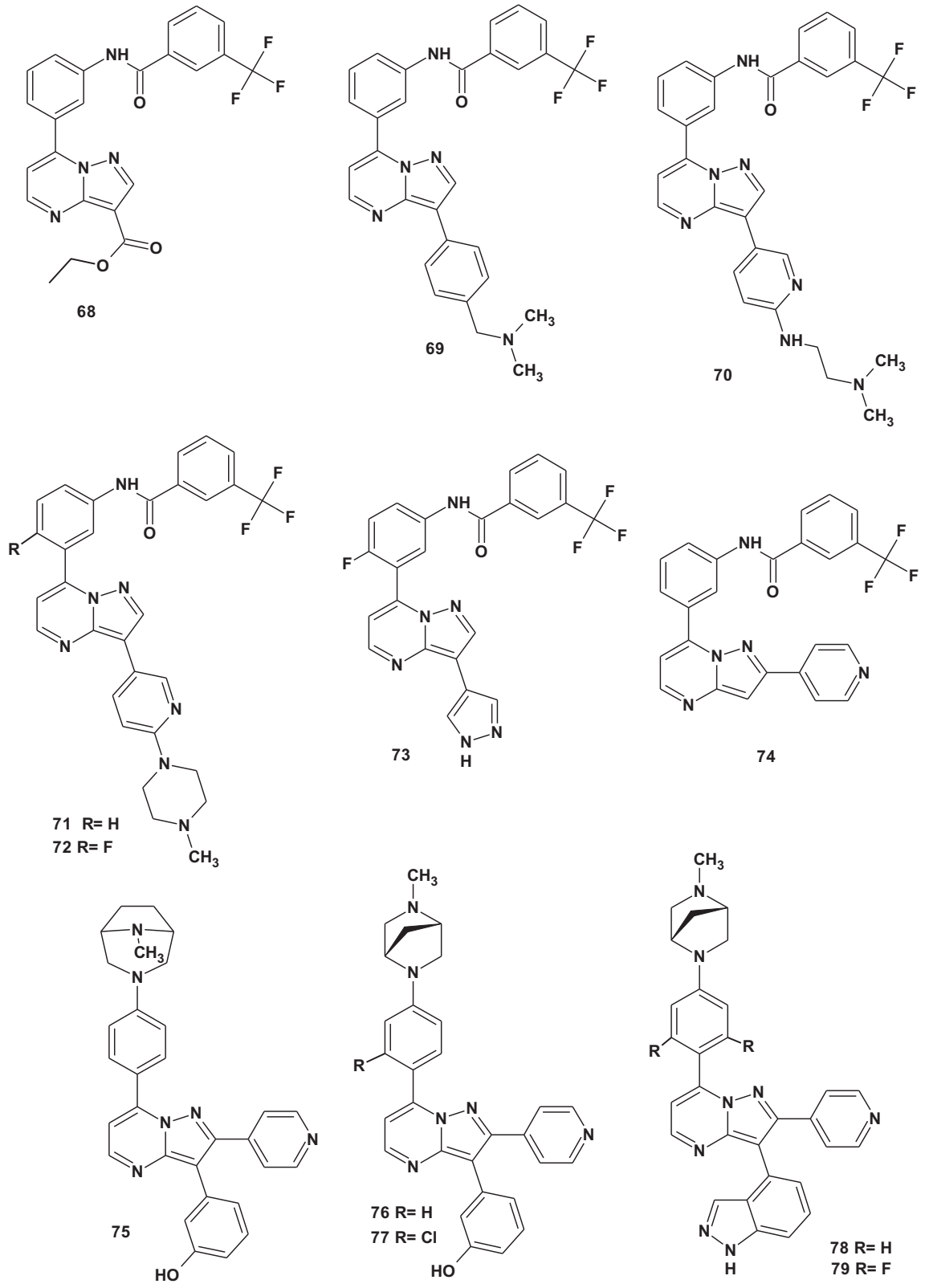

Fig. 17. Pyrazolopyrimidines as BRAF inhibitors.

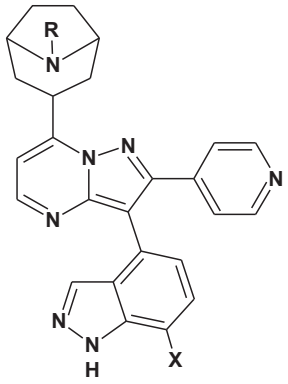

80 R= $COOC_2H_5$, X=H
81 R= $COOC_2H_5$, X=Cl
82 R= $COOC_2H_5$, X=F

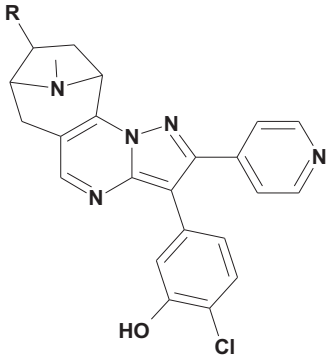

83 R= $COOCH_3$
84 R= CH_2OH
85 R= $SO_2C_6H_5$

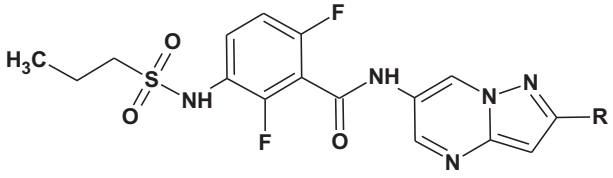

86 R= OCH_3
87 R= C_6H_5

Fig. 17. (*continued*).

2.9. Pyrazolopyrimidine derivatives

Ethyl pyrazolo[1,5-*a*]pyrimidine-3-carboxylate derivative **68** (Fig. 17) was first reported in 2009 by Gopalsamy et al. as potent and selective BRAF inhibitor that was identified through high-throughput screening [102].

Compound **68** showed BRAF IC_{50} of 1.5 μM and inhibited the growth of a variety of tumor cell lines including BXPC-3 (IC_{50} 3.25 μM), HT29 (IC_{50} 7.0 μM), A375 (IC_{50} 3.8 μM), SW620 (IC_{50} 8.3 μM), LoVo (IC_{50} 3.87 μM), WM266-4 (IC_{50} 6.2 μM) and CaCo-2 (IC_{50} 6.6 μM) [102].

Docking study of compound **68** indicated that the amide group formed two H-bonds to the enzyme: one to the side chain of Glu500 and another to the backbone NH of Asp593. The ester made hydrophobic interactions with Ile462, Trp530 and Phe582 with the ethyl group pointing toward a solvent accessible region. The aromatic ring of the amide region occupied the hydrophobic pocket consisted of Ile512, His573 and Ile571. The ring was partially exposed to solvent at the C-4 position (Fig. 18a) [102].

SAR study of pyrazolopyrimidine derivatives revealed that the presence of lipophilic group such as trifluoromethyl or trifluoromethoxy group in the *meta* position of the aromatic group in the amide region was preferred for BRAF inhibition. Also, the urea linker was optimal for enzyme activity. Replacement of the C-3 ester group with amides was tolerated with slight increase in enzyme potency and provided the opportunity for the introduction of water solubilizing groups [102].

Indeed, C-3 substitution of compound **68** was investigated and reported in the same year. Of the tested compounds, dimethylaminobenzyl derivative **69** showed potent and selective BRAF inhibitory activity with IC_{50} 0.024 μM and *in vitro* cytotoxic activity against WM266.4 and HT29 cell lines (IC_{50} 0.92 and 0.78 μM, respectively). Introduction of dimethylaminobenzyl moiety resulted in apparent improvement in the solubility over compound **68** [103].

Besides, the C-3 pyridine substituted analogs **70** and **71** bearing water solubilizing groups showed comparable BRAF inhibitory activity to the corresponding phenyl-substituted analogs (BRAF IC_{50} 0.03 and 0.044 μM, respectively). However, their cytotoxic effect on HT29 significantly improved (HT29 IC_{50} 0.46 and 0.31 μM, respectively) [103].

SAR study also indicated that C-3 substitution with five-membered rings like furyl alone or linked to water-solubilizing groups like pyrrolidine and piperazine afforded less potent analogs than derivatives with six-membered rings like pyridyl and pyrimidinyl [103].

Regarding the substitution on the central phenyl ring (at C-7), it was found that both fluoro and chloro substitution *para* to amide linkage and *ortho* to the pyrazolopyrimidine core enhanced the enzyme activity, while methoxy substitution decreased the enzyme activity [103].

The fluoro analog of compound **71** (compound **72**) showed BRAF IC_{50} of 0.03 μM with HT29 IC_{50} 0.63 μM. Also, the fluoro analog **73** was the most active of the compounds in the pyrazolo[1,5-*a*]pyrimidine series with BRAF IC_{50} of 0.018 μM, although its cellular activity was moderate [103].

X-ray crystallography studies revealed that compound **69** bound to BRAF without forming a hinge-binding H-bond and thus it was bound to the inactive (DFG-out) conformation of the enzyme (PDB code: 3II5). Two H-bonds were formed with Asp593 and Glu500. The trifluoromethylbenzamide moiety fit well in a hydrophobic pocket consisting of Ile512, Leu566, His573, and Ile591. Additionally, the C-3 phenyl ring made significant hydrophobic interactions with the residues of Ile462 and Leu596. The *para*-basic amine substituted C-3 aromatic ring was readily exposed to the aqueous environment around the enzyme (Fig. 18b) [103].

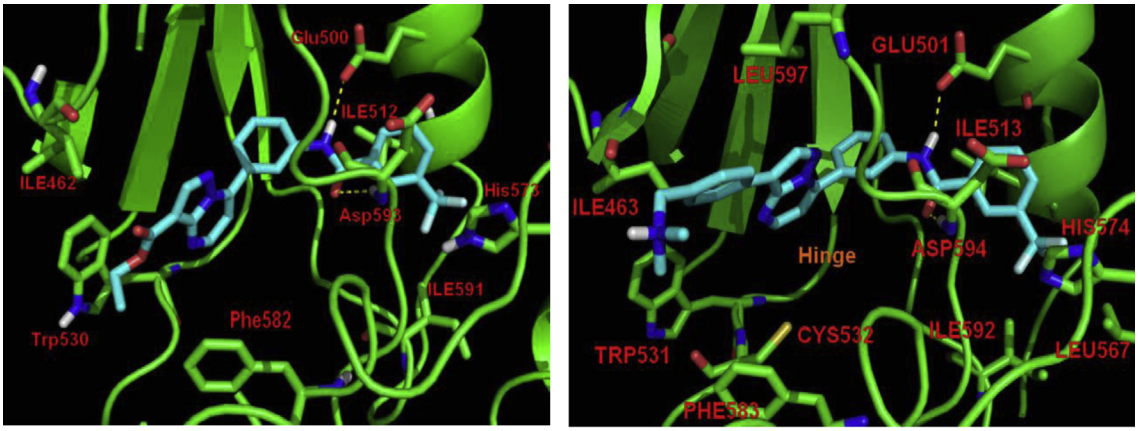

Fig. 18. (a) Docked conformation of compound **68** in the active site of BRAF. Gopalsamy et al. [102]. (b) Representation of compound **69** bound to $BRAF^{WT}$ based on the crystallographic data obtained at 2.9 Å resolution (PDB code: 3II5). Berger et al. [103].

Further optimization of the pyrazolo[1,5-*a*]pyrimidine scaffold was performed by introducing kinase hinge region interacting groups in the 2-position of the scaffold and eliminating the metabolically labile ester group. These efforts led to the identification of compound **74** with improved enzyme and cellular potency as well as good selectivity for BRAF enzyme over other kinases (BRAF IC_{50} 0.032 μM). This improvement in enzyme and cellular potency was reflected in further improvement in the antiproliferative activity compared to compound **68** [BXPC-3 (IC_{50} 3.1 μM), HT29 (IC_{50} 0.35 μM), A375 (IC_{50} 0.28 μM), LoVo (IC_{50} 0.40 μM), WM266-4 (IC_{50} 3.5 μM) and CaCo-2 (IC_{50} 2.6 μM)]. Besides, Compound **74** showed good permeability and microsomal stability [104].

Regarding the C-2 substitution, it was reported that phenyl, substituted phenyl and heteroaromatic derivatives abolished the enzyme activity. However, only the 4-pyridinyl analog **74** showed significant enhancement in the BRAF inhibitory activity. It was postulated that the 4-pyridyl group was ideally positioned so that the nitrogen atom formed H-bond to Cys531 in the hinge region [104].

This improvement in enzyme and cellular potency was also observed with C-2 imidazole and morpholine analogs which were capable of maintaining this H-bond interaction with Cys531. Furthermore, C-6 substitution of the pyridyl ring with water solubilizing groups was tolerated and it was thought that these groups were exposed to the solvent [104].

2,3-Diarylsubstituted pyrazolo[1,5-*a*]pyrimidines were also reported in 2009 in an attempt to prepare type I BRAF inhibitors. The strategy focused on C-2 and C-3 substitution of pyrazolo[1,5-*a*]pyrimidine with pyridyl and phenolic moieties, respectively, to mimic the triarylimidazole scaffold [105].

As a result, the highly potent new lead compound **75**, [3-(3-hydroxyphenyl)-2-(pyridin-4-yl)pyrazolo[1,5-*a*]pyrimidine], was identified with BRAF IC_{50} 0.9 nM. Compound **75** displayed good antiproliferative activity against different tumor cell lines [$BRAF^{V600E}$ including A375 (IC_{50} 0.30 μM) and HT29 (IC_{50} 0.27 μM)] with less potency against a wild-type BRAF cell line CaCo-2 (IC_{50} 1.3 μM) [105].

SAR study of the designed compounds indicated that C-7 substitution with aryl or heteroaryl groups carrying basic amines improved the enzyme activity. Besides, the phenolic hydrogen was essential for the activity and the introduction of a halogen atom next to the hydroxyl group enhanced the enzyme activity. Also, the presence of *N*-methyl-diazabicyclo[2.2.1]heptanyl group on the phenyl group at C-7 improved the enzyme and cellular activities. Finally, the introduction of small *ortho*-group like methyl and halogens on the phenyl group at C-7 resulted in extremely potent analogs like compounds **76** and **77** in terms of enzyme activity (BRAF IC_{50} 0.38 nM and <0.32 nM, respectively), and antiproliferative activity (A375 IC_{50} 0.077 μM and <0.010 μM, respectively) [105].

Nevertheless, compounds **76** and **77** were labile in microsomes and metabolite identification studies indicated that the phenol was glucuronidated in liver microsomes. To overcome this problem, replacement of the phenolic group with indazole group was investigated and indeed resulted in compound **78** with excellent microsomal stability although the enzyme and cellular potency were slightly reduced (BRAF kinase IC_{50} 1.2 nM and A375 IC_{50} 0.202 μM) [105].

Further structure optimization of indazolylpyrazolo[1,5-*a*]pyrimidine analog **78** was published in 2010 by researchers from Pfizer Global Research and Development in order to enhance its cellular and antiproliferative activities [106]. The result of the study highlighted that substituents on the C-7 phenyl linker had dramatic effect on the cellular and enzymatic potency. The introduction of two *ortho* fluorine atoms on the C-7 phenyl group led to the identification of the extremely potent and selective compound **79** (BRAF IC_{50} 0.16 nM and A375 IC_{50} 0.024 μM). Compound **79** exhibited potent antitumor activity in the BRAF mutant xenograft mouse model with no effect on tumor cell lines with wild type BRAF. In addition, compound **79** was metabolically stable and showed a favorable pharmacokinetic profile in nude mice [106].

In a similar study, pyrazolo[1,5-*a*]pyrimidines bearing a phenol moiety at C-3 and substituted tropanes at C-7 were prepared as potent BRAF inhibitors. Here also, indazole group replaced the C-3 phenol group to reduce the metabolism of the resulting analogs and different groups were introduced on the tropane ring. Consequently, compounds **80**–**82** were discovered as extremely potent and selective BRAF inhibitors. Compounds **80**–**82** showed BRAF IC_{50} of 0.002 μM, 0.0004 μM and 0.0004 μM, respectively. These derivatives also potently inhibited cell proliferation in the A375 and WM266 cell lines [107].

Regarding the substitution on the tropane ring, it was found that *N*-carboethoxy group gave 10–25 times more potent inhibitors than the ethyl analogs. It is noteworthy that fusing the tropane ring to the pyrimidine ring as in compounds **83**–**85** resulted in highly potent analogs (BRAF IC_{50} 0.0016 μM, 0.0006 μM and 0.0008 μM, respectively). However, their cellular activities were only modest [107].

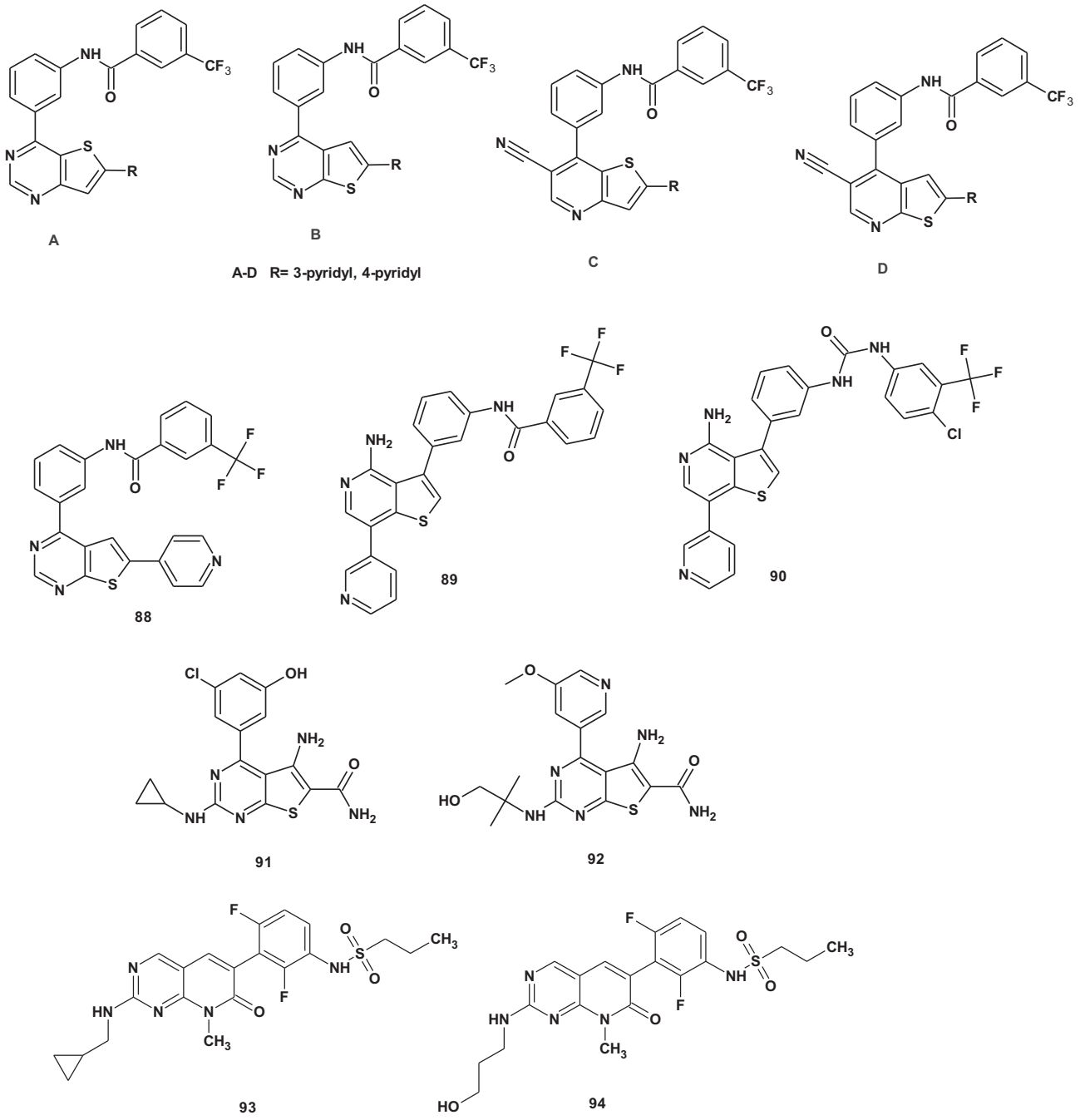

Fig. 19. Thienopyridines, thienopyrimidine and pyridopyrimidines as BRAF inhibitors.

In 2012, pyrazolo[1,5-*a*]pyrimidine derivative **86** emerged as a potent, selective and orally available $BRAF^{V600E}$ inhibitor with enhanced physicochemical and pharmacokinetic properties (BRAF IC_{50} 43 nM, pERK IC_{50} 68 nM) [108]. This derivative was designed to optimize the pyrazolopyridine derivative **38** [83] which suffered from its low solubility that inhibited the use of crystalline suspension formulations in efficacy and toxicology studies [108]. The main idea was to replace the dual hinge binding pyrazolopyridine moiety by its bioisosteric pyrazolopyrimidine ring which could form only one H-bond with the hinge region and meanwhile disrupted the opportunity for dimer formation. The propyl sulfonamide moiety was maintained as it was considered as the key feature for the DFG-in/C-helix shifted binding mode [108].

Compared to pyrazolopyridine derivative **38**, crystalline **86** showed lower melting point (182 °C vs 229 °C) which indicated a lower crystal packing energy associated with the pyrazolopyrimidine template. The decreased melting point coupled with a lower *C*log *P* (1.2 vs 1.6) for **86** translated into a fivefold improvement in solubility (21 μg/mL at pH 6.5) [108]. Compound **86** was characterized by its good permeability and microsomal stability. Furthermore, it was found that the oral exposure of **86** as a crystalline suspension in 1% methylcellulose/0.5% Tween 80 in water was equivalent to solution dosing. This improvement could be attributed to the improved aqueous solubility of **86** [108].

Although C-2 alkoxyl substituted pyrazolopyrimidines were proved to be more potent than C-2 aromatic substitutions, some C-

2 aryl analogs like compound **87** was also as potent as **38** with BRAF IC_{50} 7 nM and pERK IC_{50} of 17 nM. Heteroaromatics such as 3-pyridinyl- and (1-methylpyrazolo-4-yl) at C-2 position were also tolerated and were similarly active with BRAF IC_{50} 13 nM [108].

2.10. Thienopyridine and thienopyrimidine derivatives

Thienopyridine ring system was identified as structure analog of the potent $BRAF^{V600E}$ inhibitor pyrazolo[1,5-*a*]pyrimidine derivative **74** [104] while preservation the key pharmacophores for the proper binding of the ligand (the 4-pyridyl ring which made H-bond interactions at hinge region and the 3-trifluoromethyl substituted benzamide moiety which made hydrophobic interactions with the ATP binding site) [109].

Gopalsamy et al. assumed that the bicyclic core pyrazolo[1,5-*a*] pyrimidine act as the scaffold that properly positioned the pyridyl and the benzamide moieties and provided the required directionality for these groups to bind to the enzyme. Therefore, it could be replaced by other bicyclic scaffolds like thienopyrimidines and cyanothienopyridines [109].

The results indicated that thienopyrimidine scaffolds A and B (Fig. 19) afforded more potent inhibitors than cyanothienopyridine scaffolds C and D, however all the derivatives tested were less potent than the lead compound **74** [109]. Among the thienopyrimidine analogs, scaffold B (thieno[2,3-*d*]pyrimidine) was more active than scaffold A (thieno[3,2-*d*]pyrimidine). The thienopyrimidine derivative **88** was discovered as the most potent and selective $BRAF^{V600E}$ inhibitor in that study with IC_{50} of 0.08 μM [109]. Compound **88** also exhibited potent cytotoxic activity against a variety of tumor cell lines with high selectivity towards $BRAF^{V600E}$ [109].

Recently, 4-aminothienopyridine derivatives **89** and **90** were reported as selective $BRAF^{V600E}$ kinase inhibitors with IC_{50} equal to 5.1 and 16.6 nM, respectively. Both compounds exhibited potent cellular activity with IC_{50} of 0.2 μM [110]. The compounds were designed to act as type I kinase inhibitors and hence they were designed to fit well in the ATP binding site of the enzyme. Thus, the aminopyridine moiety of the thienopyridine scaffold bound to the hinge region through H-bond interactions, the 3-aryl moiety would fill the inner hydrophobic pocket, the 7-aryl moiety would be exposed to the outer hydrophobic pocket and the urea or amide moieties were used as a linker to connect the inner hydrophobic moiety to the induced fit moiety [110].

Thieno[2,3-*d*]pyrimidines were reported as BRAF inhibitors in 2012 [111]. These derivatives were identified from a series of PDE4 inhibitors. SAR study was done on the discovered compounds in order to decrease the PDE4 inhibitory activity and enhance the BRAF inhibitory activity. The study demonstrated that both C-5 amino and C-6 carboxamide moieties were required for BRAF inhibitory activity. The results showed also that the presence of small amino substituents at C-2 was essential for potent PDE4 inhibitory activity. However, removal of the C-2 substituent or use of larger substituents favored BRAF inhibitory activity [111]. Furthermore, C-4 *meta*-phenolic derivatives proved to be very potent BRAF inhibitors and were selective against PDE4. For example, phenolic derivative **91** showed very potent BRAF inhibitory activity (BRAF IC_{50} 0.002 μM) with potent cellular activity (pMEK IC_{50} 0.025 μM). An *in vivo* biomarker study was performed on compound **91** in SCID mice bearing A375 melanoma tumors measuring the phosphorylation of both MEK and ERK. Compound **91** displayed significant knockdown of both pMEK and pERK (60% and 80%, respectively), at 30-min post dose [111].

However, this compound suffered from poor hepatocyte stability correlated to rapid *in vivo* clearance. The C-4 phenolic group of compound **91** was identified as the major site of metabolism (glucuronidation). Therefore, its replacement or stabilization was expected to improve the bioavailability of the resulting analogs [111]. Indeed, C-4 methoxypyridine and C-4 aryl urea analogs were reported as potent and metabolically stable BRAF inhibitors. The combination of potent and stable C-2 and C-4 substituents led to identification of compound **92** which proved to be a moderately orally bioavailable BRAF inhibitor (BRAF IC_{50} 0.058 μM, pMEK IC_{50} 1.01 μM). Compound **92** demonstrated excellent hepatocyte stability and was cleared much more slowly than the C-4 phenolic analogs [111].

2.11. Pyridopyrimidine derivatives

Pyridopyrimidin-7-ones were discovered *via* structure based drug design as ATP competitive BRAF inhibitors. Structure optimization led to the identification of compound **93** (Fig. 19) (BRAF IC_{50} 3 nM and pERK IC_{50} 27 nM) as a potent, selective and orally bioavailable agent with excellent pharmacokinetic properties and tumor growth inhibition in xenograft studies [112].

Pyridopyrimidin-7-ones were identified in an attempt to raise the chemical and metabolic stability of the aminopyridine amide derivative **34** [83].

It was hypothesized that connecting the amide to the 4-position of the pyridine derivative **34** to form a fused heterocycles might afford BRAF inhibitor with the appropriate torsion angle between the bicycle and the propyl sulfonamide bearing phenyl ring. Thus, pyridopyrimidin-7-ones such as **93** and **94** were discovered and proved to be potent and selective BRAF inhibitors. Furthermore, X-ray crystal structure of $BRAF^{WT}$ in complex with compound **94** (BRAF IC_{50} 7 nM and pERK IC_{50} 41 nM) showed that the compound fit well in the ATP pocket of the enzyme and the hydroxypropyl group established H-bond with the side chain of Ser536 [112].

In contrast to pyridine derivatives, pyridopyrimidin-7-ones **93** and **94** were highly permeable in Caco-2 permeability assay and were stable in mouse hepatocytes with good oral exposure [112].

2.12. Isoquinoline and quinazoline derivatives

In 2009, Smith et al. reported the discovery and optimization of a novel series of aminoisoquinolines as potent, selective, and orally bioavailable inhibitors of $BRAF^{V600E}$ [113]. The aminoisoquinolines were discovered by structure optimization of the *N*-linked pyridylpyrimidine benzamide derivative **95** (Fig. 20) which was identified *via* high throughput screening as a potent, modestly selective inhibitor of the BRAF enzyme (BRAF IC_{50} 0.46 nM). Compound **95** was found to be highly potent inhibitor of other kinases with smaller gatekeeper residues and known DFG-out binding modes, including p38α, KDR, Lck, and Tie-2 [113]. In searching for more selective BRAF inhibitors, it was found that replacement of the benzamide moiety with an aminoisoquinoline core significantly improved the kinase selectivity and provided favorable pharmacokinetic properties. Thus, the pyridylpurine aminoisoquinoline derivative **96** was discovered as a potent and selective BRAF inhibitor (BRAF IC_{50} 1.6 nM and A375 pERK IC_{50} 1.8 nM) that exhibited also antitumor activity in xenograft models [113].

A cocrystal structure of compound **96** with BRAF (PDB: 3IDP) revealed that the purine ring formed an additional H-bond with Cys532 and also allowed favorable π-stacking interaction with the side chain of Trp531 which was probably responsible for the improvement in potency [113].

In 2011, aryl phenyl ureas substituted with 4-quinazolinoxy at the *meta*-position of the phenyl ring were described as potent inhibitors of both mutant and wild type BRAF kinases. Compound **97** [(1-(5-*tert*-butylisoxazol-3-yl)-3-(3-(6,7-dimethoxyquinazolin-4-yloxy)phenyl)urea hydrochloride)] displayed BRAF inhibitory

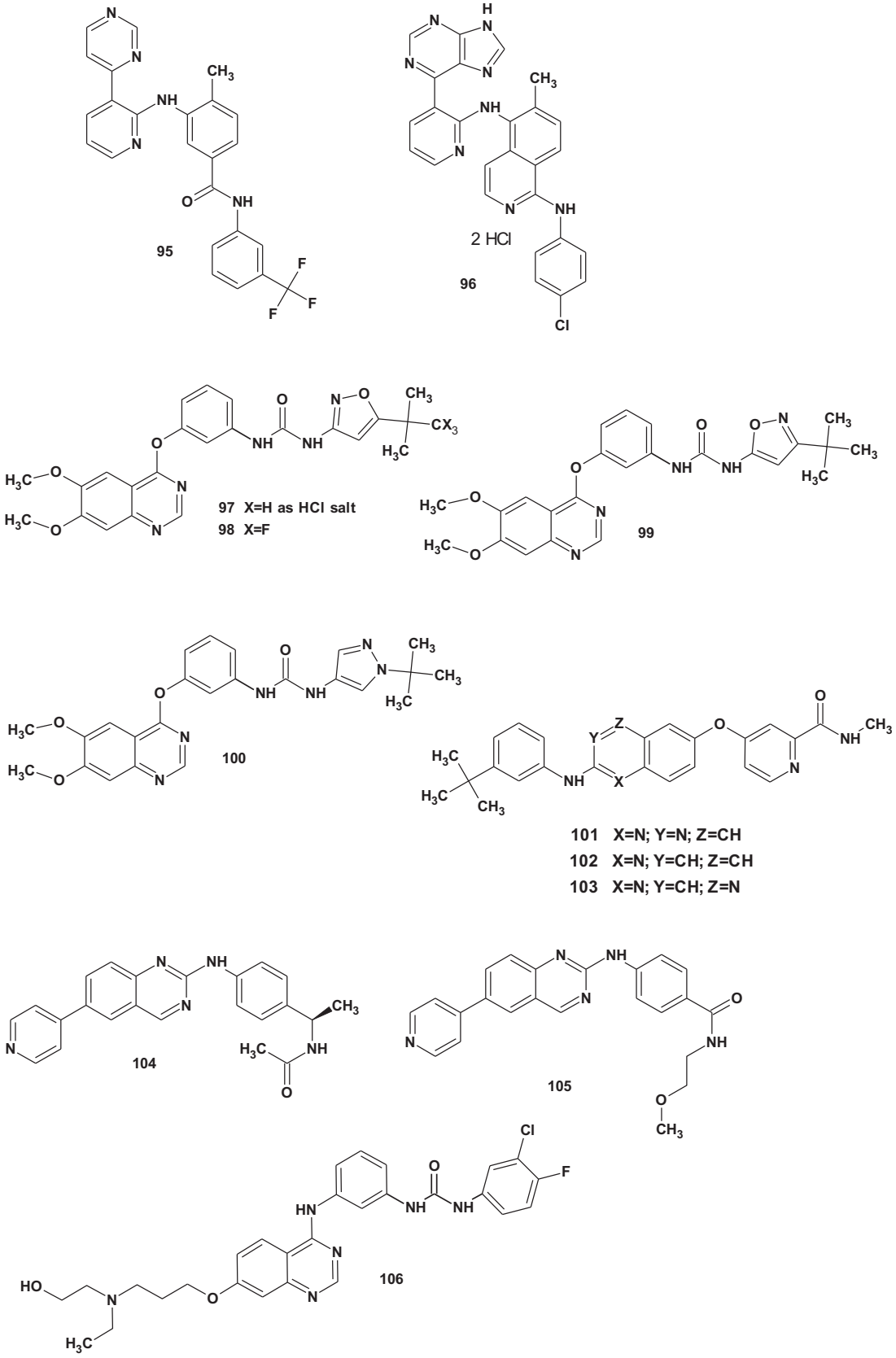

Fig. 20. Isoquinolines and quinazolines as BRAF inhibitors.

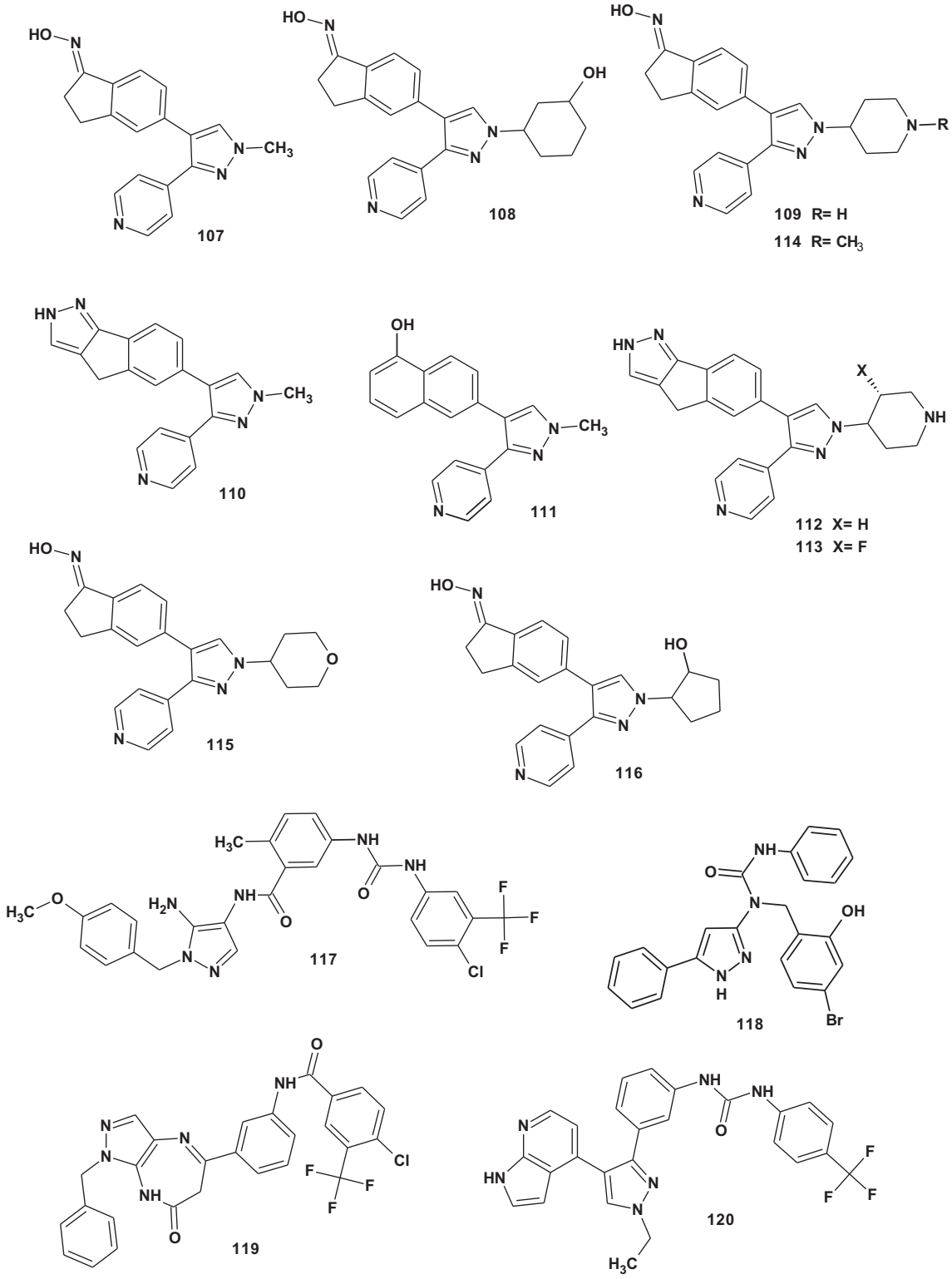

Fig. 21. Pyrazoles as BRAF inhibitors.

activity with K_d of 73 nM and A375 pMEK IC_{50} 121 nM. This compound also was moderately selective across a panel of 290 kinases, demonstrated good pharmacokinetic properties in rat and mouse and was reported to be efficacious in a mouse tumor xenograft model following oral dosing [114].

Regarding the linkers between the central phenyl ring and quinazoline ring, it was reported that the presence of NH linker provided more selective BRAF inhibitors than S or O linkers, although, all these linkers showed potent binding affinity and cellular activity. Nevertheless, derivatives with NH linker exhibited inferior pharmacokinetic properties compared to those with O or S linkers [114].

Replacing the methoxy group on either the 6- or 7-position of the quinazoline ring with hydroxy, ethoxy, methoxyethoxy, or

aminoalkoxy groups was well tolerated with respect to cellular activity and binding affinity, consistent with the hypothesis that this region of the molecule extended outside the catalytic cleft toward the solvent [114].

However, *in vitro* metabolite profiling studies conducted on compound **97** indicated that, in both rat and human liver microsomes, hydroxylation of the *tert*-butyl moiety and subsequent oxidation to the carboxylate moiety occurred to a significant degree which led to reduced cellular activities [115]. Further optimization of the 4-quinazolinyloxy-diaryl urea derivative **97** was done to decrease the metabolism and this effort led to identification of compound **98** (CEP-32496) [115]. Structure optimization was achieved by bioisosteric replacement of the metabolically sensitive *tert*-butyl group in compound **97** with fluorinated alkyl moieties. Compound **98** [5-(1,1,1-trifluoro-2-methylpropan-2-yl)-isoxazol-3-yl derivative] displayed potent binding ($BRAF^{V600E}$ K_d 14 nM) and cellular activity (pMEK IC_{50} 82 nM and A375 proliferation IC_{50} 78 nM). Its activity in the proliferation assay was approximately 4-fold greater than that observed with the *tert*-butyl analog **97**. Besides, compound **98** (CEP-32496) exhibited high potency and selectivity against several $BRAF^{V600E}$-dependent cell lines. Compound **98** also showed an excellent PK profile across multiple preclinical species [115].

In addition, compound **98** exhibited good stability in mouse, dog, monkey, and human liver microsomal preparations, predicting low phase I hepatic clearance in these species. Metabolite profiling of compound **98** in all these species indicated that both mono *O*-demethylation (of the quinazoline methoxy groups) and oxidation of the (1,1,1-trifluoro-2-methylpropan-2-yl)isoxazol-3-yl moiety occurred to some extent [115].

Besides, SAR study of these quinazoline derivatives indicated that the 3-(*tert*-butyl)isoxazole-5-urea derivative **99** was equipotent to compound **97** in both binding and cellular assays with comparable selectivity profile. In addition, substitution of the *tert*-butyl group for the smaller methyl group or the larger phenyl group led to a loss in both binding affinity and cellular potency which reflected the effect of size and lipophilicity of the substituent at this position on the activity [115]. Substitution of the isoxazole moiety with an *N*-1-(*tert*-butyl)pyrazole-4-urea motif resulted also in good binding affinity for $BRAF^{V600E}$ (compound **100**). However, this compound was inactive in the A375 cell proliferation assay [115].

In 2012, Ramurthy and coworkers from Novartis Institutes for Biomedical Research reported the identification of quinazolines, quinolines and quinoxalines derivatives **101**–**103** as analogs of the potent BRAF inhibitor 3-*tert*-butylphenylaminobenzimidazole amide **20** (BRAF IC_{50} = 0.12 μM) [74]. All the test compounds showed potent BRAF inhibitory activity with IC_{50} of 0.045, 0.026, and 0.025 μM, respectively. Thus, quinoline **102** and quinoxaline **103** derivatives were six times more potent than benzimidazole derivative **20** [116].

Regarding the structure–activity relationship of the aniline and amide functionalities in the quinazoline series, it was found that *ortho* substituents on the aniline moiety led to significant loss of affinity. While, *meta* and *para* substituents were in general similarly potent compared to *meta* and *para* substituents in the benzimidazole series. The 3-OCF_3 substituted phenyl showed the best affinity in the *meta*-substituted sub-series. For substituents in the *para*-position of the phenyl ring, affinity appeared to improve with increasing the hydrophobic nature of the substituents. However, larger groups in the *para*-position of the phenyl ring such as phenoxy and 3-pyridyl lowered the affinity [116].

Nevertheless, compounds **101**–**103** did not inhibit phosphorylation of ERK in cells, which was attributed by the authors to permeability and solubility limitations. The lack of cellular potency discouraged further development of these analogs [116].

In 2013, a group of researchers from AstraZeneca reported the discovery of the aminoquinazoline derivative **104** as potent BRAF inhibitor ($BRAF^{V600E}$ IC_{50} 19 nm and A375 perk IC_{50} 34 nm). This compound also inhibited the growth of a $BRAF^{V600E}$ A375 xenograft *in vivo* at a well-tolerated dose [117].

The aminoquinazoline derivative **105** was firstly identified from a kinase subset screening effort as a hit BRAF inhibitor ($BRAF^{V600E}$ IC_{50} 77 nM and A375 pERK IC_{50} 190 nM). Compound **105** inhibited mutant $BRAF^{V600E}$ but was much less potent against $CRAF^{WT}$ and inactive against $BRAF^{WT}$ [117].

Studying the SAR of these aminoquinazoline derivatives revealed that the presence of 4-pyridyl ring at position 6 of the quinazoline ring enhanced the selectivity profile, in particular against other tyrosine and serine/threonine kinases [117]. The group substituted on the amide linkage was believed to be exposed to the solvent and hence its optimization greatly affected the aqueous solubility. Since the presence of aromatic aniline moiety may confer potential mutagenic liability, trials were done to remove this functionality while maintaining potent enzyme and cellular activity and improving the pharmacokinetic profile. The results showed that incorporating an additional atom between the arene and the nitrogen such as α-methyl amino or α-methyl amides groups was tolerated and provided better aqueous solubility than compound **105**. Besides, the presence of 7- and 8-methoxy substitutions on the quinazoline ring was well tolerated. These positions were probably oriented away from the hinge binding region, whereas substitution of the aminoquinazoline at the 4- and 5-positions was expected to interfere with hinge binding [117].

Further structure optimization of compound **105** led to identification of compound **104**. The latter was believed to be DFG-in binding inhibitor of mutant $BRAF^{V600E}$. However, the $BRAF^{V600E}$ selective nature of compound **104** led to elevation of the level of pERK in nonmutant BRAF cell lines *in vitro* [117].

On the other hand, 4-anilinoquinazoline urea derivatives were registered as multikinase inhibitors of BRAF, $BRAF^{V600E}$, VEGFR-2 and EGFR in 2013 [118]. Upon designing these compounds, C-6 group was removed to reduce the molecular weight and to avoid any potential metabolic liability. In addition, C-7 position was substituted *via* ether link to Tethered aliphatic tertiary amino groups. The latter group was found to control the selectivity of the resulting inhibitors [118]. The best result was obtained with the ethyl (2-hydroxyethyl)amino derivative **106** which was 5-fold more potent toward BRAF, and 3-fold more potent toward $BRAF^{V600E}$ than Sorafenib (BRAF IC_{50} 22 nM, $BRAF^{V600E}$ IC_{50} 13 nM, VEGFR IC_{50} 95 nM and EGFR IC_{50} 165 nM) [118].

2.13. Pyrazole derivatives

Pyrazole derivatives **107**–**109** (Fig. 21) were developed as ATP competitive BRAF inhibitors by Hansen and collaborators. Those inhibitors showed excellent enzyme inhibitory activity (BRAF IC_{50} 0.02 nM, 0.04 nM and 0.03 nM, respectively), potent cellular potency (pERK IC_{50} 33 nM, 7 nM and 9 nM, respectively) as well as striking BRAF selectivity. Besides, Compound **108** displayed significant *in vivo* inhibition of pERK in subcutaneous LOX tumor xenograft studies [119].

The authors pointed out that substitution of the pyrazole core at *N*-1 enhanced the solubility and enzyme potency, and the best activity was obtained with cyclohexyl and piperidinyl groups as shown for compounds **108** and **109**. Furthermore, the presence of H-bond acceptor group at C-3 was essential for activity and 4-pyridyl group afforded optimal result. Replacement of 4-pyridyl ring with indazole or 3-pyridyl ring was detrimental to the cellular activity [119].

Fig. 22a showed X-ray crystal structure of the BRAF co-crystallized with inhibitor **109** which indicated that the oxime act as both H-bond donor and acceptor to the enzyme and therefore was essential for enzyme and cellular potency [119].

In spite of the potency of compound **107**, this compound suffered from metabolic degradation in a simulated gastric fluid assay to its indane ketone with a half-life of 1.3 h. Therefore, non-oxime pyrazole analogs were investigated in an attempt to obtain more metabolically stable BRAF inhibitors. The oxime moiety was replaced by 2,4-dihydroindeno[1,2-*c*]pyrazole to afford compound **110** with excellent enzyme potency (BRAF IC_{50} 2.2 nM), although less potent than compound **107**. Compound **110** displayed encouraging cellular activity (pERK IC_{50} 1900 nM) and no degradation in a simulated gastric fluid assay [120].

Further structure optimization of the fused pyrazole **110** led to the discovery of the lipophilic naphthol **111** that exhibited very potent BRAF inhibitory activity (BRAF IC_{50} 1.4 nM) and had excellent cellular activity (pERK IC_{50} 78 nM). However, **111** suffered from a high predicted clearance in human hepatocytes [120].

Structure modification of compound **110** by varying the substituents at the *N*-1 tail of the pyrazole resulted in compound **112** (4-piperidinyl substituent at *N*-1) with improved enzyme activity compared to compound **110** (BRAF IC_{50} 3 nM) yet high clearance rate as well [120]. Fig. 22b showed the X-ray crystal structure of compound **112** in complex with BRAF which indicated that indeno [1,2-*c*]pyrazole moiety bound to the ATP binding site of the BRAF in a similar manner to oxime moiety [120].

On the other hand, attempts were done to reduce the basicity of piperidine to enhance the physicochemical properties and oral absorption. The best result was obtained by introduction of fluorine atom on the piperidine moiety to give compound **113** (BRAF IC_{50} 1.4 nM and pERK IC_{50} 700 nM). Compound **113** showed good kinase selectivity together with modest oral absorption in mice [120].

Three of the molecules reported by Hansen et al. [119] were subjected to docking study and molecular dynamics (MD) simulations by Alzate-Morales and coworkers [121]. These derivatives were the BRAF active compound *N*-(4-piperidinyl)pyrazole derivative **109** (BRAF IC_{50} 0.03 nM and pERK 9 nM) and the less active pyrazole analogous with 1-methyl-4-piperidinyl (compound **114**, BRAF IC_{50} 0.34 nM) and tetrahydro-2*H*-pyran-4-yl group at position 1 of pyrazole (compound **115**) (BRAF IC_{50} 0.22 nM) [121].

The results indicated that the most active compound **109** formed interactions with residues Ile463 and His539. In addition, a water wire was identified for the most active compound **109** which connected *N*-2 of the pyrazole ring with Cys532, and Ser536. Some differences in the water wire H-bond network were detected for the less active compounds **114** and **115** which might explain the differences in activity between the three compounds [121].

A similar study was reported in 2011 where four other BRAF inhibitors (*N*-1 Hydroxy substituted cycloalkyl) also described by Hansen et al. [119] were subjected to docking study and molecular dynamics (MD) simulations, and hybrid calculation methods (Quantum Mechanics/Molecular Mechanics (QM/MM)). Here, docking of the inhibitors showed the same orientation as the X-ray crystal structure of the compound **109** (Fig. 22a) [119]. MD simulations of the most active diastereomer of compound **108** containing *cis*- and *trans*-3-hydroxycyclohexyl moiety (BRAF IC_{50} 0.04 nM and 0.09 nM, respectively) showed stable interactions with residue Ile463 at the entrance of the BRAF active site. Whilst, the less active diastereomer of compound **116** containing *cis*- and *trans*-2-hydroxycyclopentyl substituents (BRAF IC_{50} 3.91 nM and 0.33 nM, respectively) showed interactions with inner residues Asn580 and Ser465 [122]. MD simulations showed that all the compounds established dynamically stable H-bond interactions with residues Glu501 and Cys532 and formed the previously described water wire connecting *N*-2 of pyrazole ring with Cys532 and Ser536. Groups at *N*-1 of the pyrazole ring interacted with residues at the entrance of the active site [122].

Furthermore, 3D-QSAR study of the pyrazole derivatives described by Hansen et al. together with several BRAF inhibitors from different scaffolds was described in 2011 [123]. The results of all these studies could be used to develop novel, potent and highly selective BRAF inhibitors.

Amino-1*H*-pyrazole amide derivatives were reported in 2011 as potent BRAF inhibitors that displayed competitive antiproliferative activities to Sorafenib (compound **1**) against A375P melanoma cell line [124]. In particular, *N*-(5-amino-1-(4-methoxybenzyl)-1*H*-pyrazol-4-yl)-5-(3-(4-chloro-3-(trifluoromethyl)phenyl) ureido)-2-methylbenzamide (**117**) exhibited potent cytotoxic activity (GI_{50} 0.27 μM). Compound **117** was found to be a potent and selective $BRAF^{V600E}$ and C-RAF inhibitor (IC_{50} 0.26 μM and IC_{50} 0.11 μM, respectively) [124].

Here in, the presence of *p*-methoxybenzyl group on *N*-1 of pyrazole moiety seemed to be essential for activity since its replacement with benzyl group resulted in dramatic drop in the antiproliferative potency. In addition, urea derivatives were more potent than amide derivatives especially 2-methyl-5-aminophenylurea derivatives [124].

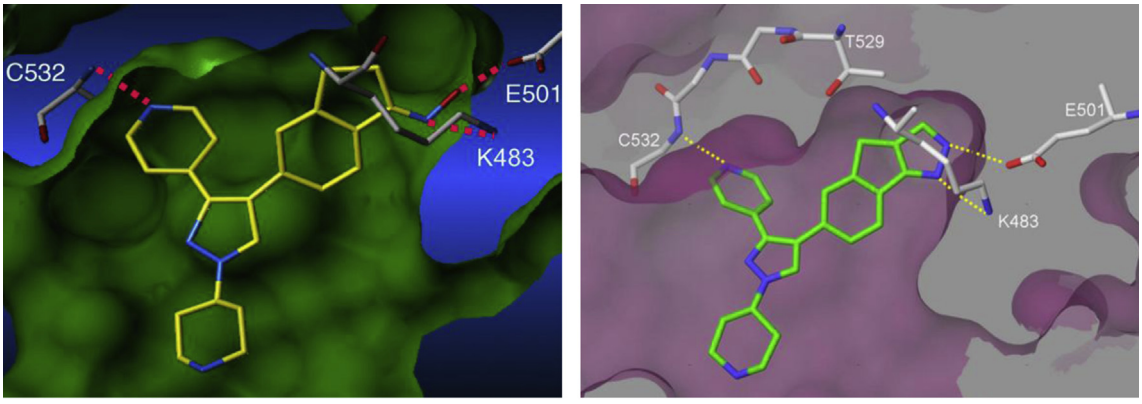

Fig. 22. (a) Cut away view of compound **109** on surface of BRAF. H-bonds are depicted as dashed red lines. Hansen et al. [119]. (b) X-ray crystal structure of compound **112** (3.6 Å resolution) in complex with BRAF. H-bonds are depicted as dashed yellow lines (PDB code: 3PSD). Newhouse et al. [120]. (For interpretation of the references to color in this figure legend, the reader is referred to the web version of this article.)

Recently, a series of 5-phenyl-1*H*-pyrazol derivatives were developed as $BRAF^{V600E}$ inhibitors. Compound **118** [1-(4-bromo-2-hydroxybenzyl)-3-phenyl-1-(5-phenyl-1*H*-pyrazol-3-yl)urea] was the most potent BRAF inhibitor discovered in that study ($BRAF^{V600E}$ IC_{50} 0.19 μM). This compound showed high *in vitro* antiproliferative activity comparable to Vemurafenib against cell lines WM266.4 and A375 (IC_{50} 1.50 and 1.32 μM, respectively). Docking studies suggested that compound **118** bound tightly to the active site of $BRAF^{V600E}$ [125].

In 2011, Kim et al. reported the synthesis of phenyl-6,8-dihydropyrazolo[3,4-*b*] [1,4]diazepin-7(1*H*)-one derivatives as selective BRAF inhibitors with potent antiproliferative activity on A375P melanoma cell line and U937 hematopoietic cell line. These compounds were developed as conformationally rigid analogs to the previously reported *N*-(5-amino-1-(4-methoxybenzyl)-1*H*-pyrazol-4-yl amide derivatives, such as **117**, which were structurally analogs to Sorafenib (compound **1**) [126].

Docking study of the aminopyrazole derivatives suggested that the pyrazole ring made two H-bonds in the hinge region and one intramolecular H-bond between the hydrogen of the 5-amino group and the carbonyl oxygen in the 4-amide group [124]. Therefore, the seven-membered ring pyrazolobenzodiazepine analogs were introduced to mimic this intramolecular H-bond (conformation restricted analogs) [126].

Among the synthesized compounds, compound **119** exhibited potent BRAF inhibitory activity (BRAF IC_{50} 655 nM) as well as potent antiproliferative activity (A375P GI_{50} 0.43 μM and U937 GI_{50} 0.06 μM) [126].

On the other hand, Tang and coworkers from GlaxoSmithKline reported the discovery of pyrazole derivatives substituted with 7-azaindole moiety as novel, selective and potent BRAF kinase inhibitors [127].

The 7-azaindole analogs were designed to act as ATP-competitive kinase inhibitors. In this design, the 7-azaindole moiety act as the hinge binder, the inner hydrophobic pocket was filled by an aromatic ring or one of its bioisosteres. Another substituted or unsubstituted hydrophobic aromatic ring was used to occupy the induced fit pocket [a relatively big pocket featuring a flexible phenylalanine (Phe594)]. In addition, urea was used as a linker to connect the two aromatic rings and meanwhile could make additional donor–acceptor interactions with Glu500. The outer hydrophobic pocket could be occupied by lipophilic ring systems to control the enzymatic potency and selectivity. Besides, water soluble residues could be introduced to occupy the solvent front area and enhanced the solubility and physicochemical properties of the resulting inhibitor. Finally, 1,3,4-trisubstituted-1*H*-pyrazole was used as an organizer motif that allowed each fragment to fit precisely into the desired pockets [127].

Consequently, the azaindole derivative **120** was introduced as BRAF inhibitor with an excellent potency in the enzyme assay (BRAF IC_{50} 2.5 nM) and the cellular assay (pMEK1 IC_{50} 63 nM) [127].

2.14. Pyrazoline derivatives

N-Aroylpyrazoline derivatives were first reported as BRAF kinase inhibitors in 2010 by Blackburn et al. Pyrazoline derivative **121** (Fig. 23) was identified *via* high throughput screening as potent and selective inhibitor of $BRAF^{V600E}$ ($BRAF^{V600E}$ IC_{50} 200 nM and pERK IC_{50} 1800 nM). Further structure optimization through modification of the aroyl group led to the identification of several potent inhibitors in terms of both enzymatic and cellular assays (pERK) such as compound **122** ($BRAF^{V600E}$ IC_{50} 19 nM and pERK IC_{50} 180 nM) [128].

SAR study of *N*-substituted pyrazolines revealed that small acyl groups such as cyclopropyl were tolerated but these derivatives showed little cellular activity. Similarly, *N*-sulfonyl derivatives (aliphatic, benzylic, and arylsulfonyl) showed no significant $BRAF^{V600E}$ inhibitory activity and no cellular activity as well. Whilst, *N*-aroyl groups displayed a wide range of activity determined by conformational effects. Nevertheless, 1-naphthyl and related quinolines were inactive. Besides, compounds with large *ortho*-substituents aroyl group (phenyl, phenoxy or trifluoromethyl) showed no inhibitory activity against $BRAF^{V600E}$. However, transfer of the phenoxy or trifluoromethyl groups to the *meta* position improved the enzyme inhibitory activity [128]. *N*-Heteroaroyl groups like furan, benzofuran, pyrrole and thiophene groups also exhibited good enzyme inhibitory activity against $BRAF^{V600E}$ superior to compound **121**. Further substitution of the five membered heteroaroyl ring with additional ring substitution or fusion led to identification of compounds **123** and **124** with better $BRAF^{V600E}$ enzymatic inhibitory activity (IC_{50} 14 and 9 nM, respectively) together with improved cellular activity compared to compound **121** (pERK IC_{50} 130 and 61 nM, respectively) [128].

Regarding the 5-phenyl substituent, it was found that the *ortho*-hydroxyl group was essential for the enzyme inhibitory activity and its transfer to the *meta* position resulted in complete loss of activity [128].

In spite of the pronounced potency of compound **122** against BRAF enzyme, it suffered from poor aqueous solubility (5.8 μg/mL) which precluded IV formulations for pharmacokinetic experiments. Further optimization of compound **122** was reported in the same year aiming to improve its potency, physicochemical and PK properties [129].

Docking studies of compound **122** showed that the nitrogen of the 3-pyridyl ring formed H-bond to the NH of Cys532. Another intramolecular H-bond was formed between the hydrogen of the phenolic OH and the carbonyl of the pyrazoline amide which organized the phenol in a hydrophobic pocket. Besides, the thiophene–pyridine moiety extended out towards the solvent [129]. Therefore, replacement of this pyridyl group with other solubilizing group might increase the aqueous solubility while retaining the enzyme inhibitory activity and the cellular potency. Indeed, it was reported that replacement of the pyridyl group with benzyl, benzylamines or other heterocycles such as thiazole or pyrazole maintained enzyme and cell potency. However, significant increases in cell potency were observed upon using constrained amines such as the isomeric tetrahydroisoquinoline and the isoindoline moieties [129].

Here also the presence of *ortho* OH group on 5-phenyl moiety was essential for BRAF inhibitory activity and its removal or placement in the *meta* position abolished the enzyme activity. Further substitution on 5-phenol ring especially by fluorine atom at *ortho* position enhanced both the BRAF enzymatic inhibitory activity and cellular potency by approximately 2–3 folds relative to the non-fluorinated analogs [129].

Regarding the 3-pyridyl group, SAR study revealed that 3-pyridyl ring was essential for BRAF enzyme inhibitory activity. Further substitution at C-5 of the pyridyl ring by amino, acylamino and hydroxymethyl enhanced the cellular potency [129].

The results from SAR study were used to develop compound **125** as the most potent BRAF inhibitor in that study ($BRAF^{V600E}$ IC_{50} 3 nM and pERK IC_{50} 19 nM). Besides, these structure modifications were found to improve the aqueous solubility sufficiently to allow IV dosing. While, non-fluorinated analogs suffered from high clearance or low bioavailability, leading to low plasma exposures, the addition of fluorine to the 5-phenolic ring led to compounds that displayed higher bioavailability as well as lower rates of clearance from plasma. For example, the tetrahydroisoquinoline derivative **126** displayed very low clearance rate and high bioavailability [129].

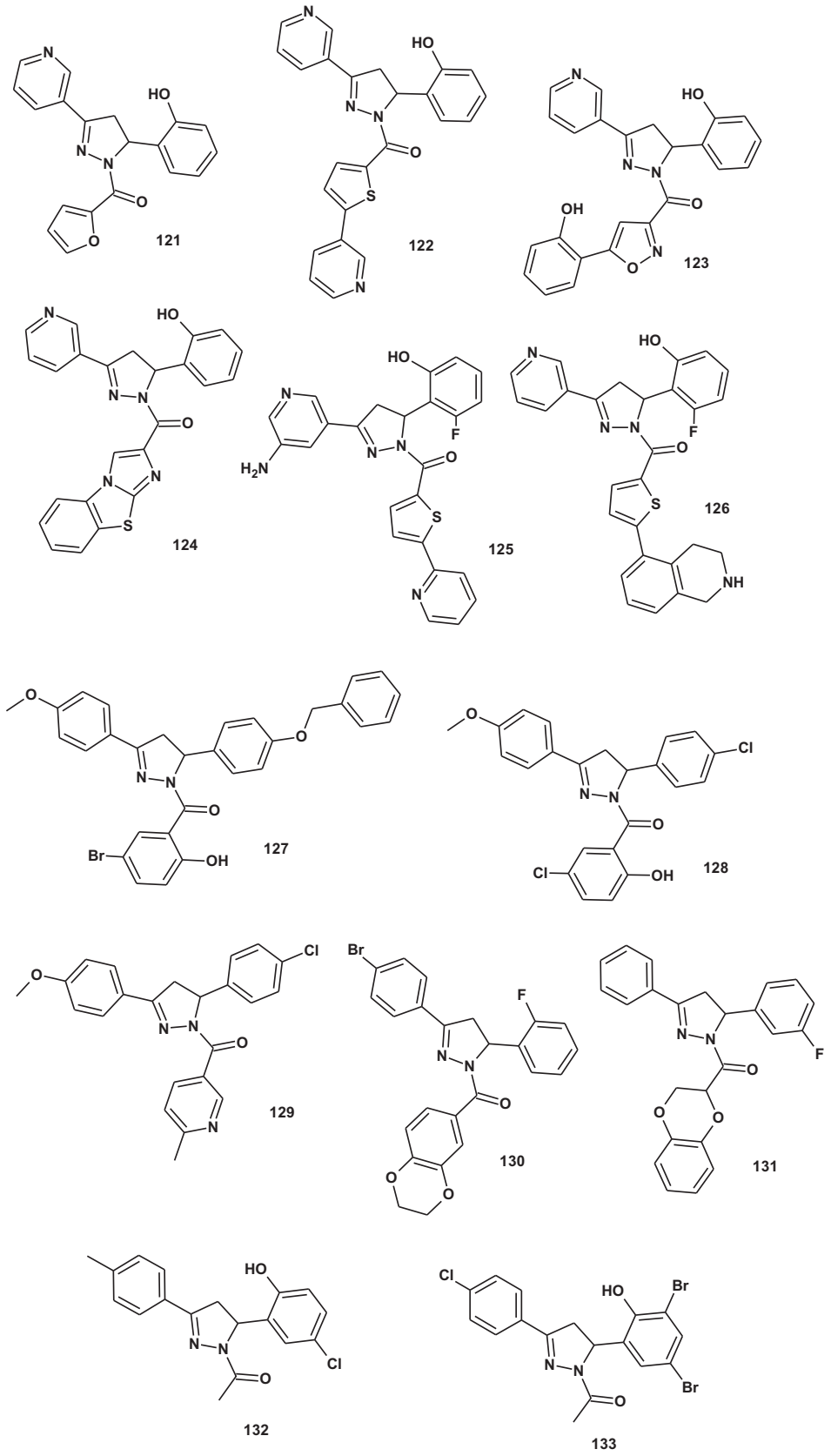

Fig. 23. Pyrazolines as BRAF inhibitors.

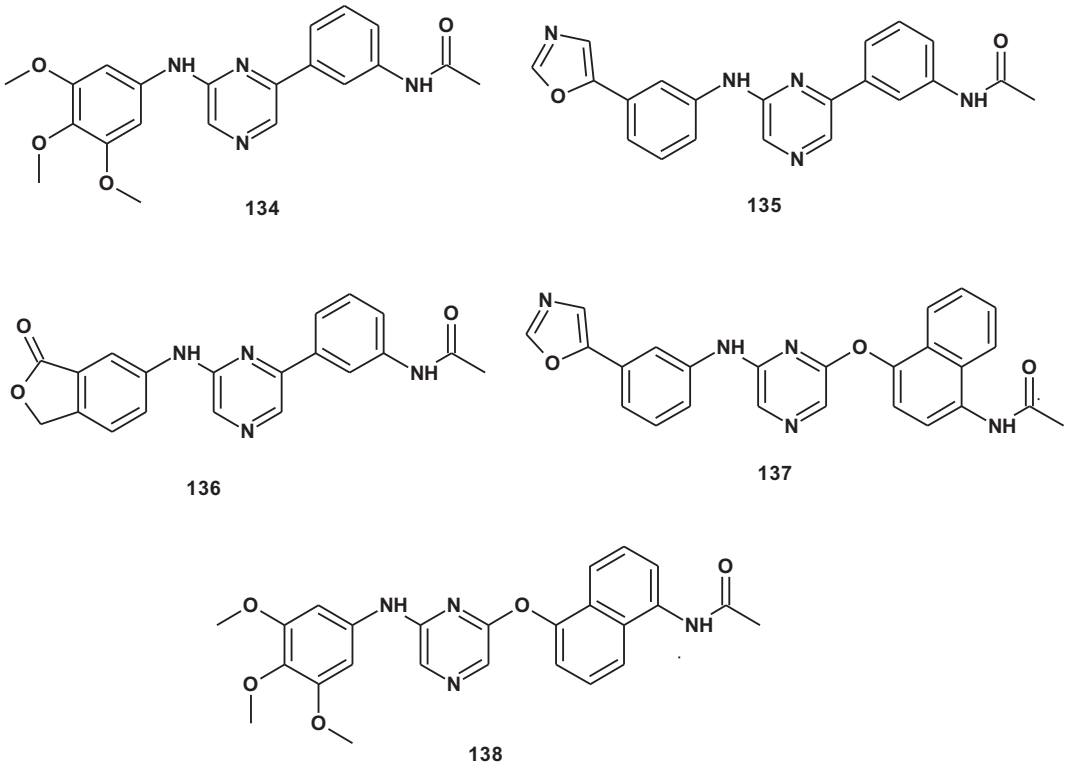

Fig. 24. Pyrazines as BRAF inhibitors.

In 2012, Li et al. reported the identification of pyrazoline salicylamide derivative **127** as $BRAF^{V600E}$ inhibitor ($BRAF^{V600E}$ IC_{50} 7.22 μM) *via in silico* and *in vitro* screening. Further structure modification afforded compound **128** as potent and selective $BRAF^{V600E}$ inhibitor ($BRAF^{V600E}$ IC_{50} 0.16 μM and pERK IC_{50} 0.81 μM). Compound **128** showed strong cytotoxic activity against mutant BRAF dependent melanoma cells WM266.4 (GI_{50} 0.24 μM) [130].

SAR study of the pyrazoline salicylamide derivatives demonstrated that *para* substitution of 5-phenyl ring with a halogen enhanced the enzyme inhibitory activity more than benzyloxy or methoxy group. Besides, strongly electron withdrawing substituents like halogens at 5 or 4 positions of salicylamide moiety were beneficial for the activity [130].

3D-QSAR study of pyrazoline salicylamide derivatives was also reported in that study. Several key features of the 3D-QSAR contour map were predicted to increase $BRAF^{V600E}$ affinity: (1) more bulk near the phenolic hydroxyl group and less bulk 5-substituent group of salicylamide ring (steric study); (2) more bulk group substituted in the *ortho* and *meta* position of 5-phenyl ring (steric study); (3) a more positive environment around the *para* position of the 4-methoxyphenyl ring and salicylamide ring (electronic study); (4) a more negative environment around the *ortho* position of salicylamide ring (electronic study) [130]. Using this result, pyrazoline derivative **129** [(5-(4-chlorophenyl)-3-(4-methoxyphenyl)-4,5-dihydro-1*H*-pyrazol-1-yl)-6-methylpyridin-3-yl methanone] was identified as potential $BRAF^{V600E}$ inhibitor ($BRAF^{V600E}$ IC_{50} 0.20 μM) with antiproliferative activity against WM266.5 human melanoma cell line (GI_{50} = 0.89 μM) [131].

Docking study of compound **129** in BRAF enzyme revealed that the molecule occupied the ATP-binding pocket and bound to an active conformation of BRAF (Type I inhibitor). The hydrophobic pocket was occupied by niacinamide substituted with methyl which confirmed the importance of hydrophobic group in niacinamide [131].

The results of 3D-QSAR models built for pyrazole niacinamide derivatives were used to modify the structure of pyrazoline inhibitors. Thus, it was assumed that replacing the niacinamide moiety with a slightly larger template which can induce a lower electron density might increase the enzyme inhibitory activity. 1,4-Benzodioxane, which was found in a variety of anticancer drugs and displayed excellent bioavailability and low cytotoxicity was tried as a template [132]. Indeed, it was reported that introduction of 2,3-dihydrobenzo[*b*][1,4]dioxin moiety greatly enhanced the $BRAF^{V600E}$ inhibitory activity of pyrazoline ring. Thus, compound **130** [2,3-dihydrobenzo[*b*][1,4]dioxin-6-yl derivative] inhibited $BRAF^{V600E}$ with IC_{50} value of 0.11 μM and showed potent cytotoxic activity against WM266.4 human melanoma cell line (GI_{50} 0.58 μM). While, compound **131** [(2,3-dihydrobenzo[*b*][1,4]dioxin-2-yl derivative] inhibited $BRAF^{V600E}$ with IC_{50} value of 1.7 μM and showed potent cytotoxic activity against WM266.4 human melanoma cell line (GI_{50} 1.45 μM) [132].

N-Acetyl pyrazoline derivatives **132** and **133** were reported in 2012 as potent and selective $BRAF^{V600E}$ inhibitors (IC_{50} 0.22 μM and 0.46 μM, respectively). Both compounds exhibited potent antiproliferative activity against MCF-7 human breast cancer cell line (IC_{50} 1.31 μM and 0.97 μM, respectively) and WM266.5 human melanoma cell line (IC_{50} 0.45 μM and 0.72 μM, respectively) [133].

SAR study of *N*-acetyl pyrazoline derivatives demonstrated that *para* electron-donating groups (like methyl and methoxy groups) at 3-phenyl ring showed more potent enzyme inhibitory activity and antiproliferative activity than analogs with *para* electron-withdrawing groups. Also, the presence of halogen atom at 3 or 5 positions of 5-phenyl ring enhanced the anticancer activity [133].

Docking study of compounds **132** and **133** in the active site of $BRAF^{V600E}$ pointed out that both compounds fit nicely in the ATP binding site of the enzyme and bound to an active conformation of $BRAF^{V600E}$. The hydroxyl group made H-bond to Ser465 and the acetamide moiety occupied the hydrophobic pocket of the ATP binding site [133].

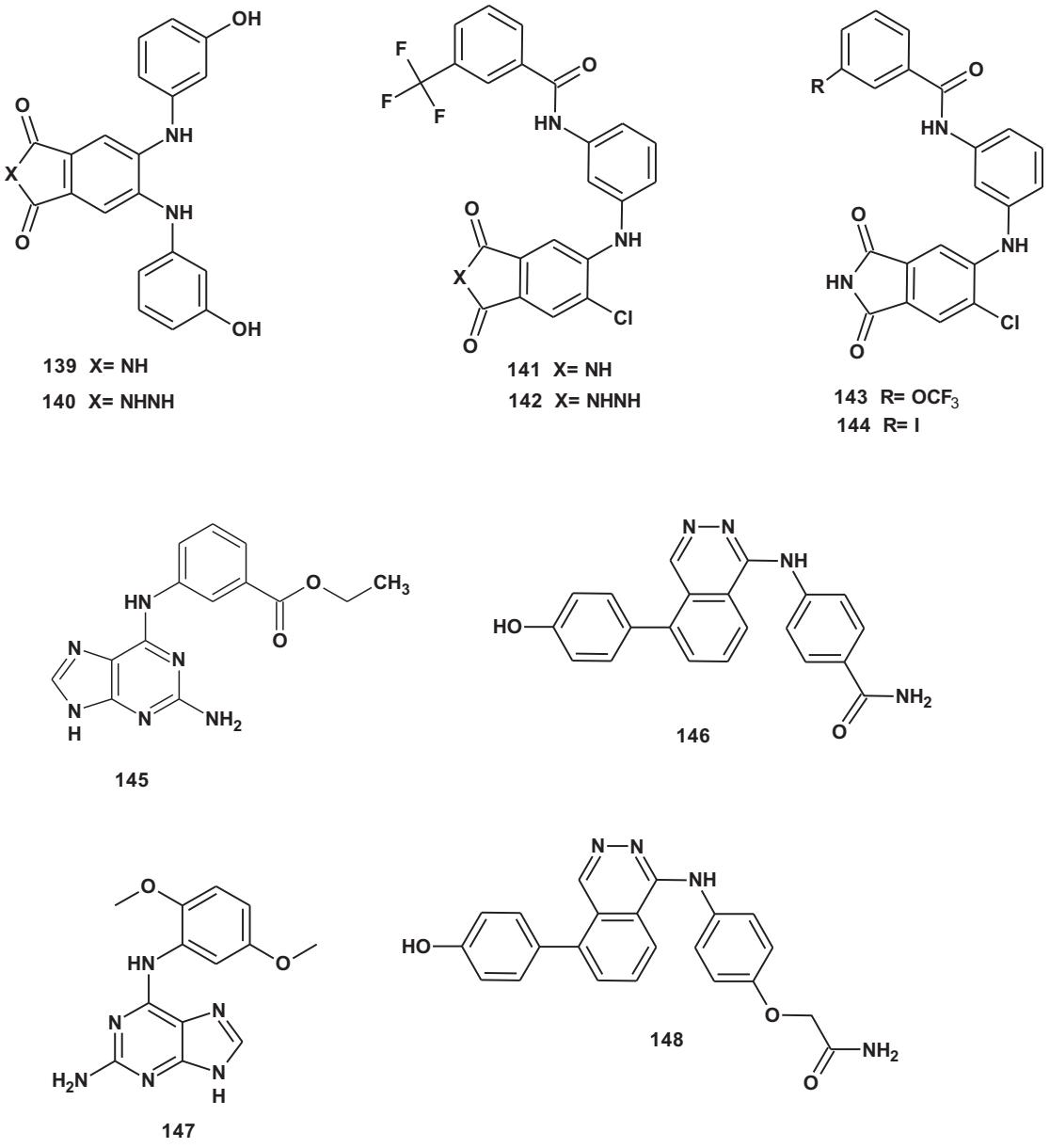

Fig. 25. Isoindoles, purines and phthalazines as BRAF inhibitors.

Recently, Tanwar and coworkers [134] reported the generation of pharmacophore model and 3D-QSAR analysis of *N*-acyl and *N*-aroylpyrazolines derivatives developed by Blackburn et al. [128].

The study demonstrated that aroyl phenyl rings should not have strong electron withdrawing substituents as they decreased both cellular and enzymatic inhibition of pyrazolines. While, addition of H-bond donor groups on aroyl groups encouraged good binding to the receptor and increased BRAF kinase inhibition. Indeed, N–H group of phenyl–pyrrole and pyrazole ring provided hydrogen atom to form H-bond with the receptor amino acids. The results also demonstrated that addition of electron withdrawing groups at pyridine ring site and phenolic ring site decreased the affinity toward $BRAF^{V600E}$ [134].

2.15. Pyrazine derivatives

In 2006, Niculescu-Duvaz and coworkers described the identification of 2-(3,4,5-trimethoxyphenylamino)-6-(3-acetamidophenyl)pyrazine **134** (Fig. 24) through high-throughput screening as potent $BRAF^{V600E}$ inhibitor with IC_{50} of 3.5 μM. Structure modification which was based mainly on replacement of 2-(3,4,5-trimethoxyphenylamino) by other aryl and heteroaryl rings led to identification of two potent $BRAF^{V600E}$ inhibitors, namely compounds **135** and **136** [135].

The 3-oxazolylphenylamino derivative **135** exhibited $BRAF^{V600E}$ inhibitory activity with IC_{50} of 0.79 μM while, 2-(3-oxo-1,3-dihydroisobenzofuran-5-ylamino) derivative **136** showed $BRAF^{V600E}$ inhibitory activity with IC_{50} of 0.74 μM [135].

SAR study of pyrazine derivatives indicated that substitution at position 4 of the phenylamino residue abolished the enzyme inhibitory activity. However, introduction of bulky substituents to improve the solubility (for example morpholine) retained the potency against $BRAF^{V600E}$. Furthermore, the NH group at position 2 of the pyrazine ring appeared to be essential for biological activity and its methylation led to complete loss of activity [135].

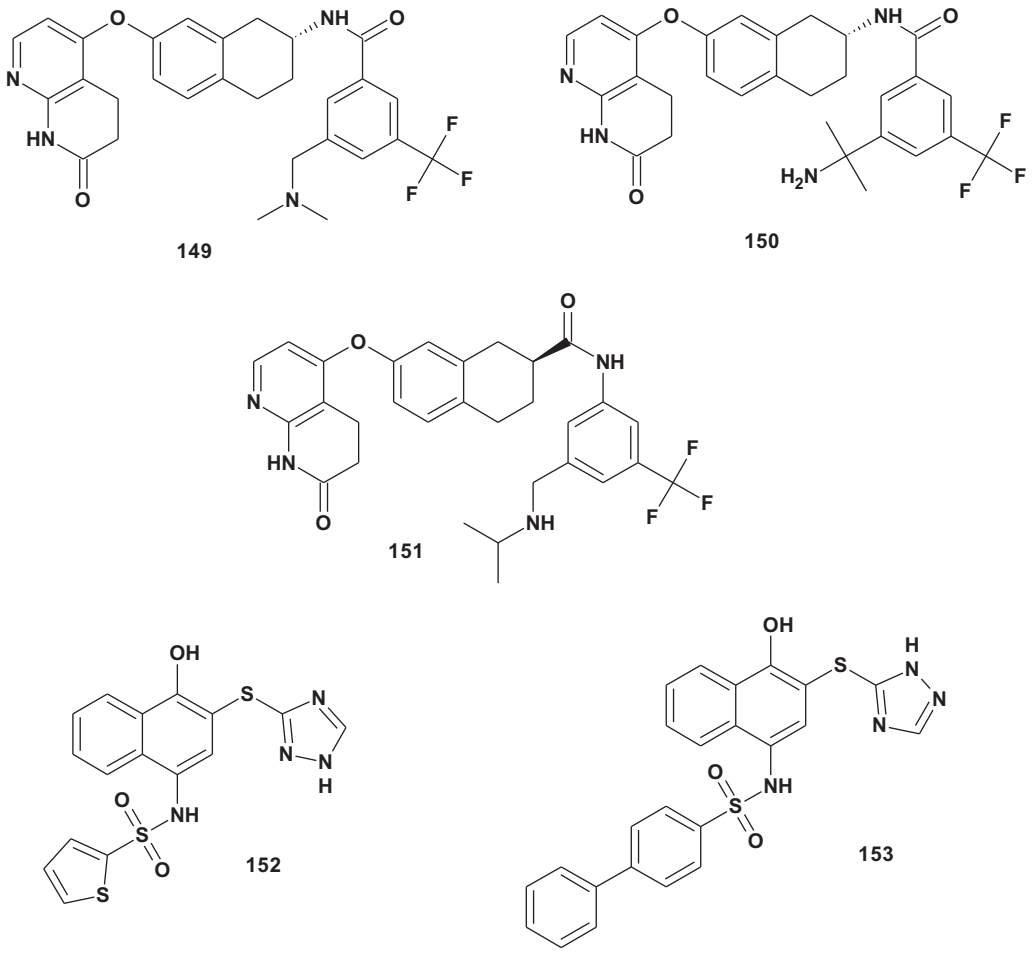

Fig. 26. Naphthalenes as BRAF inhibitors.

Structure modification of the pyrazine ring and the phenylacetamido moiety were reported two years later aiming to increase the selectivity towards $BRAF^{V600E}$ over CRAF [136]. The phenylacetamido group proved to be essential for optimum activity and the presence of the acetamide group at position 3 of the phenyl ring was also essential for the $BRAF^{V600E}$ inhibitory activity. Replacement of the pyrazine ring by other heterocycles such as pyrimidine or pyridazine abolished the activity, only pyridine ring was tolerated but yielded less active compounds. Besides, the presence of linker especially oxygen linker between the pyrazine and the phenylacetamido group was also tolerated. Combining the most effective structural feature resulting from these two studies afforded two potent pyrazine derivatives **137** and **138** with $BRAF^{V600E}$ IC_{50} of 0.31 μM and 0.41 μM, respectively [136].

2.16. Isoindole, purine and phthalazine derivatives

In 2011, Wanga and coworkers from Pfizer Worldwide Research and Development recorded the discovery of novel chemical scaffolds as type I and type II selective BRAF inhibitors using structure-guided design. The scaffolds discovered were isoindoline-1,3-dione and 2,3-dihydrophthalazine-1,4-dione. Both scaffolds showed good activity against BRAF and their potency increased upon substitution of the phenyl ring with large *meta* lipophilic substituents such as iodo and trifluoromethyl groups. Compounds **139** and **140** (Fig. 25) were considered as type I kinase inhibitors with BRAF IC_{50} equal to 0.338 μM and 0.290 μM, respectively [137].

Type II inhibitors were also developed using the same chemical scaffolds *via* incorporation of a lipophilic group at an appropriate position to fill the pocket created by the movement of DFG motif. Therefore, the phenolic group was replaced by the benzamide group which could form two H-bonds with Glu501 and Asp594, while the phenyl group could extend to the allosteric pocket in DFG-out conformation. Compounds **141**–**144** were considered as type II inhibitors and exhibited BRAF IC_{50} equal to 0.01 μM, 0.017 μM, 0.006 μM and 0.008 μM, respectively [137].

Using structure-based virtual screening, a group of Korean researchers were able to identify novel BRAF inhibitors that possessed favorable physicochemical properties. The structure-based virtual screening was conducting with docking simulations taking into consideration the effects of ligand solvation in the scoring function and thus enhancing the accuracy in predicting the binding affinity. The screened compounds were filtrated on the basis of Lipinski's 'Rule of Five' prior to the virtual screening with docking simulations to ensure good physicochemical properties of the selected compounds. Of the different scaffold identified, the 9*H*-purine derivative **145** [phenyl-(9*H*-purin-6-yl) amine] and the phthalazine derivative **146** [(phenyl-5-phenyl-phthalazin-1-yl)amine] exhibited very good binding affinity (BRAF K_d 0.7 μM and 2.1 μM, respectively). Both rings mimicked the adenine ring of ATP and thus both compounds might act as ATP competitive inhibitors, a postulation which was suggested also through careful examination of the docking modes of both compounds [138]. In analogous study, the purine and phthalazine derivatives **145** and **146** were structurally developed to afford the

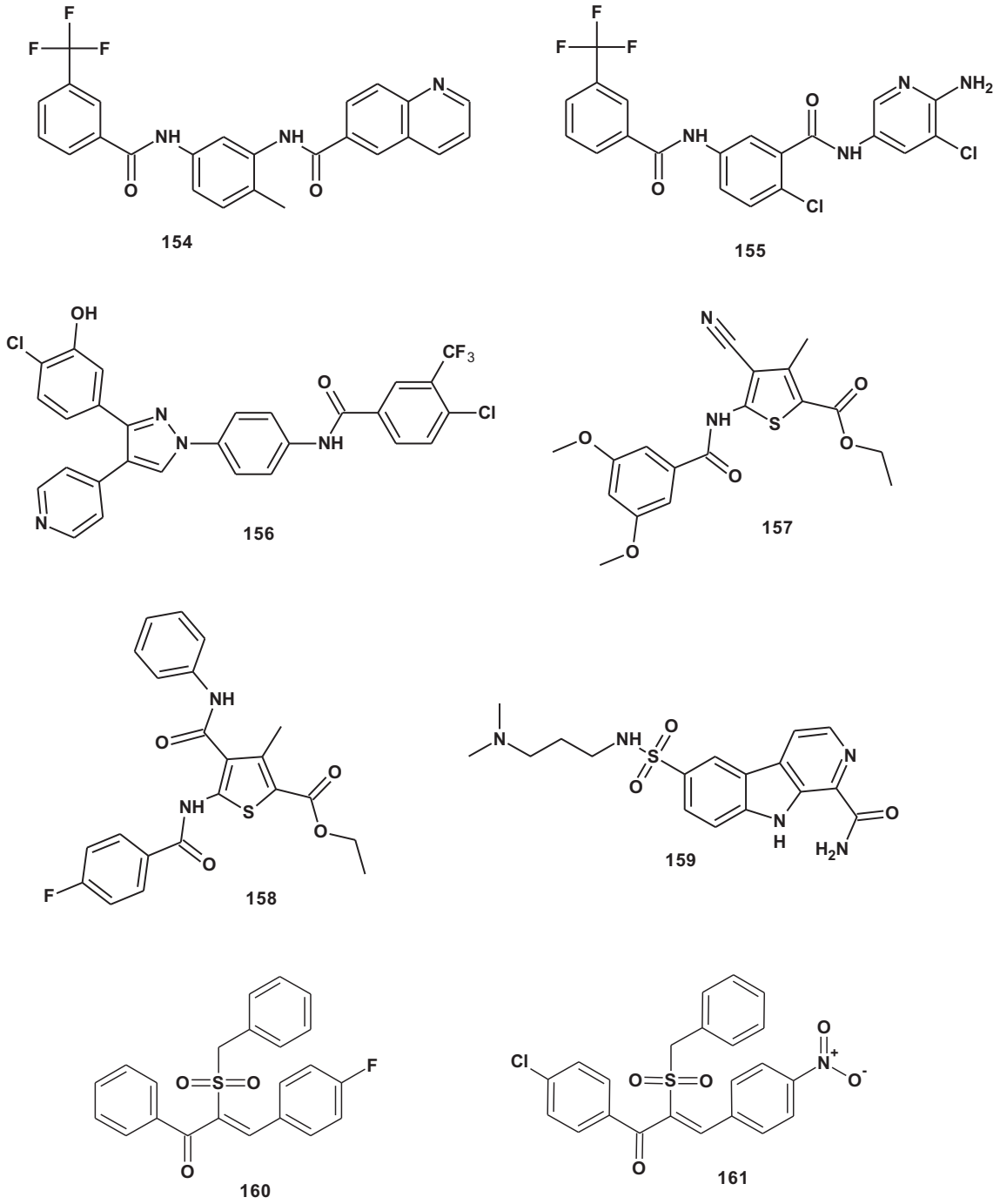

Fig. 27. Amides, ureas, carbolines and chalcones as BRAF inhibitors.

purine derivative **147** with K_d 0.43 μM and the phthalazine derivative **148** with K_d 2.5 μM [139].

2.17. Naphthalene derivatives

In 2011, Gould et al. reported the first published work on the discovery of tetrahydronaphthalene derivatives **149**–**151** (Fig. 26) as potent *in vitro* and *in vivo* inhibitors of the BRAF ($BRAF^{V600E}$ IC_{50} 2.7, 2.1 nM and 3.3 nM, respectively) (pERK IC_{50} 50 nM, 60 nM and 110 nM, respectively). Compounds **149** and **150** displayed good pharmacokinetic properties in rats and inhibited BRAF mutant tumor growth in mouse xenograft models. Compound **151** showed very good *in vivo* clearance [84].

Those compounds were developed in an attempt to modify the structure of compound **37**. Thus, cyclization of the pyridine amide group in compound **37** into a lactam ring provided potent compounds with improved oral exposures such as compound **151** [84]. Further improvement in enzyme and cellular potency was obtained by reversing the internal amide group such as in compounds **149** and **150** which displayed excellent cellular potency and PK properties [84].

ELISA based high-throughput screening was conducted to identify quinolol/naphthol derivative **152** as potent and selective inhibitor of $BRAF^{V600E}$ (BRAF IC_{50} of 100 nM) that conferred special selectivity for $BRAF^{V600E}$ over $BRAF^{WT}$ and other kinases. The X-ray crystal structure of a BRAF/quinolol complex revealed that these

compounds act as type I inhibitors that bound to the ATP pocket in the active conformation [140].

Replacement of the thiotriazole moiety in compound **152** with a hydrogen or halogen atom reduced enzyme potency. Substitutions on the naphthol ring system had significant effects on $BRAF^{V600E}$ enzyme potency. Thus, substitutions with thienylsulfonamide group as in compound **152** significantly enhanced the enzyme and cellular potency. Besides, aryl bearing sulfonamides were more potent inhibitors than aliphatic bearing sulfonamides [140].

The most potent $BRAF^{V600E}$ inhibitor identified in that study was compound **153** ($BRAF^{V600E}$ IC_{50} 0.08 μM). The latter showed significant selectivity for $BRAF^{V600E}$ and $BRAF^{WT}$ over the other kinases. Compound **153** showed *in vitro* antiproliferative activity on mutant BRAF melanoma cell line [140].

2.18. Amide and urea derivatives

In 2009, Lyne et al. from AstraZeneca reported the identification of compound **154** (Fig. 27) as promising hit compound that displayed potent inhibitory activity against $BRAF^{V600E}$ (IC_{50} 0.002 μM) with potent cellular activity (pERK IC_{50} 0.64 μM) as well as antiproliferative activity against Colo205 cell line with GI_{50} 5.9 μM [90].

SAR study of these amide analogs pointed out that replacement of quinolone ring in compound **154** with the smaller monocyclic 3-pyridyl ring afforded potent enzyme inhibitor ($BRAF^{V600E}$ IC_{50} 0.049 μM), however, the cellular potency was very low (pERK $IC_{50} > 30$ μM). A significant increase in enzymatic and cellular potency was achieved by reversing the amide linker ($BRAF^{V600E}$ IC_{50} 0.007 μM and pERK IC_{50} 1.4 μM) [90]. Furthermore, replacement the methyl group in the middle phenyl ring with chloro substituent resulted in reduced metabolism without impacting cellular potency. Also, substitution at the 2- and 3-positions of the pyridyl ring enhanced the cellular potency [90].

As a result of this study, compound **155** was identified as potent and selective $BRAF^{V600E}$ inhibitor with $BRAF^{V600E}$ IC_{50} 0.027 μM, pERK IC_{50} 0.08 μM and displayed antiproliferative activity against Colo205 cell line with GI_{50} 0.86 μM [90]. Compound **155** also displayed *in vivo* antitumor activity against A375 tumor cell line as well as good pharmacokinetic profile following oral dose in rodent [90].

Diarylureas and diarylamides carrying 1,3,4-triarylpyrazole scaffold were reported in 2011 as potent BRAF inhibitors that showed high *in vitro* antiproliferative potency against nine human melanoma cell lines [141]. Compound **156** showed high, dose-dependent inhibition of ERK kinase which might assume that the cytotoxic activity was due to inhibition of ERK or $BRAF^{V600E}$ enzymes [141]. SAR study of the synthesized compounds indicated that the hydroxyl group on position 3 of the *p*-chlorophenyl pyrazolyl moiety was optimal for the antiproliferative activity. Besides, the presence of amide linker was optimal for activity and was superior to urea linker [141].

In 2013, *N*-(thiophen-2-yl) benzamide derivatives **157** and **158** were identified through virtual screening as potent and selective $BRAF^{V600E}$ inhibitors (IC_{50} 0.77 μM and 0.63 μM, respectively) [142]. These derivatives were designed to act as type I $BRAF^{V600E}$ kinase inhibitors. SAR study of these analogs revealed that the presence of ethyl ester group at position 2 of the thiophene ring and disubstituted phenyl moiety at the benzamide group enhanced the enzyme inhibitory activity [142].

2.19. Carboline derivatives

In 2012, a group of Chinese researchers reported the synthesis of 1-carboxamide and 6-sulfonamide-substituted β-carboline derivatives as inhibitors of wild type BRAF kinase enzyme. These compounds were designed to bind to the hinge region of the enzyme [143].

The carboline scaffold was chosen to mimic Sorafenib by ring fusion of the pyridyl and phenyl rings in tricyclic ring system and scaffold hopping of the resulting ring into β-carboline ring. Besides, the sulfonamide moiety was integrated onto the 6-position of the β-carboline ring as DFG loop binder to form H-bonds as reported for the sulfonamide moiety of PLX4032 [45,95,143].

Compound **159** [1-carboxamide-6-(*N*-(3-(dimethylamino)propyl)-sulfamoyl)-β-carboline] (Fig. 27) was the most potent BRAF inhibitor discovered in that study with IC_{50} 1.62 μM [143].

Regarding the substitution on the sulfonamide moiety, it was found that *N*,*N*-dimethylaminopropyl moiety was optimal for the inhibitory activity.

Replacement of the *N*,*N*-dimethylamino group with diethylamino group had little effect on the inhibitory activity, while its deletion or replacement by methoxy or hydroxyl groups greatly decreased the inhibitory activity. In addition, unsubstituted aromatic rings and aromatic heterocycles were also tolerated at that position. On the other hand, the carboxamide group on the carboline ring was not essential for the inhibitory activity and its removal resulted in potent BRAF inhibitors [143].

2.20. Chalcone derivatives

In 2012, Li and coworkers reported the identification of (*E*)-α-benzylsulfonyl chalcone derivative **160** (Fig. 27) as a new $BRAF^{V600E}$ inhibitor ($BRAF^{V600E}$ IC_{50} 1.04 μM) through *in silico* and *in vitro* screening. Structure modification of compound **160** afforded the chalcone derivative **161** as potent and selective $BRAF^{V600E}$ inhibitor ($BRAF^{V600E}$ IC_{50} 0.17 μM). Compound **161** displayed potent antiproliferative activity against BRAF mutant melanoma cell line WM266.4 (GI_{50} 0.52 μM). The results of cell based pERK activity and cellular selectivity indicated that compound **161** selectively inhibited proliferation of mutant BRAF-dependent melanoma cell line through inhibition of oncogenic BRAF. Docking studies performed on compound **160** indicated that it was tightly embedded into the ATP-binding pocket [144].

3. Conclusion

In summary, many BRAF inhibitors have been discovered that act by either ATP competitive inhibition (type I kinase inhibitors) or by binding in an allosteric site of BRAF (type II kinase inhibitors). These inhibitors block the RAS/BRAF/MEK/ERK pathway and arrest many cellular functions resulting in cell death in proliferative tissues.

The approval of Sorafenib and Vemurafenib by FDA for the treatment of metastatic melanoma encouraged further research to discover more potent and selective BRAF inhibitors. Indeed, many BRAF inhibitors are currently under clinical investigation in phase I–III for the treatment of different types of cancer especially melanoma.

Owing to the heterogenetic nature of cancer, multitarget drugs or drug combinations that act on different targets may provide better therapeutic strategy for cancer treatment. Indeed, compounds that act by dual inhibition of $BRAF^{V600E}$ and EGFR have been discovered and exhibited potent antitumor activity. Besides, combination of RAF and MEK inhibitors were reported to exert potent anticancer activity while alleviating the undesired proliferative effects of RAF inhibitors. This combination can also reduce the incidence of resistance to RAF inhibitors which were discovered recently in many clinical trials.

References

[1] J.A. Sparano, Ras/Raf/MEK Inhibitors, Cancer Drug Discovery and Development: Molecular Targeting in Oncology, 2008, pp. 55–73.
[2] L.M. Caronia, J.E. Phay, M.H. Shah, Clin. Cancer Res. 17 (2011) 7511–7517.
[3] J.S. Sebolt-Leopold, R. Herrera, Nat. Rev. Cancer 4 (2004) 937–947.
[4] P. Blume-Jensen, T. Hunter, Nature 411 (2001) 355–365.
[5] A. Zebisch, J. Troppmair, Cell. Mol. Life Sci. 63 (2006) 1314–1330.
[6] M. Beeram, A. Patnaik, E.K. Rowinsky, J. Clin. Oncol. 23 (2005) 6771–6790.
[7] R. Roskoski, Biochem. Biophys. Res. Commun. 399 (2010) 313–317.
[8] L.F. Stancato, M. Sakatsume, M. David, P. Dent, f. Dong, E.F. Petricoin, J.J. Krolewski, O. Silvennoinen, P. Saharinen, J. Pierce, C.J. Marshall, T. Sturgill, D.S. Finbloom, A.C. Larner, Mol. Cell. Biol. 17 (1997) 3833–3840.
[9] W. Kolch, G. Heidecker, G. Kochs, R. Hummel, H. Vahidi, H. Mischak, G. Finkenzeller, D. Marmé, U.R. Rapp, Nature 364 (1993) 249–252.
[10] B. Yao, Y. Zhang, S. Delikat, S. Mathias, S. Basu, R. Kolesnick, Nature 378 (1995) 307–310.
[11] U. Kasid, S. Suy, P. Dent, S. Ray, T.L. Whiteside, T.W. Sturgill, Nature 382 (1996) 813–816.
[12] B. Hoyos, A. Imam, I. Korichneva, E. Levi, R. Chua, U. Hammerling, J. Biol. Chem. 277 (2002) 23949–23957.
[13] P.A. Tilbrook, S.M. Colley, D.J. McCarthy, R. Marais, S.P. Klinken, Arch. Biochem. Biophys. 396 (2001) 128–132.
[14] Z. Luo, G. Tzivion, P.J. Belshaw, D. Vavvas, M. Marshall, J. Avruch, Nature 383 (1996) 181–185.
[15] C.K. Weber, J.R. Slupsky, H.A. Kalmes, U.R. Rapp, Cancer Res. 61 (2001) 3595–3598.
[16] C. Wellbrock, M. Karasarides, R. Marais, Nat. Rev. Mol. Cell Biol. 5 (2004) 875–885.
[17] P.T.C. Wan, M.J. Garnett, S.M. Roe, S. Lee, D. Niculescu-Duvaz, V.M. Good, C.M. Jones, C.J. Marshall, C.J. Springer, D. Barford, R. Marais, Cell 116 (2004) 855–867.
[18] L.K. Rushworth, A.D. Hindley, E. O'Neill, W. Kolch, Mol. Cell. Biol. 26 (2006) 2262–2272.
[19] P.I. Poulikakos, C. Zhang, G. Bollag, K.M. Shokat, N. Rosen, Nature 464 (2010) 427–430.
[20] A. Baljuls, B.N. Kholodenko, W. Kolch, Mol. BioSyst. 9 (2013) 551–558.
[21] H. Davies, G.R. Bignell, C. Cox, P. Stephens, S. Edkins, S. Clegg, J. Teague, H. Woffendin, M.J. Garnett, W. Bottomley, N. Davis, E. Dicks, R. Ewing, Y. Floyd, K. Gray, S. Hall, R. Hawes, J. Hughes, V. Kosmidou, A. Menzies, C. Mould, A. Parker, C. Stevens, S. Watt, S. Hooper, R. Wilson, H. Jayatilake, B.A. Gusterson, C. Cooper, J. Shipley, D. Hargrave, K. Pritchard-Jones, N. Maitland, G. Chenevix-Trench, G.J. Riggins, D.D. Bigner, G. Palmieri, A. Cossu, A. Flanagan, A. Nicholson, J.W.C. Ho, S.Y. Leung, S.T. Yuen, B.L. Weber, H.F. Seigler, T.L. Darrow, H. Paterson, R. Marais, C.J. Marshall, R. Wooster, M.R. Stratton, P.A. Futreal, Nature 417 (2002) 949–954.
[22] M.J. Garnett, R. Marais, Cancer Cell 6 (2004) 313–319.
[23] N.J. Dibb, S.M. Dilworth, C.D. Mol, Nat. Rev. Cancer 4 (2004) 718–727.
[24] Y. Cohen, M. Xing, E. Mambo, Z. Guo, G. Wu, B. Trink, U. Beller, W.H. Westra, P.W. Landenson, D. Sidransky, J. Natl. Cancer Inst. 95 (2003) 625–627.
[25] X. Xu, R.M. Quiros, P. Gattuso, K.B. Ain, R.A. Prinz, Cancer Res. 63 (2003) 4561–4567.
[26] J.H. Lee, E.S. Lee, Y.S. Kim, Cancer 110 (2007) 38–46.
[27] D.S. Hong, L. Vence, G. Falchook, L.G. Radvanyi, C. Liu, V. Goodman, J.J. Legos, S. Blackman, A. Scarmadio, R. Kurzrock, G. Lizee, P. Hwu, Clin. Cancer Res. 18 (2012) 2326–2335.
[28] R. Kudchadkar, K.H. Paraiso, K.S. Smalley, Cancer J. 18 (2012) 124–131.
[29] K. Kalinsky, F.G. Haluska, Expert Rev. Anticancer Ther. 7 (2007) 715–724.
[30] D.S. Dhillon, S. Hagan, O. Rath, W. Kolch, Oncogene 26 (2007) 3279–3290.
[31] C. Wellbrock, L. Ogilvie, D. Hedley, M. Karasarides, J. Martin, D. Niculescu-Duvaz, C.J. Springer, R. Marais, Cancer Res. 64 (2004) 2338–2342.
[32] V. Gray-Schopfer, C. Wellbrock, R. Marais, Nature 445 (2007) 851–857.
[33] J.A. Sommers, S. Sharma, K.M. Doherty, P. Karmakar, Q. Yang, M.K. Kenny, C.C. Harris, R.M. Brosh, Cancer Res. 65 (2005) 1223–1233.
[34] X. Wang, J. Kim, J. Med. Chem. 55 (2012) 7332–7341.
[35] G.R. Alton, E.A. Lunney, Expert Opin. Drug Discov. 3 (2008) 595–605.
[36] A. Backes, B. Zech, B. Felber, B. Klebl, G. Muller, Expert Opin. Drug Discov. 3 (2008) 1409–1425.
[37] A. Backes, B. Zech, B. Felber, B. Klebl, G. Muller, Expert Opin. Drug Discov. 3 (2008) 1427–1449.
[38] Y. Liu, N.S. Gray, Nat. Chem. Biol. 2 (2006) 358–364.
[39] J.L. Liao, Curr. Top. Med. Chem. 7 (2007) 1332–1335.
[40] F. Lovering, J. McDonald, G.A. Whitlock, P.A. Glossop, C. Phillips, A. Bent, Y. Sabnis, M. Ryan, L. Fitz, J. Lee, J.S. Chang, S. Han, R. Kurumbail, A. Thorarensen, Chem. Biol. Drug Des. 80 (2012) 657–664.
[41] A.J. King, D.R. Patrick, R.S. Batorsky, M.L. Ho, H.T. Do, S.Y. Zhang, R. Kumar, D.W. Rusnak, A.K. Takle, D.M. Wilson, E. Hugger, L. Wang, F. Karreth, J.C. Lougheed, J. Lee, D. Chau, T.J. Stout, E.W. May, C.M. Rominger, M.D. Schaber, L. Luo, A.S. Lakdawala, J.L. Adams, R.G. Contractor, K.S.M. Smalley, M. Herlyn, M.M. Morrissey, D.A. Tuveson, P.S. Huang, Cancer Res. 66 (2006) 11100–11105.
[42] D.-H. Kim, T. Sim, Arch. Pharm. Res. 35 (2012) 605–615.
[43] E. Besteman, J.-G. Bienvenu, I. Chaudhary, M. Cukierski, B. Marsh, B. Surprenant, in: Proceedings of the 101st Annual Meeting of the AACR, American Association for Cancer Research, Philadelphia, PA, 2010. Abstract 1677.
[44] J. Dietrich, C. Hulme, L.H. Hurley, Bioorg. Med. Chem. 18 (2010) 5738–5748.
[45] G. Boltag, P. Hirth, J. Tsai, J. Zhang, P.N. Ibrahim, H. Cho, W. Spevak, C. Zhang, Y. Zhang, G. Habets, E.A. Burton, B. Wong, G. Tsang, B.L. West, B. Powell, R. Shellooe, A. Marimuthu, H. Nguyen, K.Y.J. Zhang, D.R. Artis, J. Schlessinger, F. Su, B. Higgins, R. Iyer, K.D. Andrea, A. Koehler, M. Stumm, P.S. Lin, R.J. Lee, J. Grippo, I. Puzanov, K.B. Kim, A. Ribas, G.A. McArthur, J.A. Sosman, P.B. Chapman, K.T. Flaherty, X. Xu, K.L. Nathanson, K. Nolop, Nature 467 (2010) 596–599.
[46] T. Eisen, T. Ahmad, K.T. Flaherty, M. Gore, S. Kaye, R. Marais, I. Gibbens, S. Hackett, M. James, L.M. Schuchter, K.L. Nathanson, C. Xia, R. Simantov, B. Schwartz, M. Poulin-Costello, P.J. O'Dwyer, M.J. Ratain, Br. J. Cancer 95 (2006) 581–586.
[47] K.T. Flaherty, I. Puzanov, K.B. Kim, A. Ribas, G.A. McArthur, J.A. Sosman, P.J. O'Dwyer, R.J. Lee, J.F. Grippo, K. Nolop, P.B. Chapman, N. Engl. J. Med. 363 (2010) 809–819.
[48] P.B. Chapman, A. Hauschild, C. Robert, J.B. Haanen, P. Ascierto, J. Larkin, R. Dummer, C. Garbe, A. Testori, M. Maio, D. Hogg, P. Lorigan, C. Lebbe, T. Jouary, D. Schadendorf, A. Ribas, S.J. O'Day, J.A. Sosman, J.M. Kirkwood, A.M. Eggermont, B. Dreno, K. Nolop, J. Li, B. Nelson, J. Hou, R.J. Lee, K.T. Flaherty, G.A. McArthur, N. Engl. J. Med. 364 (2011) 2507–2516.
[49] K.P. Hoeflich, S. Herter, J. Tien, L. Wong, L. Berry, J. Chan, C. O'Brien, Z. Modrusan, S. Seshagiri, M. Lackner, H. Stern, E. Choo, L. Murray, L.S. Friedman, M. Belvin, Cancer Res. 69 (2009) 3042–3051.
[50] J. Carnahan, P.J. Beltran, C. Babij, Q. Le, M.J. Rose, S. Vonderfecht, J.L. Kim, A.L. Smith, K. Nagapudi, M.A. Broome, M. Fernando, H. Kha, B. Belmontes, R. Radinsky, R. Kendall, T.L. Burgess, Mol. Cancer Ther. 9 (2010) 2399–2410.
[51] E.R. Cantwell-Dorris, J.J. O'Leary, O.M. Sheils, Mol. Cancer. Ther. 10 (2011) 385–394.
[52] J.R. Infante, G.S. Falchook, D.P. Lawrence, R.F. Weber, R.F. Kefford, J.C. Bendell, R. Kurzrock, G. Shapiro, R.R. Kudchadkar, G.V. Long, H.A. Burris, K.B. Kim, A. Clements, S. Peng, B. Yi, A.J. Allred, D. Ouellet, K. Patel, P.F. Lebowitz, K.T. Flaherty, J. Clin. Oncol. 29 (Suppl.) (2011). Abstract CRA8503.
[53] V. Khazak, I. Astsaturov, I. Serebriiski, E. Golemis, Expert Opin. Ther. Targets 11 (2007) 1587–1609.
[54] N. Li, D. Batt, M. Warmuth, Curr. Opin. Invest. Drugs 8 (2007) 452–456.
[55] C. Shepherd, I. Puzanov, J.A. Sosman, Curr. Oncol. Rep. 12 (2010) 146–152.
[56] R. Dienstmann, J. Tabernero, Anti-Cancer Agents Med. Chem. 11 (2011) 285–295.
[57] A. Zambon, I. Niculescu-Duvaz, D. Niculescu-Duvaz, R. Marais, C.J. Springer, Bioorg. Med. Chem. Lett. 22 (2012) 789–792.
[58] R. Nazarian, H. Shi, Q. Wang, X. Kong, R.C. Koya, H. Lee, Z. Chen, M.K. Lee, N. Attar, H. Sazegar, T. Chodon, S.F. Nelson, G. McArthur, J.A. Sosman, A. Ribas, R.S. Lo, Nature 468 (2010) 973–977.
[59] P.I. Poulikakos, Y. Persaud, M. Janakiraman, X. Kong, C. Ng, G. Moriceau, H. Shi, M. Atefi, B. Titz, M.T. Gabay, M. Salton, K.B. Dahlman, M. Tadi, J.A. Wargo, K.T. Flaherty, M.C. Kelley, T. Misteli, P.B. Chapman, J.A. Sosman, T.G. Graeber, A. Ribas, R.S. Lo, N. Rosen, D.B. Solit, Nature 480 (2011) 387–390.
[60] D.B. Solit, N. Rosen, N. Engl. J. Med. 364 (2011) 772–774.
[61] J. Villanueva, A. Vultur, M. Herlyn, Cancer Res. 71 (2011) 7137–7140.
[62] H. Shi, G. Moriceau, X. Kong, M.K. Lee, H. Lee, R.C. Koya, C. Ng, T. Chodon, R.A. Scolyer, K.B. Dahlman, J.A. Sosman, R.F. Kefford, G.V. Long, S.F. Nelson, A. Ribas, R.S. Lo, Nat. Commun. 3 (2012) 724–739.
[63] K.H. Paraiso, K.S. Smalley, Cancer Discov. 2 (2012) 390–392.
[64] F. Su, W.D. Bradley, Q. Wang, H. Yang, L. Xu, B. Higgins, K. Kolinsky, K. Packman, M.J. Kim, K. Trunzer, R.J. Lee, K. Schostack, J. Carter, T. Albert, S. Germer, J. Rosinski, M. Martin, M.E. Simcox, B. Lestini, D. Heimbrook, G. Bollag, Cancer Res. 72 (2012) 969–978.
[65] S. Giroux, Bioorg. Med. Chem. Lett. 23 (2013) 394–401.
[66] L. Finn, S.N. Markovic, R.W. Joseph, BMC Med. 10 (2012) 23–32.
[67] A.K. Takle, M.J.B. Brown, S. Davies, D.K. Dean, G. Francis, A. Gaiba, A.W. Hird, F.D. King, P.J. Lovell, A. Naylor, A.D. Reith, J.G. Steadman, D.M. Wilson, Bioorg. Med. Chem. Lett. 16 (2006) 378–381.
[68] D. Niculescu-Duvaz, I. Niculescu-Duvaz, B.M.J.M. Suijkerbuijk, D. Ménard, A. Zambon, A. Nourry, L. Davies, H.A. Manne, F. Friedlos, L. Ogilvie, D. Hedley, A.K. Takle, D.M. Wilson, J.-F. Pons, T. Coulter, R. Kirk, N. Cantarino, S. Whittaker, R. Marais, C.J. Springer, Bioorg. Med. Chem. 18 (2010) 6934–6952.
[69] A.K. Takle, M.J. Bamford, S. Davies, R.P. Davis, D.K. Dean, A. Gaiba, E.A. Irving, F.D. King, A. Naylor, C.A. Parr, A.M. Ray, A.D. Reith, B.B. Smith, P.C. Staton, J.G.A. Steadman, T.O. Stean, D.M. Wilson, Bioorg. Med. Chem. Lett. 18 (2008) 4373–4376.
[70] J. Dietrich, V. Gokhale, X. Wanga, L.H. Hurley, G.A. Flynn, Bioorg. Med. Chem. 18 (2010) 292–304.
[71] N. Sakai, S. Imamura, N. Miyamoto, T. Hirayama, WIPO Patent Application WO 2008/016192, Feb. 7, 2008.
[72] M. Okaniwa, M. Hirose, T. Imada, T. Ohashi, Y. Hayashi, T. Miyazaki, T. Arita, M. Yabuki, K. Kakoi, J. Kato, T. Takagi, T. Kawamoto, S. Yao, A. Sumita, S. Tsutsumi, T. Tottori, H. Oki, B.-C. Sang, J. Yano, K. Aertgeerts, S. Yoshida, T. Ishikawa, J. Med. Chem. 55 (2012) 3452–3478.
[73] D. Niculescu-Duvaz, I. Niculescu-Duvaz, B.M.J.M. Suijkerbuijk, D. Ménard, A. Zambon, L. Davies, J.-F. Pons, S. Whittaker, R. Marais, C.J. Springer, Bioorg. Med. Chem. 21 (2013) 1284–1304.

[74] S. Ramurthy, S. Subramanian, M. Aikawa, P. Amiri, A. Costales, J. Dove, S. Fong, J.M. Jansen, B. Levine, S. Ma, C.M. McBride, J. Michaelian, T. Pick, D.J. Poon, S. Girish, C.M. Shafer, D. Stuart, L. Sung, P.A. Renhowe, J. Med. Chem. 51 (2008) 7049–7052.

[75] S. Ramurthy, M. Aikawa, P. Amiri, A. Costales, A. Hashash, J.M. Jansen, S. Lin, S. Ma, P.A. Renhowe, C.M. Shafer, S. Subramanian, L. Sung, J. Verhagen, Bioorg. Med. Chem. Lett. 21 (2011) 3286–3289.

[76] D. Niculescu-Duvaz, C. Gaulon, H.P. Dijkstra, I. Niculescu-Duvaz, A. Zambon, D. Menard, B.M.J.M. Suijkerbuijk, A. Nourry, L. Davies, H. Manne, F. Friedlos, L. Ogilvie, D. Hedley, S. Whittaker, R. Kirk, A. Gill, R.D. Taylor, F.I. Raynaud, J. Moreno-Farre, R. Marais, C.J. Springer, J. Med. Chem. 52 (2009) 2255–2264.

[77] D. Menard, I. Niculescu-Duvaz, H.P. Dijkstra, D. Niculescu-Duvaz, B.M.J.M. Suijkerbuijk, A. Zambon, A. Nourry, E. Roman, L. Davies, H.A. Manne, F. Friedlos, R. Kirk, S. Whittaker, A. Gill, R.D. Taylor, R. Marais, C.J. Springer, J. Med. Chem. 52 (2009) 3881–3891.

[78] A. Nourry, A. Zambon, L. Davies, I. Niculescu-Duvaz, H.P. Dijkstra, D. Menard, C. Gaulon, D. Niculescu-Duvaz, B.M.J.M. Suijkerbuijk, F. Friedlos, H.A. Manne, R. Kirk, S. Whittaker, R. Marais, C.J. Springer, J. Med. Chem. 53 (2010) 1964–1978.

[79] B.M.J.M. Suijkerbuijk, I. Niculescu-Duvaz, C. Gaulon, H.P. Dijkstra, D. Niculescu-Duvaz, D. Menard, A. Zambon, A. Nourry, L. Davies, H.A. Manne, F. Friedlos, L.M. Ogilvie, D. Hedley, F. Lopes, N.P.U. Preece, J. Moreno-Farre, F.I. Raynaud, R. Kirk, S. Whittaker, R. Marais, C.J. Springer, J. Med. Chem. 53 (2010) 2741–2756.

[80] Y. Yang, J. Qin, H. Liu, X. Yao, J. Chem. Inf. Model. 51 (2011) 680–692.

[81] A. Zambon, D. Menard, B.M.J.M. Suijkerbuijk, I. Niculescu-Duvaz, S. Whittaker, D. Niculescu-Duvaz, A. Nourry, L. Davies, H.A. Manne, F. Lopes, N. Preece, D. Hedley, L.M. Ogilvie, R. Kirk, R. Marais, C.J. Springer, J. Med. Chem. 53 (2010) 5639–5655.

[82] S. Whittaker, D. Ménard, R. Kirk, L. Ogilvie, D. Hedley, A. Zambon, F. Lopes, N. Preece, H. Manne, S. Rana, M. Lambros, J.S. Reis-Filho, R. Marais, C.J. Springer, Cancer Res. 70 (2010) 8036–8044.

[83] S. Wenglowsky, L. Ren, K.A. Ahrendt, E.R. Laird, I. Aliagas, B. Alicke, A.J. Buckmelter, E.F. Choo, V. Dinkel, B. Feng, S.L. Gloor, S.E. Gould, S. Gross, J. Gunzner-Toste, J.D. Hansen, G. Hatzivassiliou, B. Liu, K. Malesky, S. Mathieu, B. Newhouse, N.J. Raddatz, Y. Ran, S. Rana, N. Randolph, T. Risom, J. Rudolph, S. Savage, L.T. Selby, M. Shrag, K. Song, H.L. Sturgis, W.C. Voegtli, Z. Wen, B.S. Willis, R.D. Woessner, W. Wu, W.B. Young, J. Grina, ACS Med. Chem. Lett. 2 (2011) 342–347.

[84] A.E. Gould, R. Adams, S. Adhikari, K. Aertgeerts, R. Afroze, C. Blackburn, E.F. Calderwood, R. Chau, J. Chouitar, M.O. Duffey, D.B. England, C. Farrer, N. Forsyth, K. Garcia, J. Gaulin, P.D. Greenspan, R. Guo, S.J. Harrison, S.-C. Huang, N. Iartchouk, D. Janowick, M.-S. Kim, B. Kulkarni, S.P. Langston, J.X. Liu, L.-T. Ma, S. Menon, H. Mizutani, E. Paske, C.C. Renou, M. Rezaei, R.S. Rowland, M.D. Sintchak, M.D. Smith, S.G. Stroud, M. Tregay, Y. Tian, O.P. Veiby, T.J. Vos, S. Vyskocil, J. Williams, T. Xu, J.J. Yang, J. Yano, H. Zeng, D.M. Zhang, Q. Zhang, K.M. Galvin, J. Med. Chem. 54 (2011) 1836–1846.

[85] S. Wenglowsky, D. Moreno, J. Rudolph, Y. Ran, K.A. Ahrendt, A. Arrigo, B. Colson, S.L. Gloor, G. Hastings, Bioorg. Med. Chem. Lett. 22 (2013) 912–915.

[86] S. Mathieu, S.N. Gradl, L. Ren, Z. Wen, I. Aliagas, J. Gunzner-Toste, W. Lee, R. Pulk, G. Zhao, B. Alicke, J.W. Boggs, A.J. Buckmelter, E.F. Choo, V. Dinkel, S.L. Gloor, S.E. Gould, J.D. Hansen, G. Hastings, G. Hatzivassiliou, E.R. Laird, D. Moreno, Y. Ran, W.C. Voegtli, S. Wenglowsky, J. Grina, J. Rudolph, J. Med. Chem. 55 (2012) 2869–2881.

[87] S. Wenglowsky, K.A. Ahrendt, A.J. Buckmelter, B. Feng, S.L. Gloor, S. Gradl, J. Grina, J.D. Hansen, E.R. Laird, P. Lunghofer, S. Mathieu, D. Moreno, B. Newhouse, L. Ren, T. Risom, J. Rudolph, J. Seo, H.L. Sturgis, W.C. Voegtli, Z. Wen, Bioorg. Med. Chem. Lett. 21 (2011) 5533–5537.

[88] E.F. Choo, B. Alicke, J. Boggs, D. Dinkel, S. Gould, J. Grina, K. West, K. Menghrajani, Y. Ran, J. Rudolph, S. Wenglowsky, Xenobiotica 41 (2011) 1076–1087.

[89] S. Wenglowsky, D. Moreno, E.R. Laird, S.L. Gloor, L. Ren, T. Risom, J. Rudolph, H.L. Sturgis, W.C. Voegtli, Bioorg. Med. Chem. Lett. 22 (2012) 6237–6241.

[90] P.D. Lyne, B. Aquila, D.J. Cook, L.A. Dakin, J. Ezhuthachan, S. Ioannidis, T. Pontz, M. Su, Q. Ye, X. Zheng, M.H. Block, S. Cowen, T.L. Deegan, J.W. Lee, D.A. Scott, D. Custeau, L. Drew, S. Poondru, M. Shen, A. Wu, Bioorg. Med. Chem. Lett. 19 (2009) 1026–1029.

[91] M. Wang, M. Gao, K.D. Miller, Q. Zheng, Bioorg. Med. Chem. Lett. 23 (2013) 1017–1021.

[92] A.J. Buckmelter, L. Ren, E.R. Laird, B. Rast, G. Miknis, S. Wenglowsky, S. Schlachter, M. Welch, E. Tarlton, J. Grina, J. Lyssikatos, B.J. Brandhuber, T. Morales, N. Randolph, G. Vigers, M. Martinson, M. Callejo, Bioorg. Med. Chem. Lett. 21 (2012) 1248–1252.

[93] D.K. Dalvie, A.S. Kalgutkar, S.C. Khojasteh-Bakht, R.S. Obach, J.P. O'Donnell, Chem. Res. Toxicol. 15 (2002) 269–299.

[94] L. Ren, S. Wenglowsky, G. Miknis, B. Rast, A.J. Buckmelter, R.J. Ely, S. Schalachter, E.R. Laird, N. Randolph, M. Callejo, M. Martinson, S. Galbrainth, B.J. Brandhuber, G. Viger, W.C. Voegtli, T. Morales, J. Lyssikatos, Bioorg. Med. Chem. Lett. 21 (2011) 1243–1247.

[95] J.C. Stellwagen, G.M. Adjabeng, M.R. Arnone, S.H. Dickerson, C. Han, K.R. Hornberger, A.J. King, R.A. Mook, K.G. Petrov, T.R. Rheault, C.M. Rominger, O.W. Rossanese, K.N. Smitheman, A.G. Waterson, D.E. Uehling, Bioorg. Med. Chem. Lett. 21 (2011) 4436–4440.

[96] T.R. Rheault, J.C. Stellwagen, G.M. Adjabeng, K.R. Hornberger, K.G. Petrov, A.G. Waterson, S.H. Dickerson, R.A. Mook, S.G. Laquerre, A.J. King, O.W. Rossanese, M.R. Arnone, K.N. Smitheman, L.S. Kane-Carson, C. Han, G.S. Moorthy, K.G. Moss, D.E. Uehling, ACS Med. Chem. Lett. 4 (2013) 358–362.

[97] A. Hauschild, J. Grob, L. Demidov, T. Jouary, R. Gutzmer, M. Millward, P. Rutkowski, C. Blank, W. Miller, E. Kaempgen, S. Martín-Algarra, B. Karaszewska, C. Mauch, V. Chiarion-Sileni, A. Martin, S. Swann, P. Haney, B. Mirakhur, M. Guckert, V. Goodman, P. Chapman, Lancet 380 (2012) 358–365.

[98] G. Falchook, G. Long, R. Kurzrock, K. Kim, T. Arkenau, M. Brown, O. Hamid, J. Infante, M. Millward, A. Pavlick, S. O'Day, S. Blackman, C. Curtis, P. Lebowitz, B. Ma, D. Ouellet, R. Kefford, Lancet 379 (2012) 1893–1901.

[99] J. Weber, K. Flaherty, J. Infante, G. Falchook, R. Kefford, A. Daud, O. Hamid, R. Gonzalez, R. Kudchadkar, D. Lawrence, H. Burris, G. Long, A. Algazi, K. Lewis, K. Kim, I. Puzanov, P. Sun, S. Little, K. Patel, J. Sosman, ASCO Meeting Abstracts 30 (2012) 8510.

[100] Z. Xu, G. Yan, G. Wang, B. Li, J. Zhu, P. Sun, X. Zhang, C. Luo, H. Wang, W. Zhu, Bioorg. Med. Chem. Lett. 22 (2012) 5428–5437.

[101] X. Kong, J. Qin, Z. Li, A. Vultur, L. Tong, E. Feng, G. Rajan, S. Liu, J. Lu, Z. Liang, M. Zheng, W. Zhu, H. Jiang, M. Herlyn, H. Liu, R. Marmorstein, C. Luo, Org. Biomol. Chem. 10 (2012) 7402–7417.

[102] A. Gopalsamy, G. Ciszewski, Y. Hu, F. Lee, L. Feldberg, E. Frommer, S. Kim, K. Collins, D. Wojciechowicz, R. Mallon, Bioorg. Med. Chem. Lett. 19 (2009) 2735–2738.

[103] D.M. Berger, N. Torres, M. Dutia, D. Powell, G. Ciszewski, A. Gopalsamy, J.I. Levin, K.-H. Kim, W. Xu, J. Wilhelm, Y. Hu, K. Collins, L. Feldberg, S. Kim, E. Frommer, D. Wojciechowicz, R. Mallon, Bioorg. Med. Chem. Lett. 19 (2009) 6519–6523.

[104] A. Gopalsamy, G. Ciszewski, M. Shi, D. Berger, Y. Hu, F. Lee, L. Feldberg, E. Frommer, S. Kim, K. Collins, D. Wojciechowicz, R. Mallon, Bioorg. Med. Chem. Lett. 19 (2009) 6890–6892.

[105] X. Wang, D.M. Berger, E.J. Salaski, N. Torres, Y. Hu, J.I. Levin, D. Powell, D. Wojciechowicz, K. Collins, E. Frommer, Bioorg. Med. Chem. Lett. 19 (2009) 6571–6574.

[106] X. Wang, D.M. Berger, E.J. Salaski, N. Torres, M. Dutia, C. Hanna, Y. Hu, J.I. Levin, D. Powell, D. Wojciechowicz, K. Collins, E. Frommer, J. Lucas, J. Med. Chem. 53 (2010) 7874–7878.

[107] M.J. Di Grandi, D.M. Berger, D.W. Hopper, C. Zhang, M. Dutia, A.L. Dunnick, N. Torres, J.I. Levin, G. Diamantidis, C.W. Zapf, J.D. Bloom, Y. Hu, D. Powell, D. Wojciechowicz, K. Collins, E. Frommer, Bioorg. Med. Chem. Lett. 19 (2009) 6957–6961.

[108] L. Ren, E.R. Laird, A.J. Buckmelter, V. Dinkel, S.L. Gloor, J. Grina, B. Newhouse, K. Rasor, G. Hastings, S.N. Gradl, J. Rudolph, Bioorg. Med. Chem. Lett. 22 (2012) 1165–1168.

[109] A. Gopalsamy, M. Shi, Y. Hua, F. Lee, L. Feldberg, E. Frommer, S. Kim, K. Collins, D. Wojciechowicz, R. Mallon, Bioorg. Med. Chem. Lett. 20 (2010) 2431–2434.

[110] J. Tang, K.E. Lackey, S.H. Dickerson, Bioorg. Med. Chem. Lett. 23 (2013) 66–70.

[111] G.K. Packard, P. Papa, J.R. Riggs, P. Erdman, L. Tehrani, D. Robinson, R. Harris, G. Shevlin, S. Perrin-Ninkovic, R. Hilgraf, M.A. McCarrick, T. Tran, Y. Fleming, A. Bai, S. Richardson, J. Katz, Y. Tang, J. Leisten, M. Moghaddam, B. Cathers, D. Zhu, S. Sakata, Bioorg. Med. Chem. Lett. 22 (2012) 747–752.

[112] L. Ren, K.A. Ahrendt, J. Grina, E.R. Laird, A.J. Buckmelter, J.D. Hansen, B. Newhouse, D. Moreno, S. Wenglowsky, V. Dinkel, S.L. Gloor, G. Hastings, S. Rana, K. Rasor, T. Risom, H.L. Sturgis, W.C. Voegtli, S. Mathieu, Bioorg. Med. Chem. Lett. 22 (2012) 3387–3391.

[113] A.L. Smith, F.F. DeMorin, N.A. Paras, Q. Huang, J.K. Petkus, E.M. Doherty, T. Nixey, J.L. Kim, D.A. Whittington, L.F. Epstein, M.R. Lee, M.J. Rose, C. Babij, M. Fernando, K. Hess, Q. Le, P. Beltran, J. Carnahan, J. Med. Chem. 52 (2009) 6189–6192.

[114] M.W. Holladay, B.T. Campbell, M.W. Rowbottom, Q. Chao, K.G. Sprankle, A.G. Lai, S. Abraham, E. Setti, R. Faraoni, L. Tran, R.C. Armstrong, R.N. Gunawardane, M.F. Gardner, M.D. Cramer, D. Gitnick, M.A. Ator, B.D. Dorsey, B.R. Ruggeri, M. Williams, S.S. Bhagwat, J. James, Bioorg. Med. Chem. Lett. 21 (2011) 5342–5346.

[115] M.W. Rowbottom, R. Faraoni, Q. Chao, B.T. Campbell, A.G. Lai, E. Setti, M. Ezawa, K.G. Sprankle, S. Abraham, L. Tran, B. Struss, M. Gibney, R.C. Armstrong, R.N. Gunawardane, R.R. Nepomuceno, I. Valenta, H. Hua, M.F. Gardner, M.D. Cramer, D. Gitnick, D.E. Insko, J.L. Apuy, S. Jones-Bolin, A.K. Ghose, T. Herbertz, M.A. Ator, B.D. Dorsey, B. Ruggeri, M. Williams, S. Bhagwat, J. James, M.W. Holladay, J. Med. Chem. 55 (2012) 1082–1105.

[116] S. Ramurthy, A. Costales, J.M. Jansen, B. Levine, P.A. Renhowe, C.M. Shafer, S. Subramanian, Bioorg. Med. Chem. Lett. 22 (2012) 1678–1681.

[117] M.M. Vasbinder, B. Aquila, M. Augustin, H. Chen, T. Cheung, D. Cook, L. Drew, B.P. Fauber, S. Glossop, M. Grondine, E. Hennessy, J. Johannes, S. Lee, P. Lyne, M. Mörtl, C. Omer, S. Palakurthi, T. Pontz, J. Read, L. Sha, M. Shen, S. Steinbacher, H. Wang, A. Wu, M. Ye, J. Med. Chem. 56 (2013) 1996–2015.

[118] Q. Zhang, Y. Diao, F. Wang, Y. Fu, F. Tang, Q. You, H. Zhou, Med. Chem. Commun. 4 (2013) 979–986.

[119] J.D. Hansen, J. Grina, B. Newhouse, M. Welch, G. Topalov, N. Littman, M. Callejo, S. Gloor, M. Martinson, E. Laird, B.J. Brandhuber, G. Vigers, T. Morales, R. Woessner, N. Randolph, J. Lyssikatos, A. Olivero, Bioorg. Med. Chem. Lett. 18 (2008) 4692–4695.

[120] B.J. Newhouse, J.D. Hansen, J. Grina, M. Welch, G. Topalov, N. Littman, M. Callejo, M. Martinson, S. Galbraith, E.R. Laird, B.J. Brandhuber, G. Vigers, T. Morales, R. Woessner, N. Randolph, J. Lyssikatos, A. Olivero, Bioorg. Med. Chem. Lett. 21 (2011) 3488–3492.
[121] J.H. Alzate-Morales, A. Vergara-Jaque, J. Caballero, J. Chem. Inf. Model. 50 (2010) 1101–1112.
[122] J. Caballero, J.H. Alzate-Morales, A. Vergara-Jaque, J. Chem. Inf. Model. 51 (2011) 2920–2931.
[123] K.-C. Shih, C.-Y. Lin, J. Zhou, H.-C. Chi, T.-S. Chen, C.-C. Wang, H.-W. Tseng, C.-Y. Tang, J. Chem. Inf. Model. 51 (2011) 398–407.
[124] M. Kim, M. Kim, H. Yu, H. Kim, K.H. Yoo, T. Sim, J.-M. Hah, Bioorg. Med. Chem. 19 (2011) 1915–1923.
[125] J.-J. Dong, Q.-S. Li, S.-F. Wang, C.-Y. Li, X. Zhao, H.-Y. Qiu, M.-Y. Zhaoa, H.-L. Zhu, Org. Biomol. Chem. 11 (2013) 6328–6337.
[126] H. Kim, M. Kim, J. Lee, H. Yu, J.-M. Hah, Bioorg. Med. Chem. 19 (2011) 6760–6767.
[127] J. Tang, T. Hamajima, M. Nakano, H. Sato, S.H. Dickerson, K.E. Lackey, Bioorg. Med. Chem. Lett. 18 (2008) 4610–4614.
[128] C. Blackburn, M.O. Duffey, A.E. Gould, B. Kulkarni, J.X. Liu, S. Menon, M. Nagayoshi, T.J. Vos, J. Williams, Bioorg. Med. Chem. Lett. 20 (2010) 4795–4799.
[129] M.O. Duffey, R. Adams, C. Blackburn, R.W. Chau, S. Chen, K.M. Galvin, K. Garcia, A.E. Gould, P.D. Greenspan, S. Harrison, S. Huang, M. Kim, B. Kulkarni, S. Langston, J.X. Liu, L. Ma, S. Menon, M. Nagayoshi, R.S. Rowland, T.J. Vos, T. Xu, J.J. Yang, S. Yu, Q. Zhang, Bioorg. Med. Chem. Lett. 20 (2010) 4800–4804.
[130] Q. Li, X. Lv, Y. Zhang, J. Dong, W. Zhou, Y. Yang, H. Zhu, Bioorg. Med. Chem. Lett. 22 (2012) 6596–6601.
[131] C. Li, Q. Li, L. Yan, X. Sun, R. Wei, H. Gong, H. Zhu, Bioorg. Med. Chem. 20 (2012) 3746–3755.
[132] Y. Yang, Q. Li, S. Sun, Y. Zhang, X. Wang, F. Zhang, J. Tang, H. Zhu, Bioorg. Med. Chem. 20 (2012) 6048–6058.
[133] J. Liu, H. Zhang, J. Sun, Z. Wang, Y. Yang, D. Li, F. Zhang, H. Gong, H. Zhu, Bioorg. Med. Chem. 20 (2012) 6089–6096.
[134] O. Tanwar, A. Marella, S. Shrivastava, M.M. Alam, M. Akhtar, Med. Chem. Res. 22 (2013) 2174–2187.
[135] I. Niculescu-Duvaz, E. Roman, S.R. Wittaker, F. Friedlos, R. Kirk, I.J. Scanlon, L.C. Davies, D. Niculescu-Duvaz, R. Marais, C.J. Springer, J. Med. Chem. 49 (2006) 407–416.
[136] I. Niculescu-Duvaz, E. Roman, S.R. Wittaker, F. Friedlos, R. Kirk, I.J. Scanlon, L.C. Davies, D. Niculescu-Duvaz, R. Marais, C.J. Springer, J. Med. Chem. 51 (2008) 3261–3274.
[137] X. Wanga, E.J. Salaski, D.M. Berger, D. Powell, Y. Hua, D. Wojciechowicz, K. Collins, E. Frommer, Bioorg. Med. Chem. Lett. 21 (2011) 6941–6944.
[138] H. Park, H. Choi, S. Hong, S. Hong, Bioorg. Med. Chem. Lett. 21 (2011) 5753–5756.
[139] H. Park, Y. Jeong, S. Hong, Bioorg. Med. Chem. Lett. 22 (2012) 1027–1030.
[140] J. Qin, P. Xie, C. Ventocilla, G. Zhou, A. Vultur, Q. Chen, Q. Liu, M. Herlyn, J. Winkler, R. Marmorstein, J. Med. Chem. 55 (2012) 5220–5230.
[141] W.-K. Choi, M.I. El-Gamal, H.S. Choi, D. Baek, C.H. Oh, Eur. J. Med. Chem. 46 (2011) 5754–5762.
[142] Y. Xie, X. Chen, J. Qin, X. Kong, F. Ye, Y. Jiang, H. Liu, H. Jiang, R. Marmorstein, C. Luo, Bioorg. Med. Chem. Lett. 23 (2013) 2306–2312.
[143] B. Xin, W. Tang, Y. Wang, G. Lin, H. Liu, Y. Jiao, Y. Zhu, H. Yuan, Y. Chen, T. Lu, Bioorg. Med. Chem. Lett. 22 (2012) 4783–4786.
[144] Q. Li, C. Li, X. Lu, H. Zhang, H. Zhu, Eur. J. Med. Chem. 50 (2012) 288–295.